TECHNICAL REPORT ON SUSPENDED MATTER IN MERMAID SOUND, DAMPIER ARCHIPELAGO

Department of Conservation and Environment,
Perth, Western Australia

Bulletin 215 October 1985

TECHNICAL REPORT ON SUSPENDED MATTER IN MERMAID SOUND, DAMPIER ARCHIPELAGO

M.J. FORDE

DAMPIER ARCHIPELAGO MARINE STUDY

DEPARTMENT OF CONSERVATION AND ENVIRONMENT
1 MOUNT STREET
PERTH WESTERN AUSTRALIA 6000

ISBN 0 7309 0578 0

CONTENTS

FIGURES

Page

TABLES

ABSTRACT

This report presents data from a study (1981-1983) of the spatial and temporal variations in levels of suspended matter in the water column using sediment traps in Mermaid Sound, Dampier Archipelago. Seasonal wind conditions and wave energy regimes were analysed and related to suspended loads to determine the possible causes of these variations. Light attenuation was also measured and trends assessed in relation to suspended matter. Trap data were indicative of the degree of resuspension of sediment at a site and not of net sedimentation rates.

The composition of suspended material was found to vary with height above the sea-floor. The organic fraction was greatest near the water surface whereas the calcium carbonate fraction was greatest near the sea-floor. Within the study area suspended loads were found to be greater in the southern sector of the Sound ie inshore, than in the northern sector ie offshore. Levels were generally higher in summer than in winter mainly as a result of the seasonal prevailing winds.

Light attenuation values supported these broad conclusions; the offshore areas were always less turbid than those inshore, while the entire area was more turbid in summer than in winter. Light measurements alone, however, should not be used as an indication of the suspended load. The composition of material in suspension is more important to light attenuation than the total dry weight; the critical factors being organic content, grain size and grain colour. Dredging caused widespread decrease in light attenuation, particularly over the summer of 1982-83.

Inshore wind speed, wave energy and suspended load were all significantly correlated, indicating that local wind conditions regulated wave energy which in turn resuspended bottom sediments. By contrast, offshore, the suspended load did not correlate with mean wind speed although it did correlate with wave energy. Thus, a combination of wind-induced waves as well as swell energy was likely to have caused resuspension and

therefore variations in suspended load in the northern sector. Overriding these trends are the effects of cyclones which generate both swell and wind energy. Cyclones were observed to cause large-scale, short-term resuspension of sediments, considerable damage to benthic communities, the generation of calcareous rubble and considerable relocation of sediments.

ACKNOWLEDGEMENTS

I gratefully acknowledge the generous support and encouragement of Dr V.W. Talbot at all stages through this study. He also gave advice, general guidance and constructive criticisms on the report. Dr D.A. Mills is thanked for providing data and for preparing the first draft of Chapter 3. Dr R.G. Chittleborough, Dr J.R. Ottaway, Ms E. Moore, Mr C.J. Simpson and other staff of the Department of Conservation and Environment discussed the work at various stages, assisted with fieldwork and advised on the preparation of various drafts.

Associate Professor A.J. McComb and staff at the Centre for Water Research, University of Western Australia, advised on the nature of the field programme, critically read parts of the manuscript, and gave technical and logistical support. Dr R. Dunlap, Chemistry Department, University of Western Australia, Ms E. Moore and Dr J.R. Ottaway constructively edited the penultimate draft. Mr B. Stewart, Mr A. Berman and Ms E. Moore prepared this report for publication.

1. INTRODUCTION

1.1 SCOPE

Mermaid Sound, an area of 400 km^2 in the north-west of Western Australia (Fig. 1.1), is bounded by the mainland and the islands of the Dampier Archipelago. The Coastal Waters Branch of the Department of Conservation and Environment undertook a series of research projects to investigate the marine ecosystems of this region (Chittleborough, 1983; Gordon, 1983; Mills, 1985; Simpson, 1985; Talbot, 1985; Talbot and Creagh, 1985a,b) with the objective of managing and minimising human impacts.

Initial observations of water turbidity in Mermaid Sound indicated marked variation from clear oceanic waters at the northern part of the Sound to very turbid conditions near the mainland. Coincident with this turbidity range is a change in the biotic communities. For example, the outer reef supports extensive coral communities dominated by acroporids (eg. *A. hyacinthus*) and pocilloporids (eg. *P.damicornis*), while further into the Sound massive corals such as *Favia* and *Favites* are dominant. Turbidity and sediment load are important factors in coral reef development and they influence species composition. Endean (1976) has shown that the families Acroporidae and Pocilloporidae are very susceptible to sediment deposition, while many massive species are more tolerant. Thus a knowledge of variations in suspended matter is important in understanding biotic communities.

This study, initiated in September 1981, examined natural spatial and temporal variation in suspended matter in Mermaid Sound, and investigated:

- the relationship between suspended matter and vertical light attenuation,
- the relationship between marine sediments and suspended load, and
- the environmental factors which determine suspended loads.

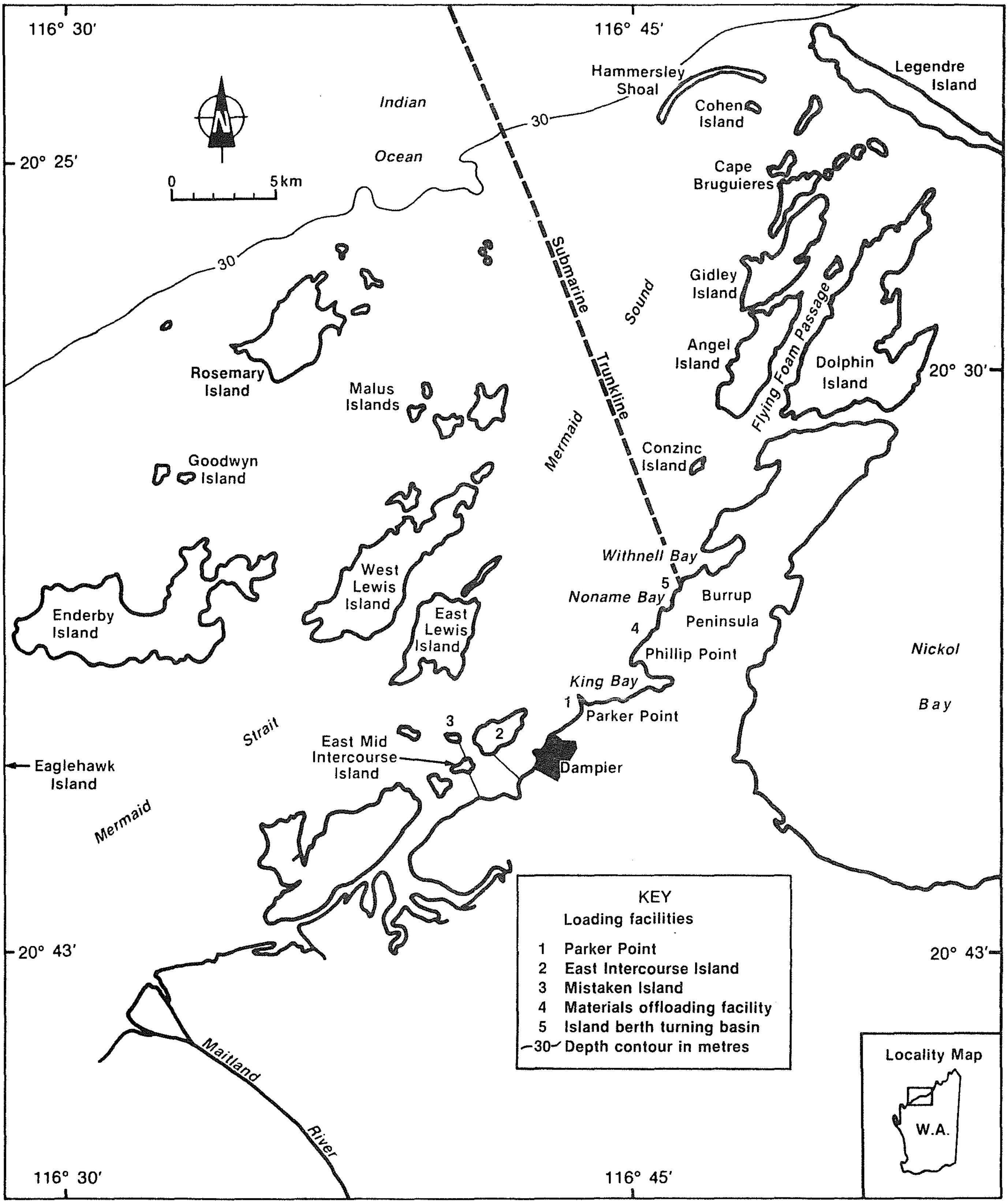

Figure 1.1 The study area; Dampier Archipelago.

1.2 STUDY AREA

The Dampier Archipelago was formed during the last postglacial marine transgression about 7000 years ago (Lawson & Treloar, 1983). Resultant flooding of the hinterland drowned the low-lying valleys and plains leaving rocky high points exposed as islands and emergent shoals. The dominant bedrock of the area is gidley granophyre, being an intrusion along the basal unconformity of the precambrian Fortescue group (Kriewaldt, 1964). Medium-grained reddish-fawn limestone occurs mainly in the outer areas of the Archipelago (Biggs & Denman, 1981). These deposits, that may be remnants of a coastal dune system of the pleistocene epoch, form an outer submarine escarpment and associated emergent rocks and islands (Lawson & Treloar, 1983).

The inshore sediments of the Archipelago are composed mainly of clay-sized material with high silica content derived from river discharge and shore erosion. Freshwater discharge to the Dampier Archipelago is from the infrequent flow of the Maitland River, and is usually associated with cyclonic rainfall. The sediments become progressively coarser (Lawson & Treloar, 1983) and increase in calcium carbonate content with distance from the mainland, as a result of decreasing terrigenous input and increasing biogenic deposition. Recent (Holocene) deposits of calcium carbonate have minimal iron staining, forming white-grey beaches, foredunes and main dunes. Relic (Pleistocene) material forms weathered, oxidised, reddish-cream deposits further inland and in isolated areas of reworking within the Archipelago (Biggs & Denman, 1981; Lawson & Treloar, 1983).

1.3 PHYSICAL ENVIRONMENT

The area is arid and tropical, with an average annual rainfall of approximately 290 mm (Dept. of the Interior, 1972) and an annual evaporation rate of 3734 mm (Bureau of Meteorology, unpublished data, 1980). The period of highest rainfall is from January to March and is associated with tropical cyclone activity. The annual range in sea temperature is 19 - 32^{0}. These limits are close to the lower and upper tolerance levels of many tropical marine organisms (Woodside Petroleum Development, 1979). The tidal range is moderate (4.5 m); tides are semidiurnal. Current speeds are generally greater in offshore areas and channels. Tidal excursion may be as much as 10 km under normal spring tide conditions. Wind energy and water movement of the region are discussed in detail in Chapters 2 and 3 respectively.

1.4 PORT OPERATION, FACILITIES AND ASSOCIATED INDUSTRIES

The sheltered waters of the Archipelago, the relatively deep water access to the mainland and the safe anchorage of Mermaid Sound, have facilitated development of the port and associated industries within the area.

Hamersley Iron Pty Ltd was first to construct a loading facility, at Parker Point (Fig. 1.1), which began operations in 1966. A second facility, located on East Intercourse Island (Fig. 1.1), started exporting iron ore in March 1972. To provide access to this island from the mainland, a solid fill causeway was constructed. Dredging was required to construct shipping channels to these terminals; 17 x 10^6 m^3 of dredge spoil were relocated within Mermaid Sound, between 1965 and 1977. Further dredging, to widen and deepen sections of these channels to facilitate larger ore carriers, resulted in 0.716 x 10^6 m^3 of spoil being relocated in 1981-82.

Dampier Salt Pty Ltd was the next major industrial company in the area. Construction began in 1967 and the first harvest of common salt (sodium chloride) occurred in 1971. A loading facility was constructed on Mistaken Island (Fig. 1.1) and was connected to the mainland by a solid fill causeway incorporating East Mid-Intercourse Island.

The most recent major industry in the area has been natural gas development by Woodside Offshore Petroleum Pty Ltd. This is still in the development stage, but four dredging operations have been undertaken to date:

- to permit access to the supply base, 1.2 x 10^6 m^3 of sediments were dredged from near Phillip Point and King Bay (Fig. 1.1) and deposited onshore behind a bund. Spoil overflow resulted in the burial and death of 1.2 ha of mangroves adjacent to the bund in May 1982.

- associated with the construction of the materials offloading facility (MOF) (Fig. 1.1) 0.14 x 10^6 m^3 of spoil were relocated 1.5 km north of the dredge site.

- for the construction of a submarine trunkline (Fig. 1.1). Blasting and clamshell dredging resulted in 0.28 x 10^6 m^3 of spoil being dredged and sidecast 500 m between December 1981 and July 1983. The later period involved backfilling and the dumping of 0.026 x 10^6 m^3 of bedding material (0-50 mm aggregate) and 0.94 x 10^6 m^3 of solid filling (0-600 mm crushed rock) over the pipeline,

- for the construction of the island turning basin offshore from Withnell Bay (Fig. 1.1) between 1 December 1982 and 21 February 1983 which involved dredging and onshore deposition of 0.55 x 10^6 m^3 of spoil in Noname Creek (Fig. 1.1).

2. WIND AND WAVE ENERGY

2.1 INTRODUCTION

Winds and pressure disturbances acting over the sea lead to a transfer of energy from air to water. Some of this energy is contained in wave motion and subsequently may be expended by friction at the sea-floor, particularly in shallow waters. In the process, sea-floor sediments may be moved and the finer fractions placed in suspension in the water column. These resuspended sediments can then be mobilised by currents.

The manner in which meteorological processes interact to form the observed seasonal wind conditions of the Archipelago is discussed in this chapter. Available wave data are analysed and effects of long and short period waves on the Archipelago are considered. Finally, occurrence, energetics and impact of tropical cyclones are examined with reference to sediment movement.

2.2 WIND

Local wind conditions of the Pilbara coast, including the Dampier Archipelago, are dominated by three meteorological processes:

- Migration of high pressure systems (anti-cyclonic belts) into the more northerly latitudes in winter.

- Formation of monsoonal depressions in summer.

- Occurrence of diurnal land/sea breeze conditions caused by the difference in land and sea temperatures. This diurnal pattern is superimposed upon the winds caused by large-scale pressure systems.

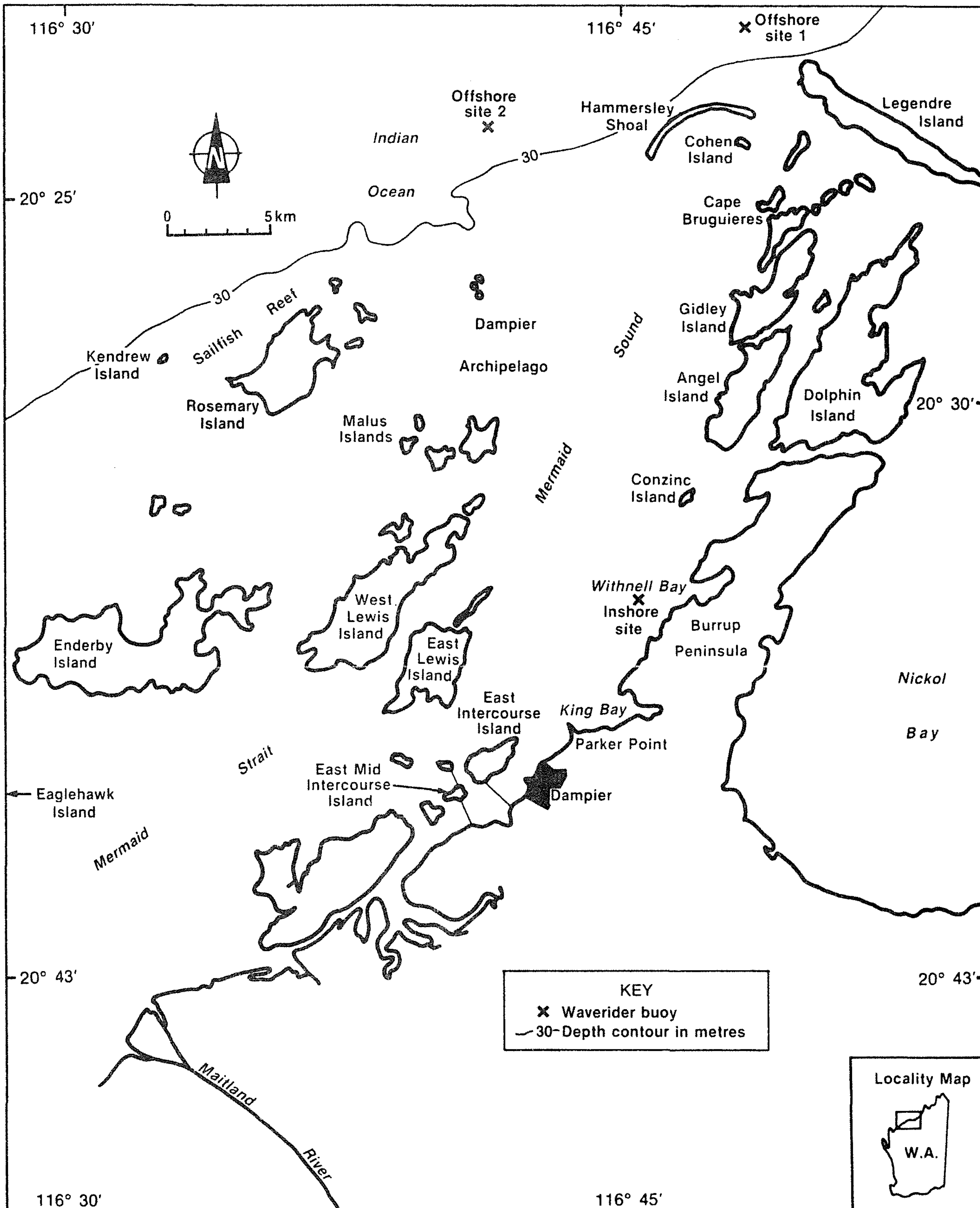

Figure 2.1 Sites of waverider buoys deployed from May 1980 to December 1982.

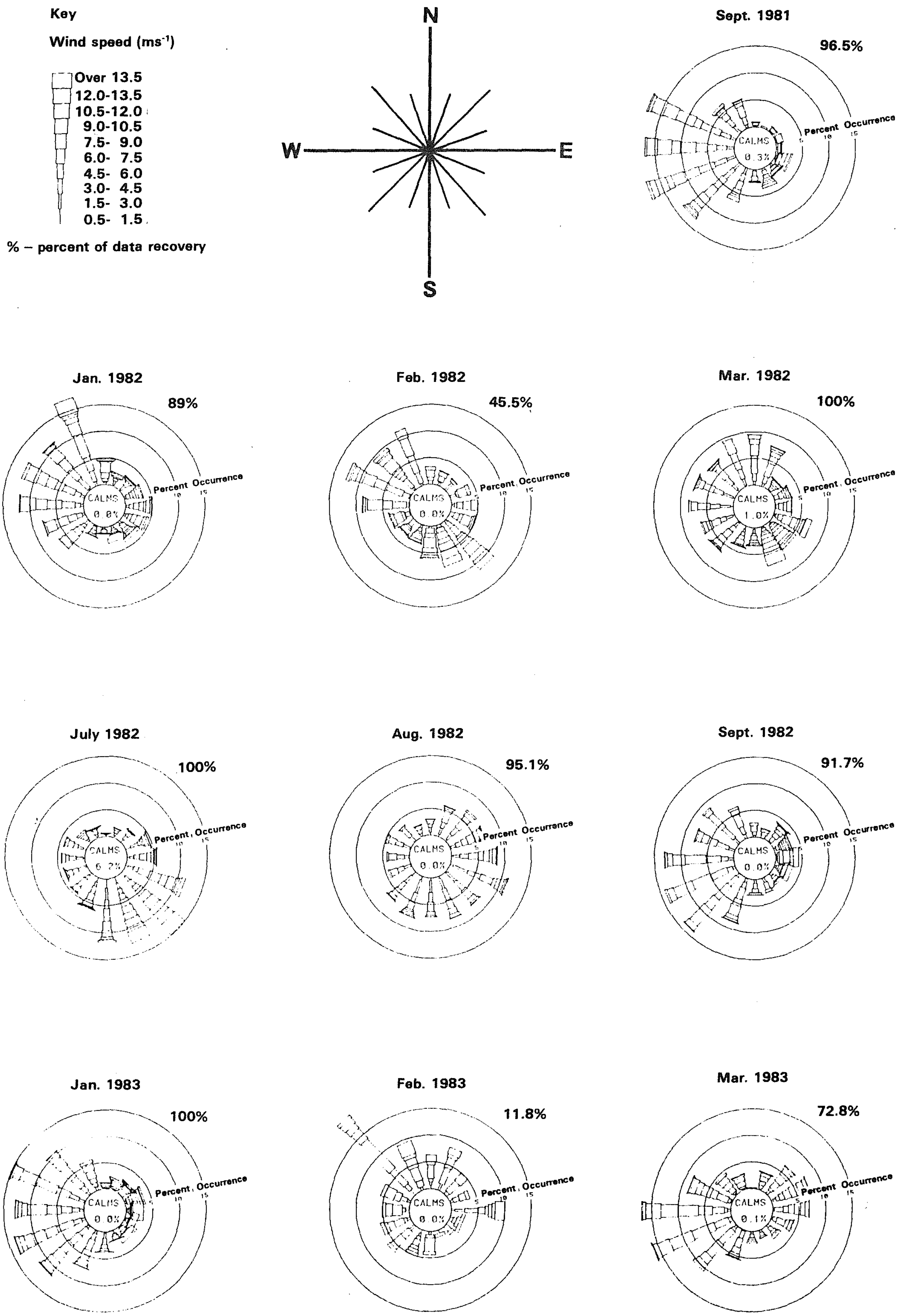

Figure 2.2 Monthly wind speed and direction roses for Conzinc Island from September 1981 to June 1983.

Oct. 1981

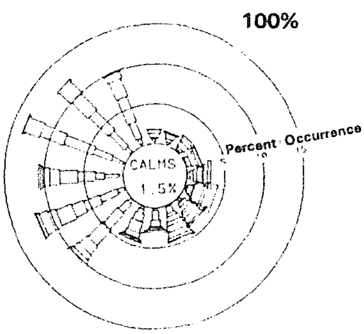

Nov. 1981

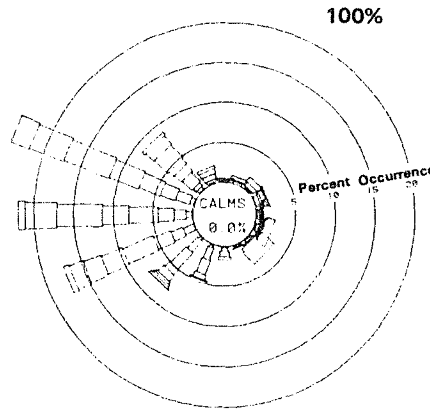

Dec. 1981

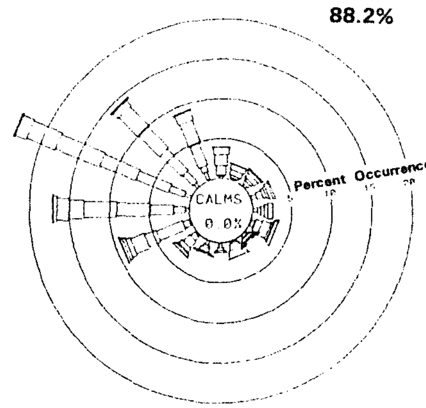

Apr. 1982

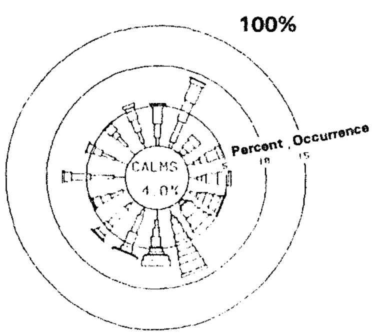

May 1982

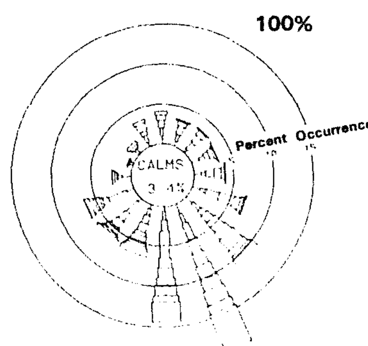

June 1982

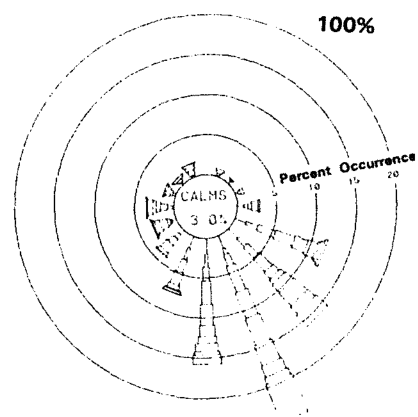

Oct. 1982

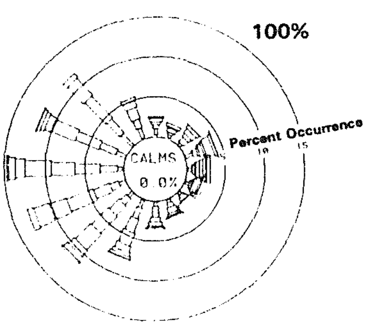

Nov. 1982

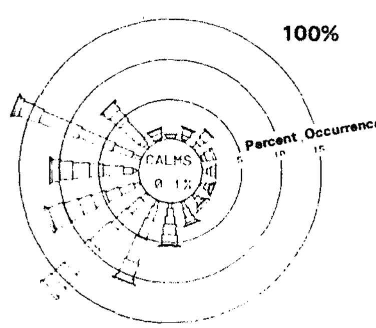

Dec. 1982

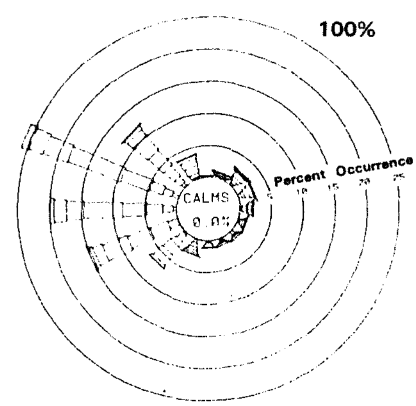

Apr. 1983

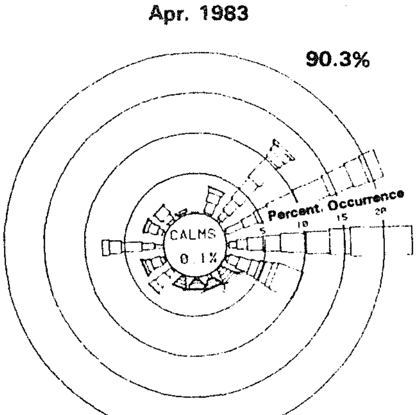

May 1983

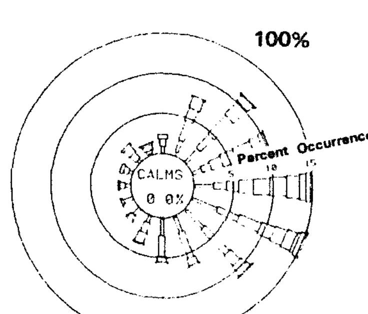

June 1983

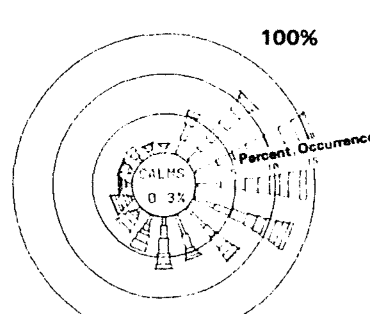

2.2.1 Methods: wind measurement

To measure wind in the Dampier Archipelago, a Woeffle anemometer was positioned 4.5 m above the highest point of Conzinc Island (Fig. 2.1) from September 1981 to July 1983. The records were digitised to obtain mean values of wind speed and direction, for consecutive 30-minute periods. These data were stored on computer and then used to calculate monthly wind roses (Fig. 2.2).

2.2.2 Discussion

Wind patterns in the Dampier Archipelago are strongly influenced by seasonal meteorological conditions; however, as these conditions do not fall neatly into the conventional seasons and as there is variation from year to year they will be discussed with reference to observed occurrence.

September-February. During this period, the belt of high pressure systems is located to the south, and monsoonal depressions generate winds with a strong westerly component (September to February 1982-83, Fig. 2.2). The prevailing pattern of these winds was typified by December records for 1982 (Fig. 2.2 and 2.3), in which 80% of the wind contained a westerly component. Superimposed upon this pattern, generated by the monsoons, were diurnal land/sea breezes, which enhanced wind speed during the afternoon and reduced it during the night and early morning (Fig. 2.3).

Wind speeds were generally high during these months, with 34% at 7.5 ms^{-1} or greater. Calm periods (winds of < 0.5 ms^{-1}) were rare (Fig. 2.2). In February 1982, the westerly pattern weakened, wind direction became variable and some strong offshore breezes were experienced.

March-April. Breakdown of the monsoonal summer pattern resulted in a transition period in March and April 1982, before the influence of the northward migrating anti-cyclonic belt became dominant. This period was characterised by fluctuating winds

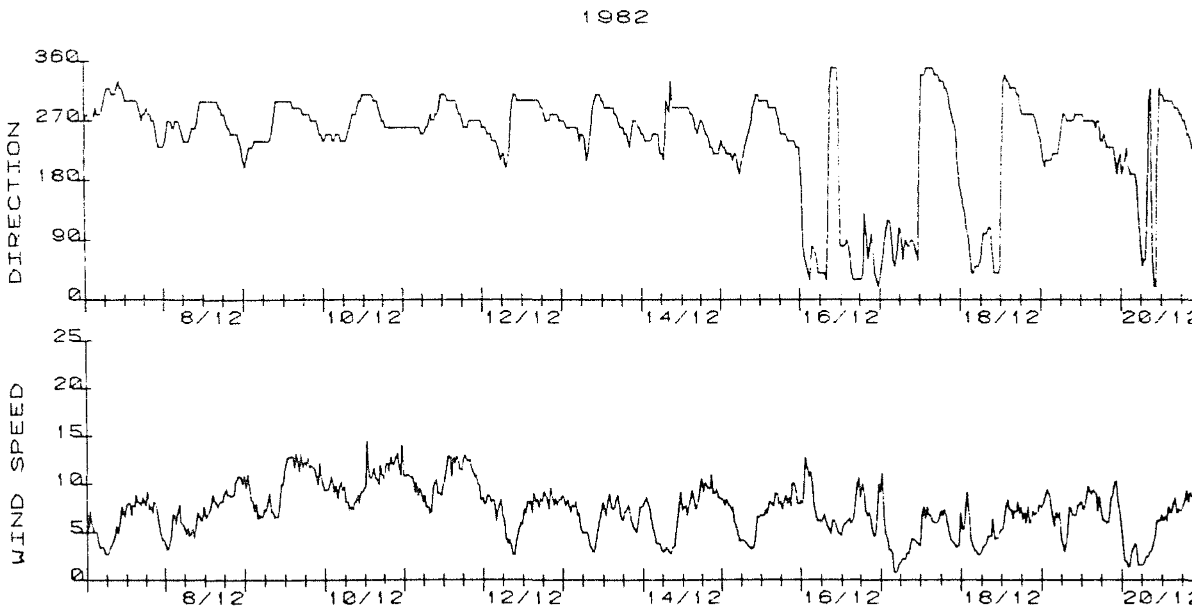

Figure 2.3 Diurnal wind patterns recorded at Conzinc Island in December 1982.

and some calm periods. April 1983, however, was dominated by strong winds with an easterly component. Hence, the timing and duration of this low energy transition period varies from year to year. Cyclonic storm events may occur in the area from November through to April, and are discussed in Section 2.4
May-July. The belt of high pressure systems moves to its most northerly extent during this period, and becomes the dominant meteorological feature of the Pilbara region (Steedman and Associates, 1982). These systems direct an easterly to southerly airstream across the Pilbara coastline. The predominant winds observed over this period, at Conzinc Island, were from the south-south-east in 1982, while the easterly component was more obvious in 1983. A diurnal land/sea breeze was again evident, reinforcing southerly to easterly winds in the morning and moderating them in the afternoon and night (Fig. 2.4). Periods of light variable winds and calms, interspersed this pattern.
August. The transition period in 1982, from the easterly to westerly pattern, was observed during August. This period was typified by light winds (only 12% were > 7.5 ms^{-1}), lacking a dominant directional component.

These conclusions concerning seasonal wind patterns in the Dampier region are consistent with those made by Woodside

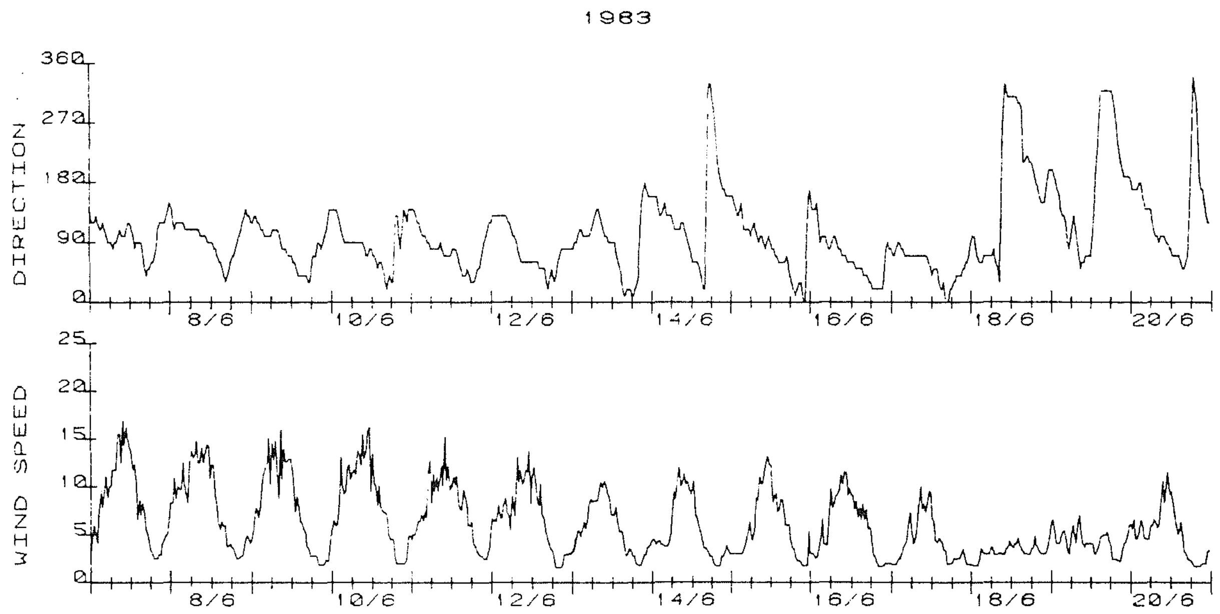

Figure 2.4 Diurnal wind patterns recorded at Conzinc Island in June 1983.

Petroleum Development Pty Ltd (1979), which collected wind data from Legendre Island (Fig. 2.1) between October 1970 and September 1971. They also analysed four to five years of wind data of Dampier Salt Pty Ltd, and from Cape Lambert (50 km east of Dampier) and Barrow Island (125 km south of Dampier).

2.3 WAVES

The transfer of energy from air to sea by surface wind stress and atomspheric pressure disturbances results in the formation of waves. Local winds generate mainly short period waves the energy of which is dependent upon the wind speed and duration, and fetch. In contrast, storm events in distant oceanic areas can generate long period waves or 'swell'. The energy of this swell in coastal waters is dependent upon the initial energy at the site of formation and the distance the swell has travelled.

Two types of oceanic storm events generate the swell which affects the coastline of the Dampier region. Tropical cyclones may form in the northern Indian Ocean from November to April, causing low pressures and above gale force winds that generate large swells; however, these events are sporadic, and the generated swell is often of short duration, although potentially significant for biotic communities and sediment distribution. In winter, storm events in the lower Indian Ocean generate swell which is attenuated into a generally low, consistent, long period waveform as it approaches the study area (Woodside Petroleum Development Pty Ltd, 1980). Winter swell is seen locally as waves breaking on Hammersley Shoal, an on Cohen, Gidley and Angel Islands (Fig. 2.1).

2.3.1 Methods

Quantitative wave data are available for the Dampier region for the period May 1980 - December 1982. These data were collected by R K Steedman and Associates for Woodside Offshore Petroleum Pty Ltd (Steedman and Associates, 1983).

Waverider buoys were located at two offshore stations, one adjacent to Legendre Island and the other near the mouth of the Hamersley Iron channel. A third buoy was placed at an inshore station, near Star Rock west of Withnell Bay (Fig. 2.1). Raw wave profiles, sampled at one second intervals for up to 20 minutes, were collected several times daily. Each of these profiles was processed and the results presented as time series of significant wave height, significant wave period, average zero crossing period and period of peak spectral ordinate. For example, Figures 2.5a and 2.5b show derived wave characteristics of the inshore and offshore sites for the months of June 1981 and March 1982.

2.3.2. Discussion

The wave data showed that significant wave heights, and therefore wave energy densities, were consistently higher at the offshore sites than at the site within Mermaid Sound (Figs. 2.5a and 2.5b).

In Chapter 5, the degree of correlation between measures of wave energy and trapped suspended matter is assessed. As measurements of suspended matter were those of loads accumulated over periods of the order of one month, the

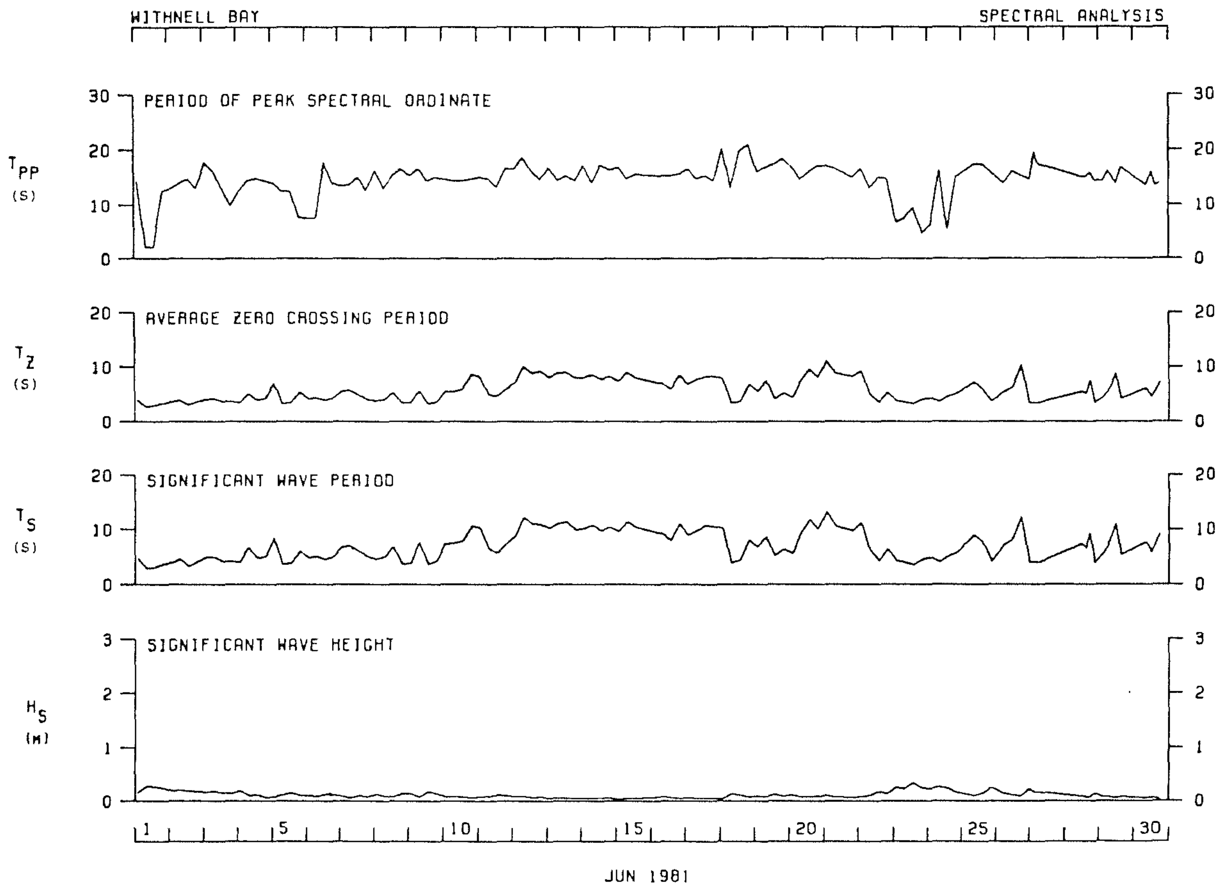

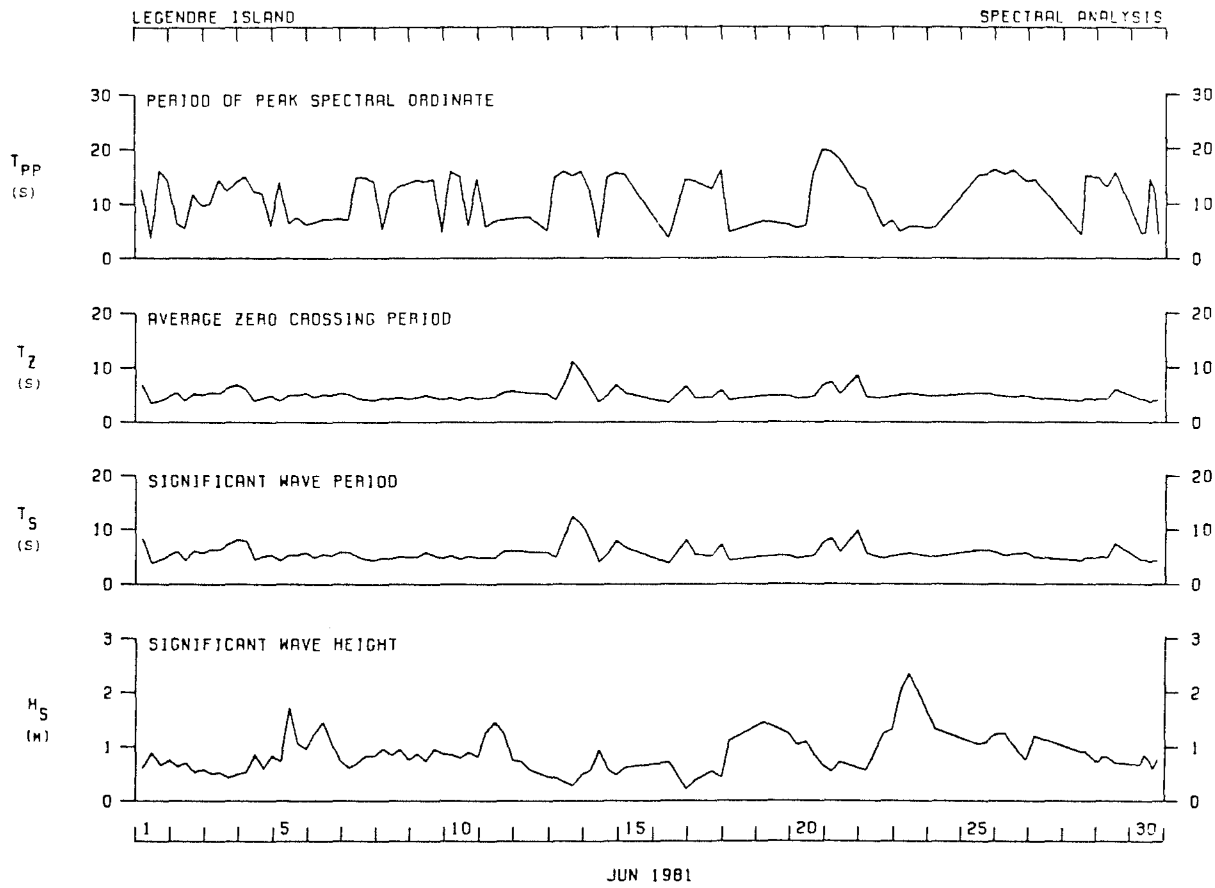

Figure 2.5a Spectral analysis of waverider buoy data from near Withnell Bay and Legendre Island, June 1981. (Data from R.K. Steedman and Associates, 1983.)

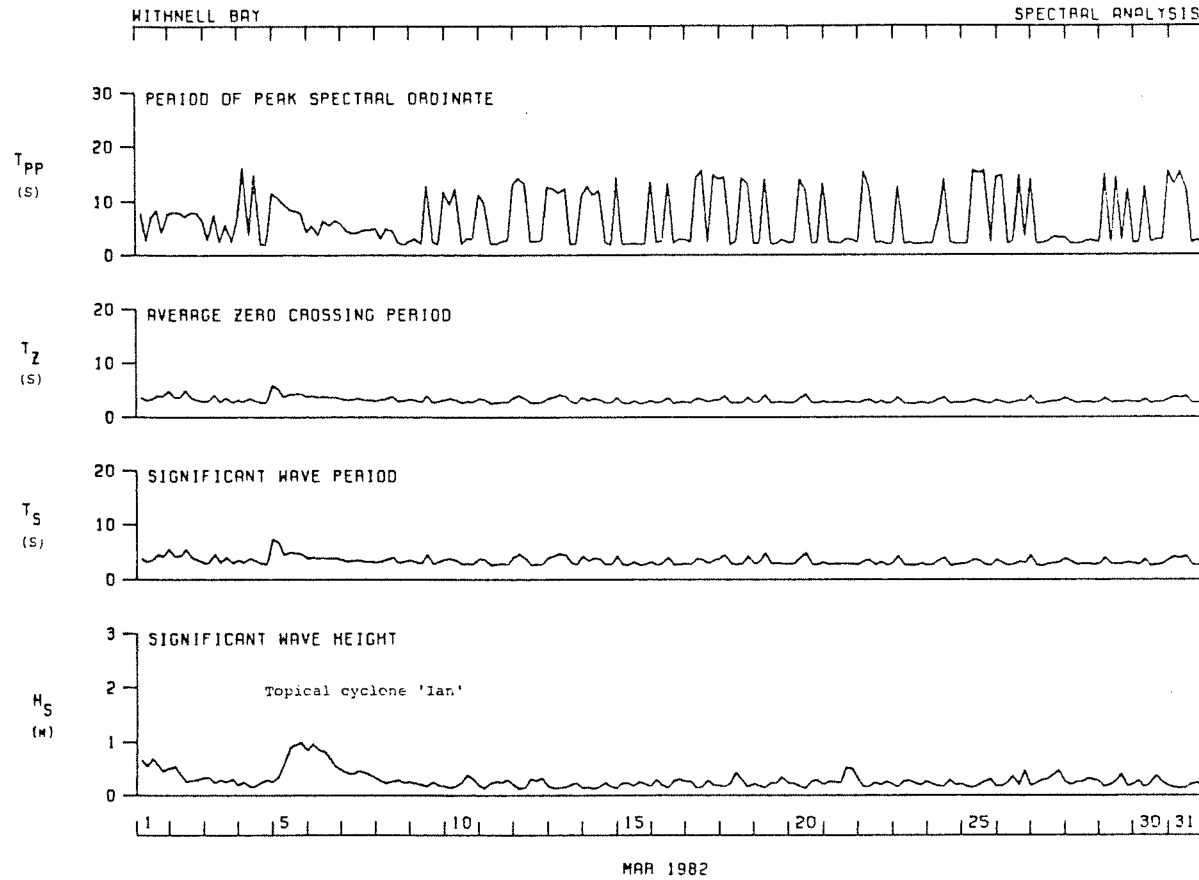

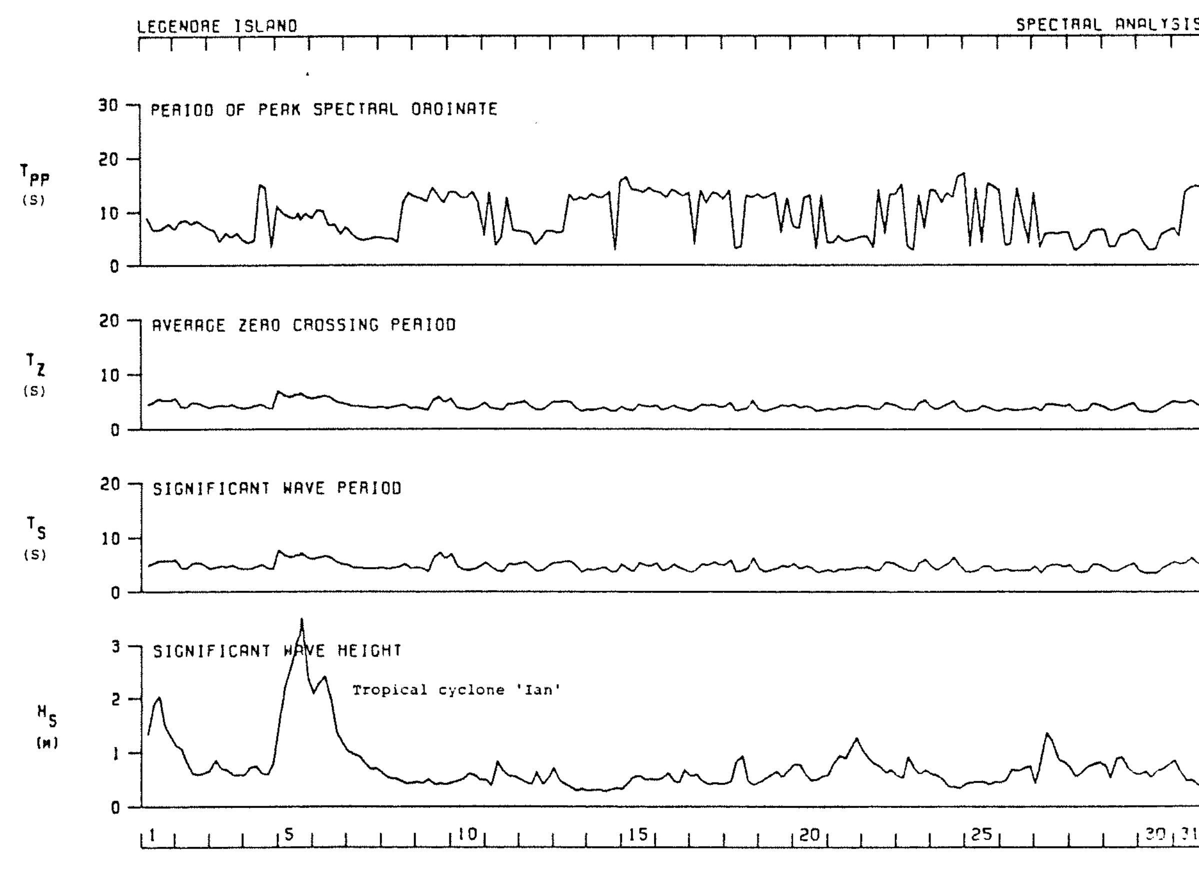

Figure 2.5b Spectral analysis of waverider buoy data from near Withnell Bay and Legendre Island, March 1982. (Data from R.K. Steedman and Associates, 1983.)

following procedure was adopted to obtain an **index of wave energy** over the corresponding periods:

Monthly means of significant wave heights were derived from data presented in Steedman and Associates (1983) and these means inserted into a theoretical expression for specific wave energy (US Army Coastal Engineering Research Centre, 1975):

$$E = \frac{\rho g h^2}{8}$$

Where ρ = density of seawater
g = gravitational acceleration
h = significant wave height

The specific wave energy is the wave energy contained in a water column with a base of 1 sq. m., given a train of sinusoidal waves.

From the calculated data presented in Table 2.1, the index of wave energy is seen to be 6-64 times greater at the outer stations than the inner one. The difference is caused largely

Table 2.1 Monthly mean of significant wave heights and wave periods, and monthly index of specific wave energy, derived from waverider data for inshore and offshore sites.

Date	Location	Monthly mean of significant wave heights (m)	Monthly mean of significant wave periods (m)	Monthly index of specific wave energy (Jm^{-2})	Energy Ratio (outer:inner)
Nov. 1980	O[1]	0.70	4.2	616	6:1
Nov. 1980	I	0.28	2.8	98	
May 1981	O[2]	0.82	4.8	850	14:1
May 1981	I	0.22	3.6	60	
June 1981	O[2]	0.78	5.2	768	64:1
June 1981	I	0.10	5.8	12	
July 1981	O[2]	1.03	4.7	1 334	33:1
July 1981	I	0.18	4.6	40	
Sept. 1981	O[2]	0.93	5.8	1 088	18:1
Sept. 1981	I	0.22	3.7	60	
Oct. 1981	O[2]	0.77	5.5	746	16:1
Oct. 1981	I	0.19	3.2	46	
Feb. 1982	O[2]	0.76	4.0	726	7:1
Feb. 1982	I	0.29	2.8	106	
Mar. 1982	O[2]	0.67	4.0	564	10:1
Mar. 1982	I	0.21	2.3	56	
Apr. 1982	O[2]	0.47	4.4	278	9:1
Apr. 1982	I	0.16	3.1	32	

Waverider data from RK Steedman and Associates, 1983
O[1] - Offshore Site 1 - near Legendre Island)Outside Dampier
O[2] - Offshore Site 2 - near mouth of Hamersley Iron channel)Archipelago
I - Inshore site - near Withnell Bay - Inside Dampier Archipelago

by the geometry of Mermaid Sound, with a long axis in a north-south direction (Fig. 2.1), while the predominant wind directions are from the east or west. The Withnell Bay site (Fig. 2.1) is also protected from the persistent winter swell, which approaches the Archipelago from a west north-westerly direction.

Wave energy is lost between the outer and inner sites through dissipation by bottom friction, involving the movement of sediments, and the breaking of waves on the shallow outer reefs and islands (Fig. 2.1).

2.4 TROPICAL CYCLONES IN THE DAMPIER REGION

Cyclones are the most energetic events to affect tropical regions. These are clockwise rotational (southern hemisphere), low-pressure systems of tropical origin, with winds of at least gale force (18 ms^{-1}) near the centre. The energy is derived mainly from surface water temperature, and from heat released when oceanic water vapour condenses to form clouds. Tropical cyclones therefore occur when water temperature is highest and affect the Pilbara coastline predominantly between December and April (Lourensz, 1981). Reliable records of cyclone occurrences and trajectories have been kept since 1959, and in the 21 years to 1980 ten cyclones passed within 150 km of Dampier (Lourensz, 1981).

An indication of the wave energy generated by cyclones can be gained from observations of storm damage to coral reefs in the Dampier Archipelago following cyclones passing within 150 km.

2.4.1 Cyclone events

Tropical cyclone 'Trixie'. Tropical cyclone 'Trixie' formed on 15 February 1975 and passed through the Dampier Archipelago on 18 February, before crossing the coast at Onslow, 180 km south-west of Dampier, on 19 February (Fig. 2.6). This very severe cyclone had a minimum pressure of 925 mb and maximum recorded

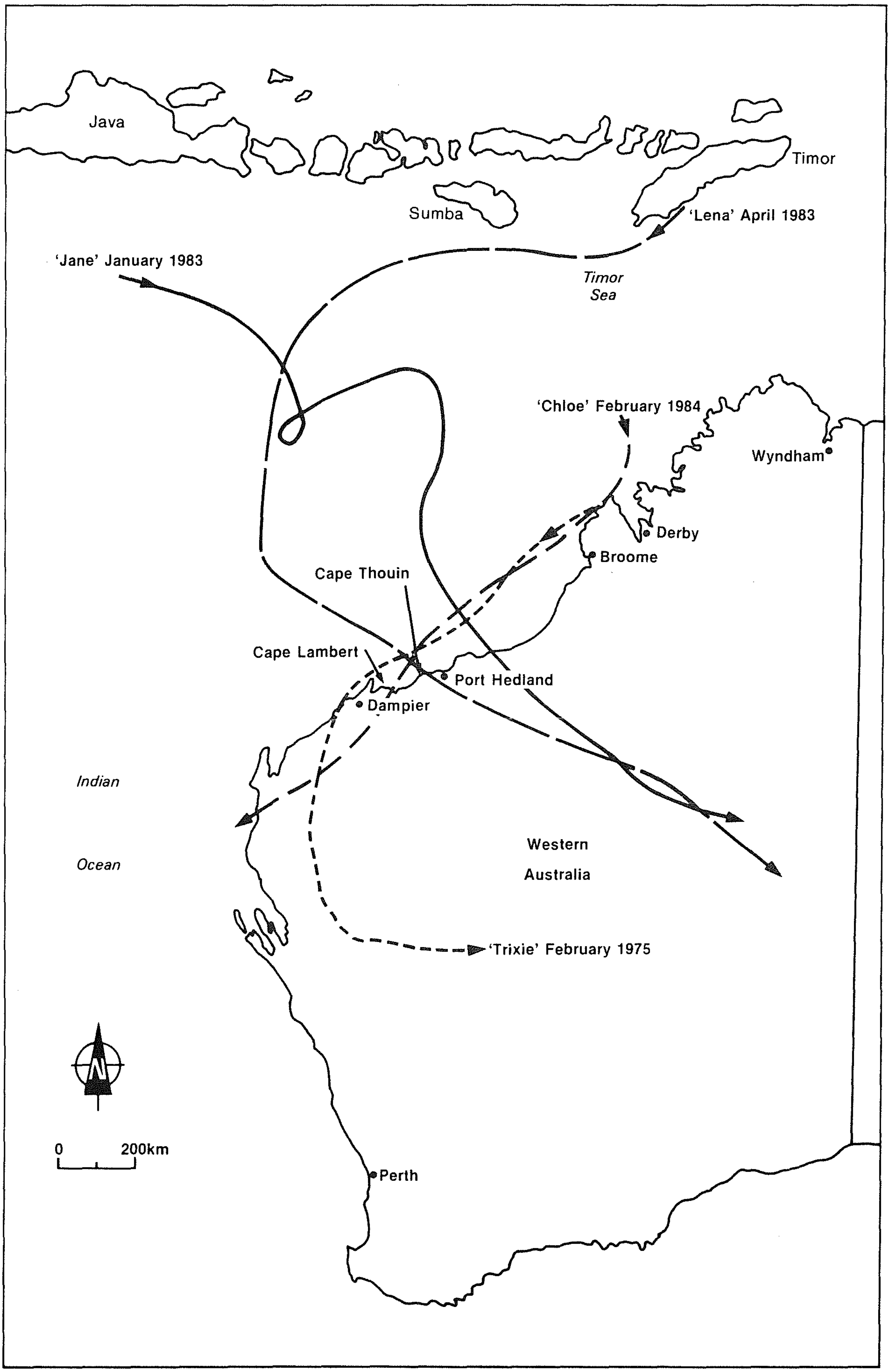

Figure 2.6 Trajectories of tropical cyclones 'Trixie', 'Jane', 'Lena' and 'Chloe'.

winds (ten min mean value) of 52.8 ms^{-1} (190 kmh^{-1}). At Dampier, the maximum gust was 63.9 ms^{-1} (120 kmh^{-1}), and for eight hours the wind was in excess of 25 ms^{-1} (90 kmh^{-1}). A peak gust of 68.9 ms^{-1} (248 kmh^{-1}) at Onslow, from 'Trixie', is the highest cyclonic wind speed recorded for Australia.

The Western Australian Museum conducted surveys of coral reefs in the Dampier Archipelago, with particular emphasis on those near Kendrew Island (Fig. 2.1), between 1972 and 1974. In 1978, it was found that the previously rich coral reefs near Kendrew Island had been markedly disturbed. This was attributed to a combination of 'Trixie' and a population increase of the crown of thorns, starfish, *Acanthaster planci* (Marsh, 1978). Two massive coral colonies *(Platygyra sinensis)*, each about 1 m diameter and observed alive on the reef flat in 1974, were found on the beach in 1978 (Marsh, pers. comm., 1981). Investigation of the Angel Island and Conzinc Island communities in 1978 revealed signs of storm damage, also possibly caused by 'Trixie' (Marsh, pers. comm., 1984).

Tropical cyclone 'Jane'. Tropical cyclone 'Jane' formed on 5 January 1983, 800 km north-west of Port Hedland, and crossed the coast at Pardoo, 270 km north-east of Dampier on 9 January (Fig. 2.6). This severe cyclone had a minimum pressure of 955 mb and winds of 38.6 ms^{-1} (139 kmh^{-1}) recorded at Port Hedland. Winds at the Conzinc Island anemometer site (Fig. 2.1) increased from 8 ms^{-1} (29 kmh^{-1}) to 22 ms^{-1} (80 kmh^{-1}) over 30 h, and were maintained at that speed for 18 h, before rapidly returning to about 8 ms^{-1} (29 kmh^{-1}). The strong winds at Dampier were from an easterly, turning to southerly, direction because the cyclone, which had a clockwise rotation, crossed the coast north-east of Dampier. Effects on the coral reefs of Nelson Rocks were evident. Massive corals *(Porites sp)* were broken from the bottom, and rolled over the more fragile branching corals such as *Acropora formosa*. Tubular corals (e.g. *A. hyacinthus)* of up to 1.5 m diameter had been overturned, and others growing on large coral heads 1.5 m from the bottom had old coral debris trapped on them. Despite the immediate mechanical damage which generated calcareous rubble and sediment, new coral growth had re-established within three months.

Tropical cyclone 'Lena'. Tropical cyclone 'Lena' formed on 5 April 1983, 850 km north north-west of Port Hedland, and crossed the coast at Cape Flourin, 120 km north-east of Dampier on 8 April (Fig 2.6). This much less intense cyclone had a minimum pressure of 994.5 mb, and winds of 42.5 ms^{-1} (153 kmh^{-1}) at Port Hedland. An anemometer positioned on the Woodside Petroleum Development Pty Ltd test pile near Withnell Bay (Fig. 2.1) recorded no winds in excess of 10 ms^{-1} (36 kmh^{-1}). Inspection of the reefs at Nelson Rocks affected by cyclone 'Jane', showed no visible damage after 'Lena'.

Tropical cyclone 'Chloe'. Tropical cyclone 'Chloe' formed on 26 February 1984, 300 km north of Derby, and crossed the coast at Cape Lambert, 50 km east of Dampier (Fig, 2.6). This intense cyclone had a minimum pressure of 962 mb, winds of 41.7 ms^{-1} (150 kmh^{-1}), and gusts of 61.1 ms^{-1} (220 kmh^{-1}), recorded at Cape Lambert. Instrument failure prevented the Bureau of Meteorology from gaining accurate wind strengths at Dampier; however, at 2400 h on 28 February, the wind was reported at 17 ms^{-1} (61 kmh^{-1}). At 0913 h on 29 February, gusts of 42 ms^{-1} (151 kmh^{-1}) were reported, and at 0500 h on 1 March of 15 ms^{-1} (54 kmh^{-1}) were being experienced. These winds, like those of 'Jane', were from an easterly turning southerly direction. The net effects on the reefs at Nelson Rocks appeared to be negligible, with no observed damage, and, apparently, little generation of new calcareous sediments.

2.4.2 Discussion

Tropical cyclone'Trixie' has had marked, and possibly long-term, effects on marine communities of the Dampier Archipelago. The full extent of these effects is unknown. Independent investigation in 1983 by Veron (Australian Institute of Marine Science) failed to find any developed coral communities, or the remains of dead ones on Sailfish Reef (Veron, pers. comm., 1984). Therefore, it seems likely that the coral communities, which were present on that reef in 1974, were destroyed by either 'Trixie' or by a combination of 'Trixie' and the crown of thorns starfish, *Acanthaster planci*. The calcareous remains of those corals may have been removed by 'Trixie', or subsequent wave action and contributed to the sediments of the area. A report of an apparent increase in coral rubble on the Kendrew Island reef flat in 1978, over that observed in 1974 (Marsh, per. comm., 1984), indicates that some of the broken coral was washed into the shallow areas.

This obvious damage to the coral reefs is a result of the wave energy associated with cyclone 'Trixie'. Winds from 'Trixie' are the strongest recorded in the area, and, additionally, the cyclone's path would have maximised the effect of the winds upon the Archipelago. Passing through the Archipelago and moving parallel to the coast, the cyclone generated winds perpendicular to the coastline. The outer areas, including Kendrew Island and Sailfish Reef, are unprotected from wind-induced waves with northerly components, such as those caused by 'Trixie'.

In contrast, tropical cyclones 'Jane', 'Lena', and 'Chloe' all crossed the coast to the north-east of the Archipelago, before dissipating in the hinterland. 'Lena' was not a severe cyclone, did not cause strong winds at Dampier and caused no observed effects on the local marine communities.

Tropical cyclones 'Jane' and 'Chloe' were intense and both generated winds of similar direction. Those from 'Chloe' were more intense at Dampier. The negligible effects from 'Chloe' indicate that damage to the biota by 'Jane' was not caused by the local wind conditions. The major difference between these two cyclones was the area of origin: 'Jane' formed north-west of Dampier, while 'Chloe' formed to the north-east. The Archipelago would, therefore, have been affected by swell energy from 'Jane', while swell from 'Chloe' would have affected the eastern shores of Dolphin Island and the Burrup Peninsula (Fig. 2.1).

2.4.3 Conclusions

Tropical cyclones form high energy, locally generated waves, and also trains of swell wind waves. Both of these wave types have affected the Dampier Archipelago, and may result in catastrophic disturbance of the benthos. The destruction of calcareous structures, such as corals, results in the formation of calcareous rubble and sediments.

The effect a cyclone has upon the Archipelago is dependent upon the intensity of the cyclone and the approach direction. Cyclones which pass to seaward of, and close to, the Archipelago are the most disruptive of Archipelago marine communities.

3. WATER MOVEMENT

3.1 INTRODUCTION

Water movement and circulation in and around the Dampier Archipelago is influenced by tides, wind, cyclonic activity, regional continental shelf currents and seasonal formation of water density structure.

Areas of strong and weak currents are identified. The maxima are generally associated with peak spring tides, and occasionally with extreme wind conditions. The longer-term circulation of water through the Archipelago is thought to be determined principally by seasonal winds (Chapter 2).

In addition to the referenced sources, the information presented here is derived from field measurements of water currents, water temperature and salinity conducted by the Department of Conservation and Environment.

3.2 METHODS: CURRENT MEASUREMENT

Neil Brown acoustic current meters were mounted on tautline, U-shaped moorings or suspended from bottom-resting tripods (Fig. 3.1). Deployment periods ranged from ten days to three months. Trivane drogues of area 3.5 m^2 and minimal windage were tracked using standard surveying techniques. Temperature-salinity measurements were made with a Yeo-kal Autolab Portable Salinity-Temperature Bridge, Model 602.

A two dimensional numerical hydrodynamic model (Mills, 1985) was applied to the western Archipelago. Simulations were made of spring tidal currents, wind-driven flows and the flushing of coastal basins by continental shelf current through-flow.

Geographical names and instrument locations referred to in this chapter are shown in Figure 3.1.

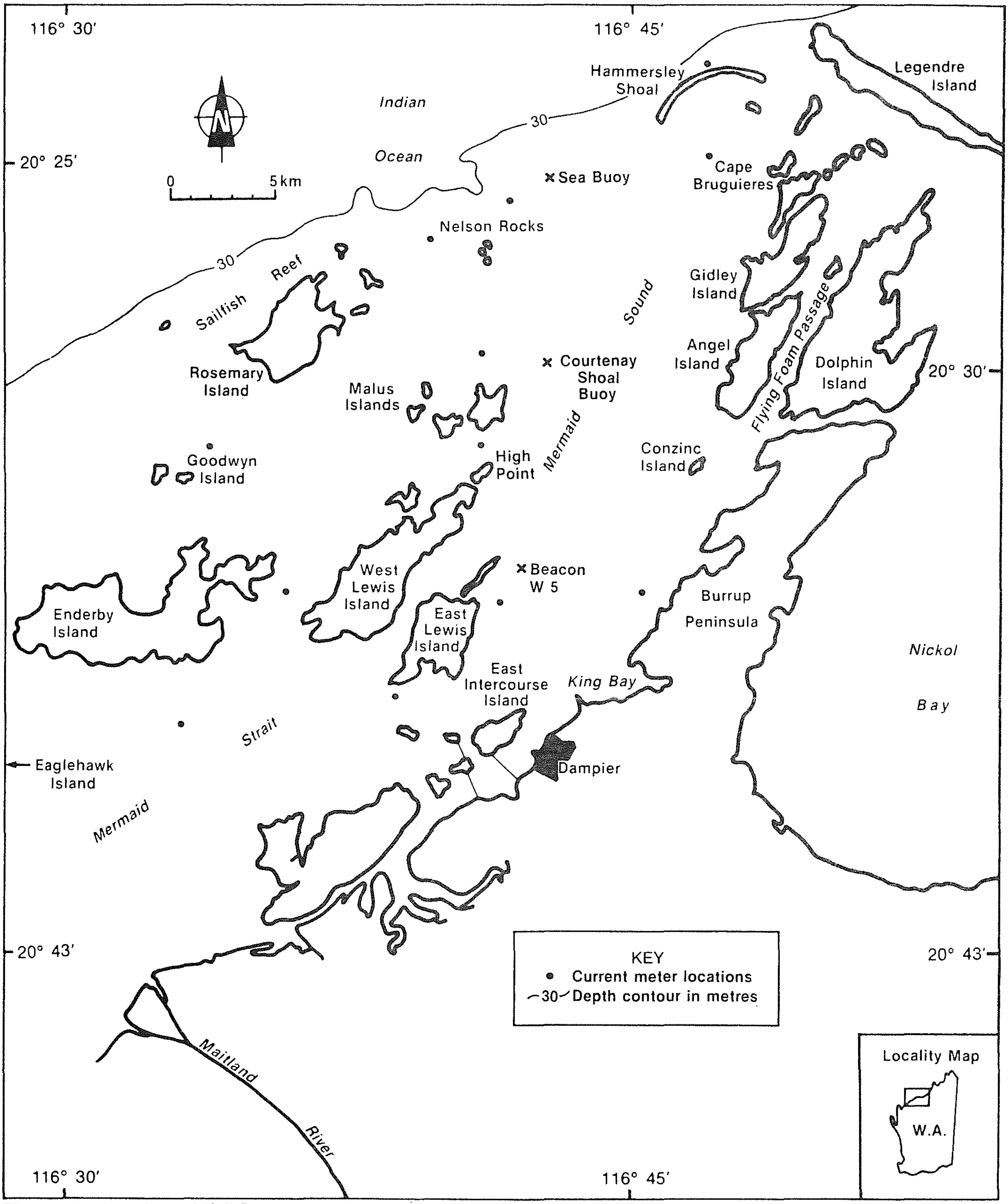

Figure 3.1 Locations of Neil Brown acoustic current meters.

3.3 RESULTS

3.3.1 Tidal currents

The dominant tides of the North-West Shelf are semi-diurnal. Within Mermaid Sound, the mean spring range of the tide is 3.52 m and the mean neap range is 0.93 m (derived from harmonic analysis of one year's tide heights at Withnell Bay, Public Works Department, W.A.: unpublished).

The semi-diurnal tidal currents contribute most to the total instantaneous water movements in the region. However, since these currents reverse direction twice every tidal cycle, they advect water particles less than about 10 km, which is much less than the length of the Archipelago (≃ 60 km).

The modelled peak ebb current velocity field for a mean spring tidal range is depicted in Figure 3.2. The distribution of the peak flood currents is very similar, except reversed in direction.

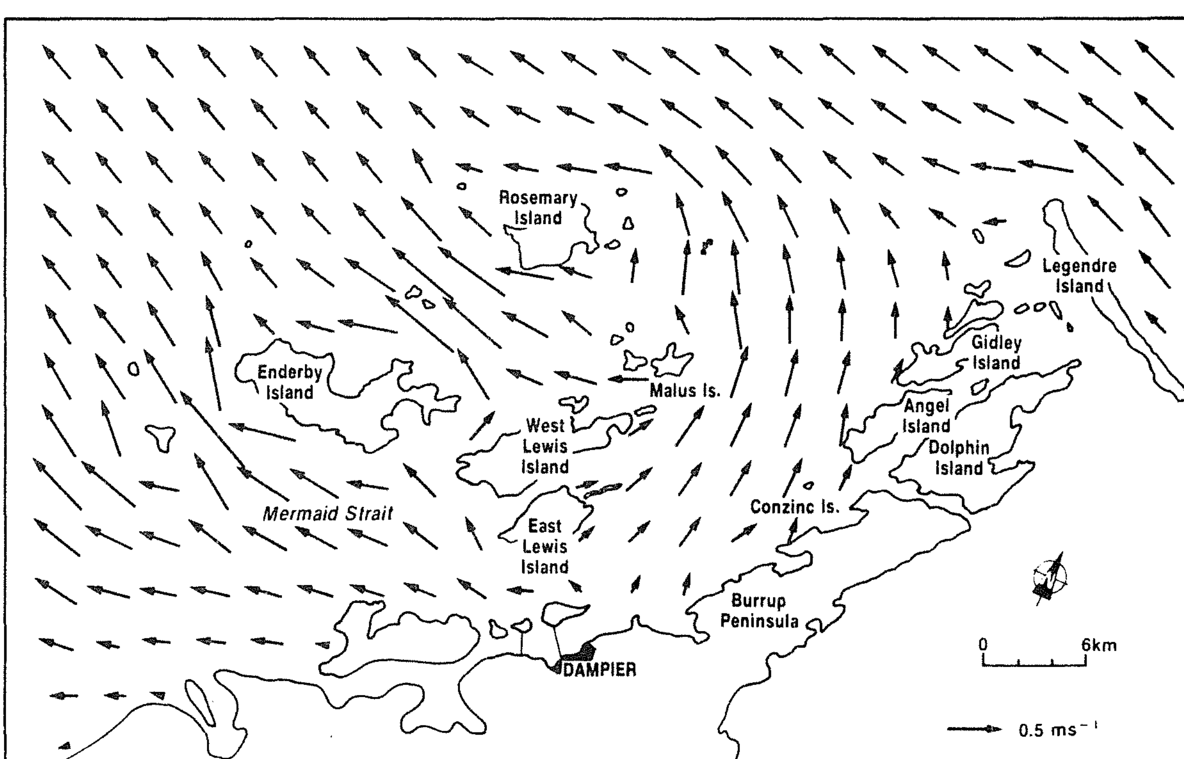

Figure 3.2 Computer model simulation of spring ebb tidal currents, Dampier Archipelago (adapted from Mills, 1985).

On the inner continental shelf, in water depths of about 40 m, the direction of peak ebb current is about 300^0, and that of peak flood about 120^0. The tidal currents deviate little entering and leaving Mermaid Strait and the area between Rosemary Island and Enderby Island. However, the water is forced to turn almost perpendicular as it flows into and out of Mermaid Sound.

The areas of strongest tidal current are generally found toward the outer extremities of the Archipelago and occur when the water level is falling or rising most rapidly.

Immediately north of Cape Legendre, peak spring tidal currents reach 0.5 - 0.6 ms^{-1}. Along the seaward reaches of the Hamersley Iron shipping channel, from Courtenay Buoy to Sea Buoy, peak spring tidal currents are in excess of 0.4 ms^{-1} and at times exceed 0.5 ms^{-1}. The currents over the shallow reef crest and reef flats immediately west of Nelson Rocks have similar speeds. Passing to the north-eastern side of Goodwyn Island is a deep channel which has tidal flow speeds of up to 0.7 - 0.8 ms^{-1}. Comparable speeds are achieved in the channel between Eaglehawk Island and Enderby Island. Tidal speeds of up to 0.5 ms^{-1} may occur in the vicinity of Southwest Reef.

Some of the inter-island channels are also subject to strong flows; for example, Flying Foam Passage. The few current measurements that have been made in this channel suggest that peak spring tidal flows exceed 2 ms^{-1}. The current floods northwards and ebbs to the south. Spring tidal excursions along this channel may be large enough to exchange Nickol Bay and Mermaid Sound waters. The tidal current regime of Mermaid Sound is influenced up to at least 5 km from the southern opening of Flying Foam Passage. At a location 1 km north of Conzinc Island, and 3 km due west of the Passage mouth, peak ebb velocity on spring tides is north-west at about 0.5 ms^{-1}, whereas the corresponding flood velocity to the south south-east does not exceed 0.25 ms^{-1} (Woodside Petroleum Development, 1979). This energetic, directionally-biased current regime is likely to have a significant influence on sediment transport.

In the channel between West Lewis Island and Enderby Island, maximum tidal currents reach 0.6 ms^{-1}. Between Malus Islands and High Point, spring tidal currents of 0.45 ms^{-1} are attained.

The localities described above experience strong tidal currents; however, equally significant to sediment transport and deposition are regions with low current velocities. Some of these are located adjacent to areas with high water current flow.

Weak tidal streams, that rarely exceed 0.2 ms^{-1}, occur to the south-west of Cape Legendre, on and inside Hammersley Shoal. Along the northern side of Malus Islands, and between the north-western end of this island group and Rosemary Island, peak spring tidal currents rarely exceed 0.2 ms^{-1}. Similarly, weak tidal currents occur in an area between the south-western shore of Goodwyn Island and the northern shore of Enderby Island. The inner reaches of Mermaid Sound and Mermaid Strait undergo weak tidal oscillations with speeds of up to 0.2 ms^{-1}; however, tidal currents strengthen in the main channel connecting these two water expanses, with peak currents occurring close to times of high and low water.

Residual water movement associated with the tidal streams is generally low: of the order of 0.01 ms^{-1}. A notable exception to this is the previously-described, directionally-biased regime occurring within, and adjacent to, the Flying Foam Passage.

3.3.2 Local wind-driven currents

Locally occurring wind modifies the motion of the Archipelago waters, first in a thin surface layer, and after several hours within the entire water body. Elevations or depressions of water level adjacent to coastlines give rise to water surface slopes and pressure gradient forces. These, in conjunction with the applied wind stress and bottom friction stress, determine the resultant wind-induced transport.

Wind-driven model simulations and current meter measurements (Woodside Petroleum Development 1979; Lawson and Treloar, 1981; Mills, Department of Conservation and Environment, unpublished data) suggest the existence of two main modes of wind-driven circulation.

Prevailing spring and summer winds from the south and west drive water eastward through Mermaid Strait and between Rosemary and Enderby Islands, while water in Mermaid Sound is forced northwards towards the seaward entrance.

Easterly and northerly winds induce southward flow into and through Mermaid Sound and drive water westward in between the islands of the Archipelago. These winds may occur occasionally in association with cyclones during summer and autumn, or as a winter pattern of diurnally fluctuating winds (Chapter 2).

Examination of current meter records shows that the effect of wind stress on water movement is most marked about times of neap tide. This is partly a relative effect, owing to the weakness of the neap tidal currents; however, the energy imparted by wind to water is more efficiently transformed into advective kinetic energy at times of neap tides, when the flow less turbulent and energy dissipation, by bottom friction, occurs at a lesser rate.

Strong (>10 ms^{-1}) persistent winds enhance peak spring tidal currents by 0.5 to 0.1 ms^{-1} (Lawson and Treloar, 1981). Moderate to strong persistent winds (>10 ms^{-1}) distort or completely nullifye the neap tidal current reversals, resulting in a large net excursion of water with peak speed of about 0.2 ms^{-1} DCE current records).

As examples of extreme forcing, the passages of tropical cyclones 'Ian' and 'Jane' near the Archipelago, in March 1982 and January 1983 respectively, were examined. 'Ian' brought southerly winds > 20 ms^{-1} (72 kmh^{-1}) on 5 March, before slowly swinging northerly and moderating to 7 ms^{-1} (25.2 kmh^{-1}) by 8 March. Currents recorded 2 m above the sea-floor, in the 18 m (depth) channel between Malus Island and West Lewis Island, flowed consistently to the west for 36 h, before turning east for a further 12 h. Current speeds peaked at 0.4 ms^{-1} in both directions and the net current run was 18.2 km to the west. This event occurred within a few days of neap tides.

The winds during 'Jane' were initially east-north-east at 10 ms^{-1} (36 kmh^{-1}) on 7 January, before increasing to more than 20 ms^{-1} (72 kmh^{-1}) two days later. Currents recorded 4 m above the sea-floor near the shipping Beacon W5, initially flowed south for 46 h, followed by a 26 h northerly reversal. Current speeds of about 0.35 ms^{-1} were recorded in both directions, and the net current run was 16.6 km. As on the previous occasion, these abnormal currents were measured within a few days of neap tides.

3.3.3 Large-scale continental shelf currents

These currents are thought to be driven principally by a persistent sea level gradient along the Western Australian coastline (Godfrey & Ridgway, 1984). Holloway & Nye (1984), gave monthly averages of currents measured at several locations on the southern part of the North-West Shelf during 1982-83. The most significant feature was a south-west flowing current (thought to be part of the Leeuwin Current) of greatest strength and duration from February to July. Weakening or short-term reversals of the current may occur during periods of strong south-westerly winds. On the inner shelf, the flow regime is expected to be similar, with monthly speeds of 0.01-0.1 ms^{-1} and a predominantly westerly flow; however, the frequency and duration of wind-driven reversals is likely to be greater than for the outer shelf.

Numerical model simulations, assuming a steady long-shore pressure gradient to drive shelf currents, suggest that the Dampier Archipelago waters are partially sheltered from the influence of currents on the shelf. The model predicted that water flows through the inner portion of Mermaid Sound at reduced speeds; less than 25% of the current speeds on the shelf.

3.3.4 Density effects

Seasonal variation in air temperature, combined with annual excess of potential evaporation over rainfall in the Dampier region, results in spatial and temporal variations in the hydrological structure of the Archipelago. From April to August, waters near the mainland are both cooler and more saline than those offshore (Fig. 3.3). This denser, inner water leaves the Sound as near-bottom gravity flow along the deepest parts of the outer bathymetry, moving counter to a wind-induced inflow of surface water.

During October to March, the inner water is more saline but warmer than the offshore waters (Fig. 3.3), which display a density structure more typical of that below the seasonal continental shelf thermocline. The prevailing south-west winds of this period force the inner water toward the northern and seaward boundaries of the Sound, leaving as a low density surface layer.

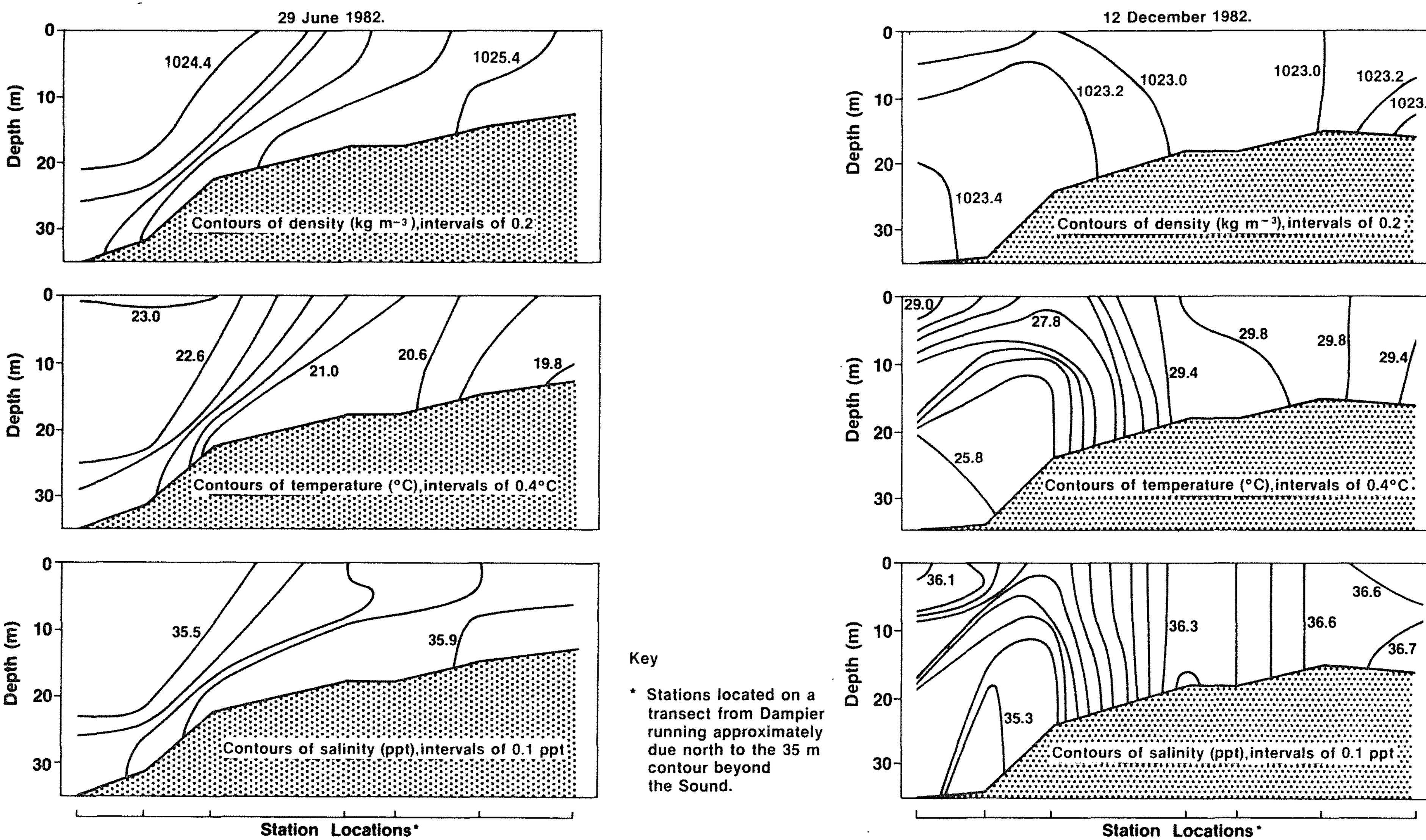

Figure 3.3 Hydrographic sections through Mermaid Sound showing density, temperature and salinity contours.

4. LIGHT ATTENUATION

4.1 INTRODUCTION

Vertical attenuation of light through water is caused by a combination of absorption and scattering processes. Water alone absorbs and reflects light, but these effects are greatly enhanced by suspended phytoplankton, inanimate particulate matter and dissolved coloured material (Kirk, 1981). Dissolved coloured material has been assumed unimportant in Dampier Archipelago waters, as that of freshwater origin (eg humic substances) flocculates and precipitates under marine conditions (Duinker, 1980).

Suspended material indirectly affects marine communities by increasing light attenuation, which limits primary production. Light levels limit the depths to which benthic primary producers may occur (Chapman & Chapman, 1973). Limited light may be the reason why macroalgae and many coral species of the Archipelago have ranges confined to the shallows (Woodside Petroleum Development, 1979).

At present, the light requirements of the Archipelago's primary producers are unknown. Recent research has shown that primary producers in marine environments display photoadaptations similar to those found in terrestrial plants. For example, corals on the Great Barrier Reef have been shown to be adapted to either high (300 μ Einsteins m^{-2} s^{-1}) or low (100 μ Einsteins m^{-2} s^{-1})light levels (Chalker et al, 1983). Photo-adaptions have also been found amongst the algae, with ranges of 50-200 and 500-1000 μ Einsteins m^{-2} s^{-1}reported for shade and sun loving species respectively (Raven & Glidewell, 1975). Less is known of the light requirements of *Sargassum* and *Caulerpa* species, the principal macroalgal species in the Archipelago (Borowitzka, personal communication, 1984). Larkum (1983) reports that neither the photosynthetic capacity nor the contribution made to primary productivity, by these plants, is known.

In addition to this indirect effect of light attenuation, the physical presence of suspended material can directly affect biota. Filter-feeding organisms are dependent upon suspended organic matter for food; however, suspended matter can have adverse effects on biota. For example, certain corals are susceptible to excessive sediment load. Lasker (1980) noted three mechanisms by which coral growth is affected by suspended sediment:

(i) Planula settlement is prevented by sediment inundation of suitable substrates.

(ii) Coral growth is inhibited by settling sediment because sediment rejection requires energy.

(iii) Rapid settlement of suspended material can cause inundation and suffocation of coral colonies.

These adverse effects are not limited to corals. Bakus (1969) refers to suspended material stressing both sponges and ascidians by burial, canal clogging and chamber clogging.

This chapter, however, will be limited to the relationship between light attenuation and suspended solids, and spatial and temporal variation in light attenuation within Mermaid Sound.

4.2 MATERIALS AND METHODS

To determine the experimental error in the estimation of suspended mass and organic content, a series of ten water sample replicates were collected in August 1982. Some 50 litres of water were collected from near Nelson Rocks, divided into 5 litre subsamples, filtered, frozen and subsequently analysed. To assess the relationship between suspended matter and vertical light attenuation, a series of water samples were taken in conjunction with light attenuation profiles in March and December, 1983. In March, 15 samples were taken from seven sites at a depth of 1-2 m, and another 1-2 m sample was taken simultaneously with a 4-5 m sample at Nelson Rocks. In December, 11 samples were taken from three sites at two depths, namely, 1-2 m and 7-8 m (Fig. 4.1).

Water samples were taken in March 1983 using a 5 litre Niscan sampling bottle at 1-2 m depth. Three litres were used for assessment of suspended load and organic content, while the remaining 2 litres were used for chlorophyll a and phaeophytin determination.

The 3 litre samples were filtered through pre-combusted, pre-weighed glass fibre filters of pore size 0.8-1.2 micron. Following filtration, the filters were rinsed with about 100 ml of deionized water, to remove any salt residues, and frozen.

Samples were later dried to constant weight in a 120^{o}C constant temperature oven, before being weighed to 0.00001 g on a Sartorius digital balance (model 2004 MP6). Organic weight of the filtrate was determined by loss on ignition after heating at 600^{o}C for 90 min in a muffle furnace (Kiln Manufacturers, WA: model LFB-14). To prevent contamination from condensation, the filters were cooled on all occasions in a desiccator prior to weighing.

The 2 litre samples were filtered through identical, but untreated, filters and frozen prior to analysis for chlorophyll a and phaeophytin pigments using acetone extraction method (Strickland & Parsons, 1972).

The light profiles done in conjunction with the sampling for suspended matter were determined using a Licor-188B integrating quantum meter, fitted with a Licor-192S underwater quantum sensor, measuring the photosynthetic photon flux density (PPFD) in the 400-700 μm range. Light intensity readings were taken at 1 m intervals, starting at 1 m depth. An above-surface reference reading was also taken.

The attenuation of PPFD is approximated by the equation

$$Q = Q_0 e^{-ukz}$$

where Q and Q_0 are the downward photon flux in the photosynthetic waveband at depth z metres and at the surface respectively and where k is the (natural logarithm) vertical light attenuation coefficient (units are in quanta $m^{-2}s^{-1}$; Kirk, 1977). The vertical attenuation of light through natural waters with depth is therefore approximately exponential. On this basis, attenuation coefficients were calculated by regressing the natural logarithm of the PPFD against depth, the slope of the line being the vertical light attenuation coefficient. This attenuation coefficient was used as an index of turbidity and compared with the suspended loads obtained using the filtration method.

A separate series of light profiles were taken at 23 sites, extending from the headwaters of the Sound to a site 7.5 km north of Sea Buoy (Fig. 4.1), on six occasions between April 1982 and March 1983. Temperature and salinity profiles were taken in conjunction with these, using a Yeo-Kal Autolab Portable Salinity-Temperature Bridge, Model 602 (Chapter 3). Readings were taken between 0930 h and 1630 h, during neap tide and on cloudless days in order to minimise environmental variables (Kirk, 1977).

The attenuation coeffients calculated from these profiles were plotted using a contouring computer package (SYMAPS) and then examined for spatial and temporal variation.

A further set of seven light profiles was taken at approximately hourly intervals between 0920 h and 1500 h at Nelson Rocks on 28 June 1982.

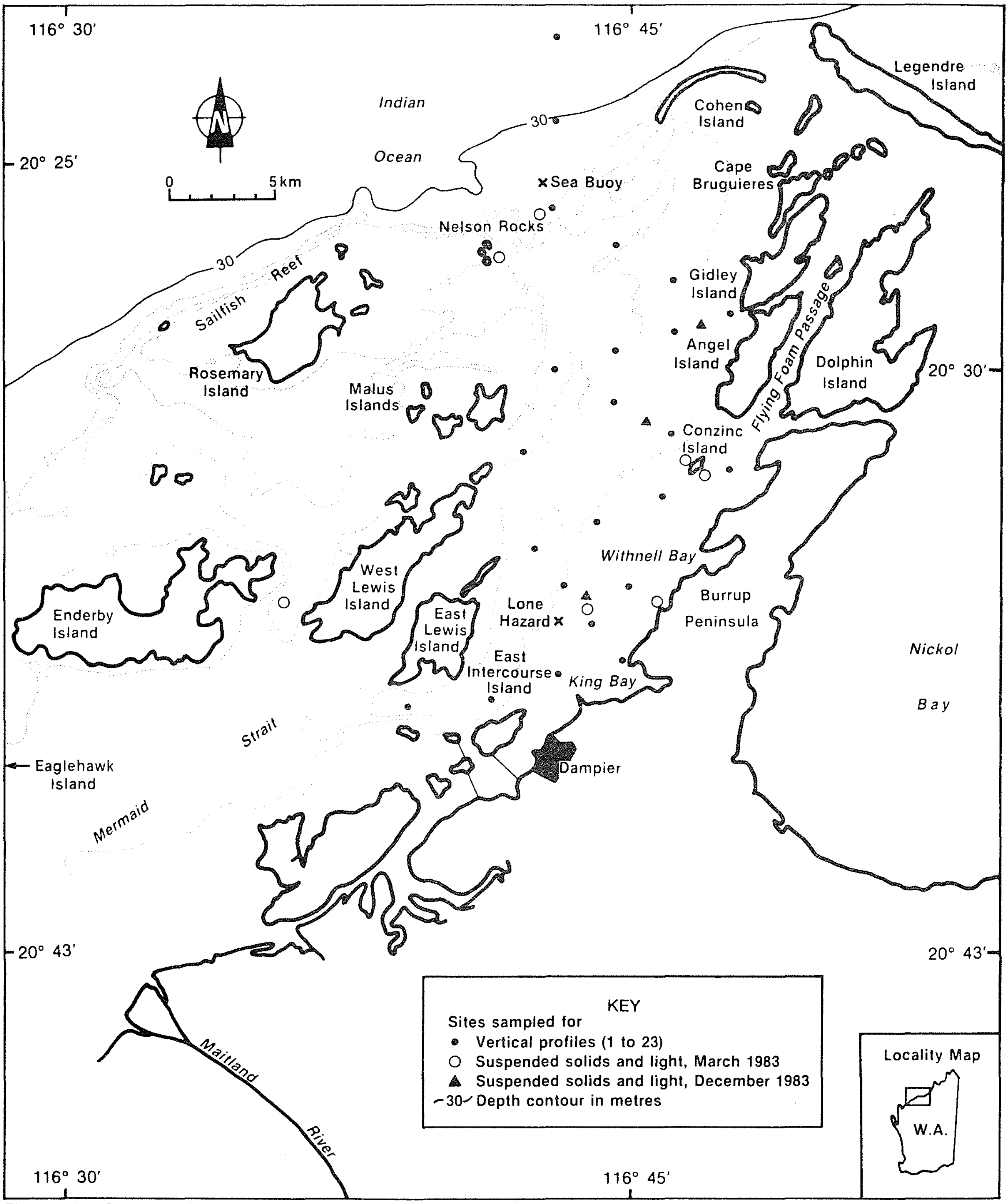

Figure 4.1 Sampling sites for light attenuation data.

4.3 RESULTS

4.3.1 Vertical light attenuation and suspended load

The ten replicates analysed for total load and organic content to determine experimental error displayed standard deviations of about 15% of the mean for both analyses (Table 4.1). Of the light profiles determined in March 1983, two exhibited anomalous values probably because of patchy cloud conditions; hence were discarded. Of the water samples analysed, the two taken simultaneously, at different depths at Nelson Rocks, were very similar and were averaged for comparison with the light profile (Table 4.2).

Table 4.1 Values of total load and organic load, derived from ten replicate samples taken at Nelson Rocks, 1 March 1983, to determine experimental error.

	Total load mgL^{-1}	Organic load mgL^{-1}	Organic %
	0.550	0.404	73.4
	0.584	0.430	73.6
	0.702	0.424	60.4
	0.680	0.430	63.2
	0.596	0.402	67.5
	0.622	0.538	68.5
	0.678	0.420	61.9
	0.576	0.330	57.3
	0.748	0.436	58.3
	0.488	0.330	67.6
$\bar{x}$	0.622	0.414	67.0
SD	0.079	0.059	8.9

When compared, the vertical light attenuation coefficients were found to be significantly negatively correlated to both total dry weight (r_{11} = -0.846, $p < 0.001$; Fig. 4.2) and organic dry weight (r_{11} = 0.790, $p < 0.002$; Fig. 4.3). Pigment analyses were not determined for the March samples, through technical oversight.

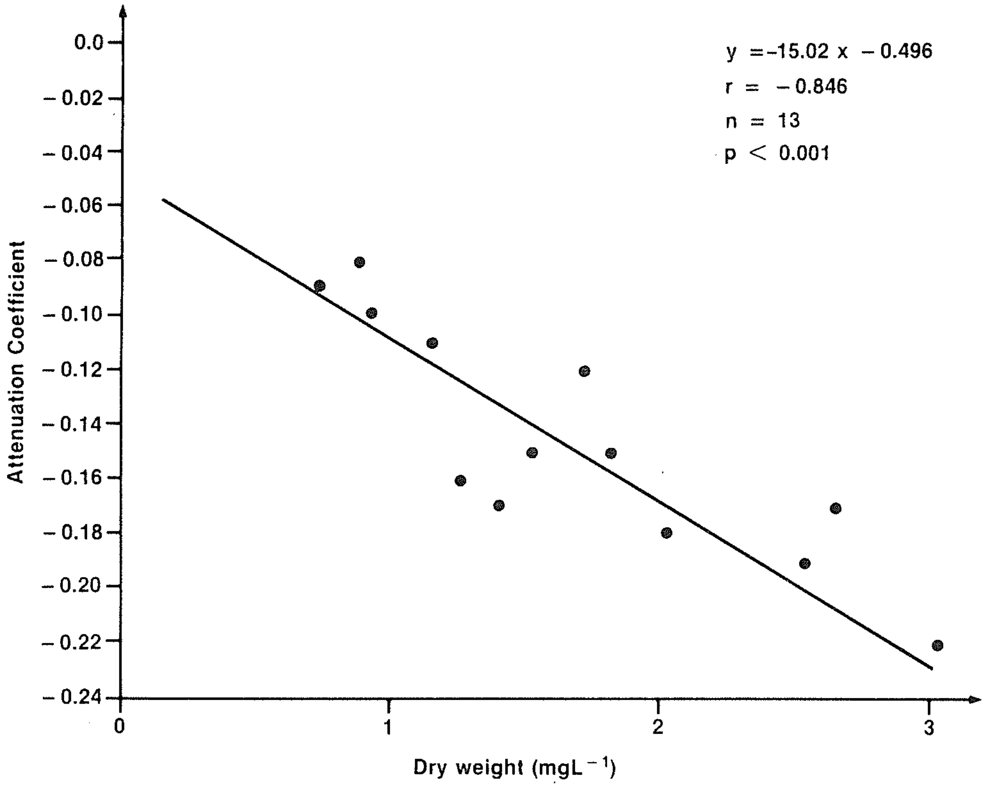

Figure 4.2 The relationship between light attenuation coefficient and total suspended mass in March, 1983.

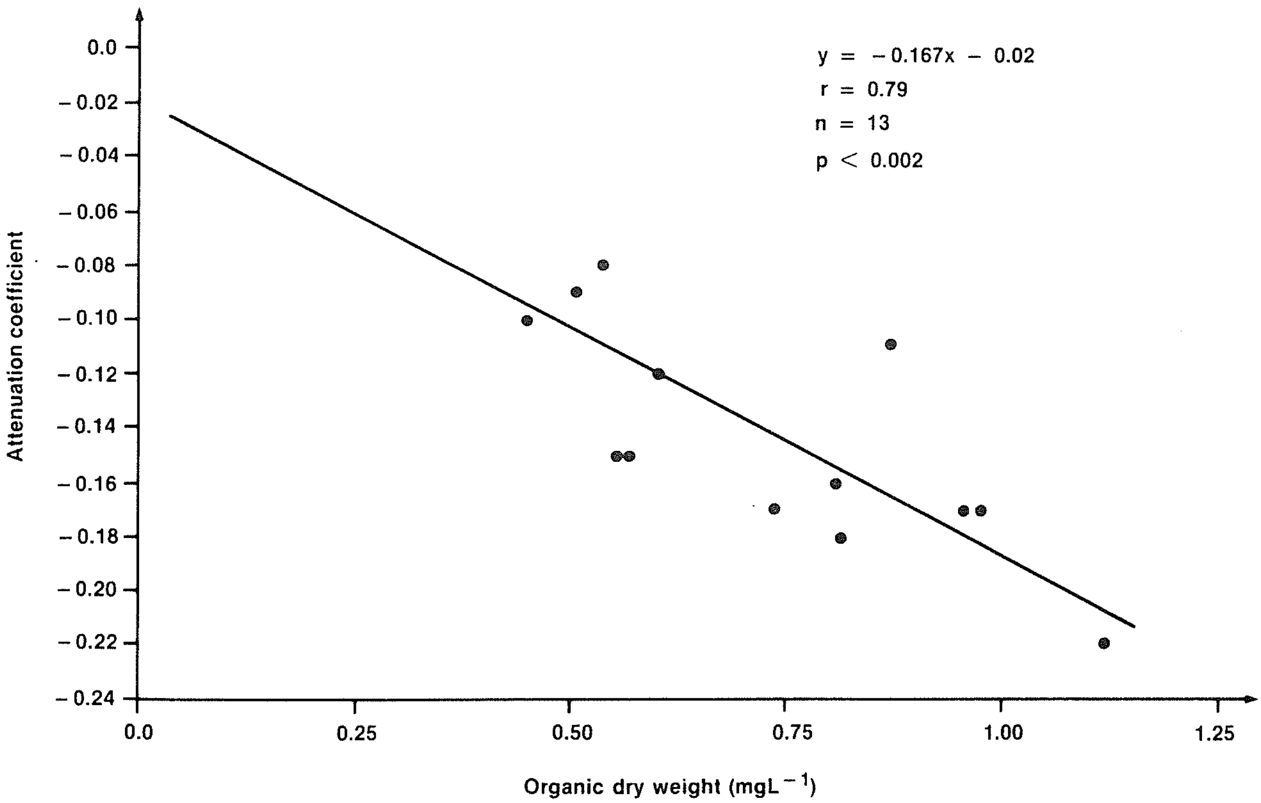

Figure 4.3 **The relationship between light attenuation coefficient and suspended mass of organic matter in March, 1983.**

Table 4.2 Suspended loads derived from seawater sample collected in March 1983 and light attenuation coefficients recorded concurrently.

Date	Station	*	Total load mg L^{-1}	Organic load mg L^{-1}	Organic %	Light attenuation coefficient
4 March	Conzinc East	T	2.06	0.83	40	-0.18
	Noname Rock	T	1.4	0.73	50.2	-0.17
	Conzinc West	T	1.82	0.6	30	-0.15
7 March	Conzinc East	T	2.64	0.94	36	-0.17
9 March	Enderby	T	1.74	0.65	38	-0.12
	Nelson	T	1.26	0.81	64	-0.16
	Nelson	B	1.21	0.8	66	
	Nelson	T	1.15	0.86	75	-0.11
	Noname Rocks	T	3.02	1.13	38	-0.22
	Conzinc East	T	1.53	0.62	40	-0.15
10 March	Sea Buoy	T	0.72	0.52	72	-0.09
	Conzinc West	T	0.92	0.45	49	-0.1
	Lone Hazard	T	0.88	0.57	65	-0.08
	Noname Rocks	B	2.54	0.91	36	-0.17

* T = top (1m from top)

B = bottom (1m from bottom)

When the second series of samples were taken in December blooms of the blue-green alga *Trichodesmium* were widespread. These were not observed in March. The blooms were patchily distributed into dense surface windrows, or appeared to be well mixed in at least the surface water. Comparison of the vertical light attenuation coefficients with the total suspended organic or pigment content of sampled water revealed no significant correlations (Table 4.3, page 42).

4.3.2 Spatial and temporal variation in light attenuation

The contour maps of the vertical light attenuation coefficients are presented (Fig. 4.4). Although temperature and salinity were determined for sites on six occasions, unsatisfactory incident light conditions limited the number of light profiles at different times. However, from the contour maps, a persistent gradient of increasing light attenuation, from the outer sites to those closest to the base of the Sound, can be seen. This pattern remained consistent throughout the entire sampling programme.

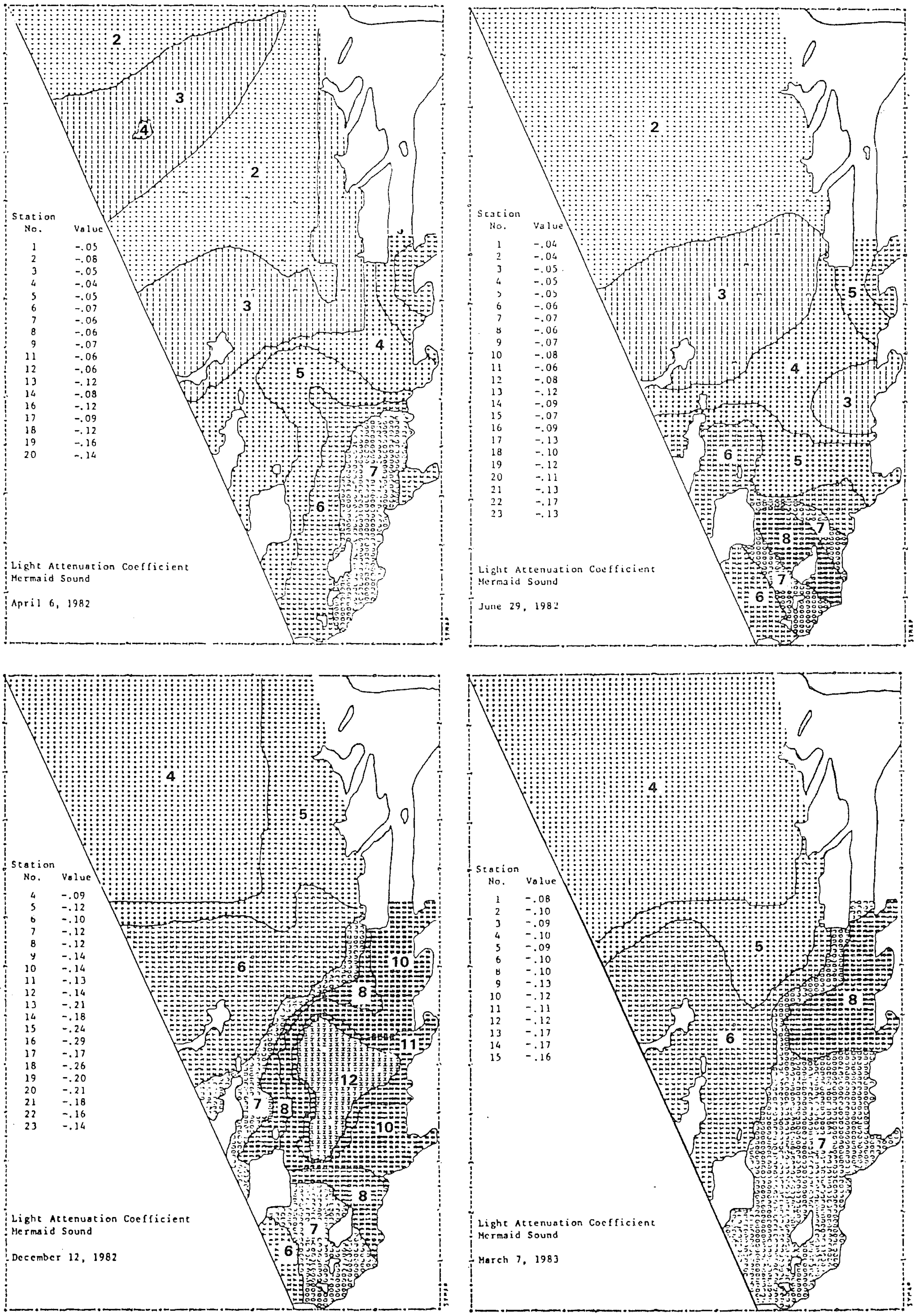

Figure 4.4 Contour maps of light attentuation coefficients (m^{-1}) recorded in Mermaid Sound between April, 1982 and March, 1983.

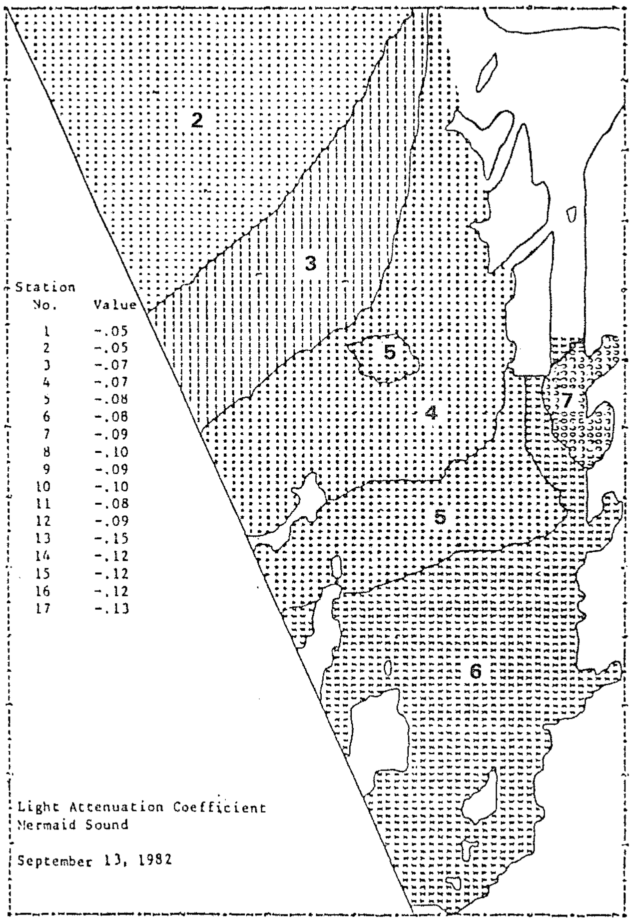

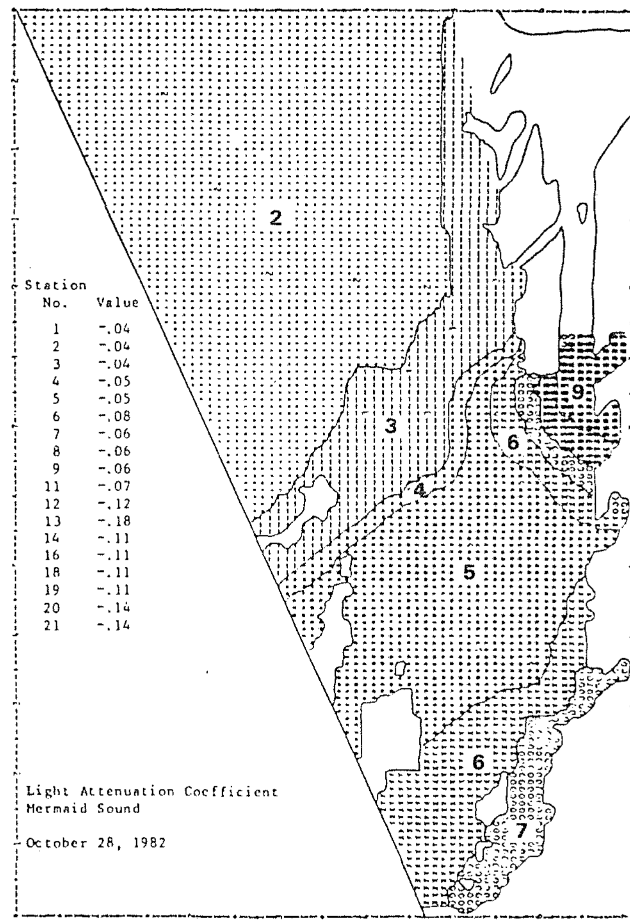

Key

Absolute value range applying to each level.
('maximum' included in highest level only)

Level	Minimum	Maximum
2	-.04	-.05
3	-.05	-.07
4	-.07	-.08
5	-.08	-.09
6	-.09	-.11
7	-.11	-.12
8	-.12	-.13
9	-.13	-.14
10	-.14	-.16
11	-.16	-.17
12	> -.17	

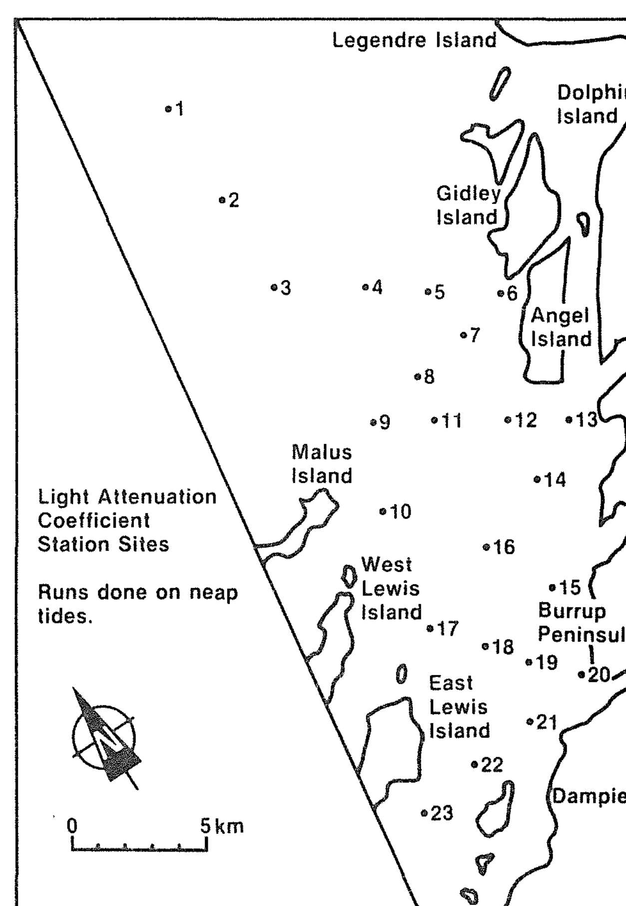

Figure 4.4 Cont.

Table 4.3 Suspended solid and pigment loads derived from December 1983 seawater samples, and light attenuation coefficients recorded concurrently.

Date & Station	*	Total load mg L^{-1}	Organic load mg L^{-1}	Organic %	Chlorophyll a	Phaeophytin	Light attenuation coefficient
3 Dec							
Lone Hazard	T	1.99	1.22	61.4	0.37	0.18	-0.13
	B	2.12	0.79	37.3	0.42	0.29	
Conzinc Is.	T	2.02	1.18	58.6	2.72	0.08	-0.23
	B	3.71	1.4	37.7	1.11	0.81	
4 Dec							
Lone Hazard	T	1.94	0.81	41.9	0.61	0.35	-0.1
	B	2.8	1.13	40.5	0.74	0.37	
Conzinc Is.	T	7.54	4.73	62.7	1.15	0.76	-0.11
	B	8.64	2.73	31.6	0.91	0.50	
Angel Is.	T	2.57	1.33	51.6	0.73	0.45	-0.08
	B	1.27	0.76	60.0	0.91	0.45	
5 Dec							
Angel Is.	T	3.18	1.57	49.5	0.90	0.53	-0.09
	B	2.03	1.05	51,9	0.97	0.48	
Conzinc Is.	T	2.27	0.97	42.7	0.61	0.53	-0.11
	B	2.64	0.92	35.0	0.85	0.42	
Lone Hazard	T	3.39	1.18	34.7	0.91	0.45	-0.16
	B	3.58	1.21	33.8	0.90	0.53	
6 Dec	T	1.93	0.83	42.9	0.48	0.24	-0.13
Conzinc Is.	B	2.92	0.99	33.8	0.61	0.53	
Lone Hazard	T	2.00	0.83	41.6	0.54	0.36	-0.19
	B	4.25	1.33	31.4	1.03	0.61	
Angel Is.	T	1.96	0.83	42.4	0.73	0.45	-0.18
	B	3.23	1.21	37.5	0.79	0.44	

*T = top (1 m from top); B = bottom (7-8 m depth).

The most obvious temporal trend for the area sampled, including the outermost station 7.5 km north of the mouth of the Sound, was towards greater turbidity in summer than in winter. Despite this seasonal trend, the outer and inner sites remained, throughout the year, relatively clear and turbid respectively. The transition area between the offshore and inshore conditions, in terms of light attenuation, occurred in the central region between the Malus Islands and the southern end of Angel Island (Fig. 4.1). This area also had the greatest seasonal range in turbidity.

One area of persistently higher turbidity occurred near Conzinc Island and Flying Foam Passage (Fig. 4.1). The December 1982 light profiles showed another area of unusually turbid water near Withnell Bay (Fig 4.4). It was the site of the most turbid water recorded during the study.

The light profiles taken at Nelson Rocks showed that light attenuation decreased by about 60% over the six-hour period. This change coincided with an incoming tide, causing a depth increase of approximately 2 m over the sampling period (Fig. 4.5).

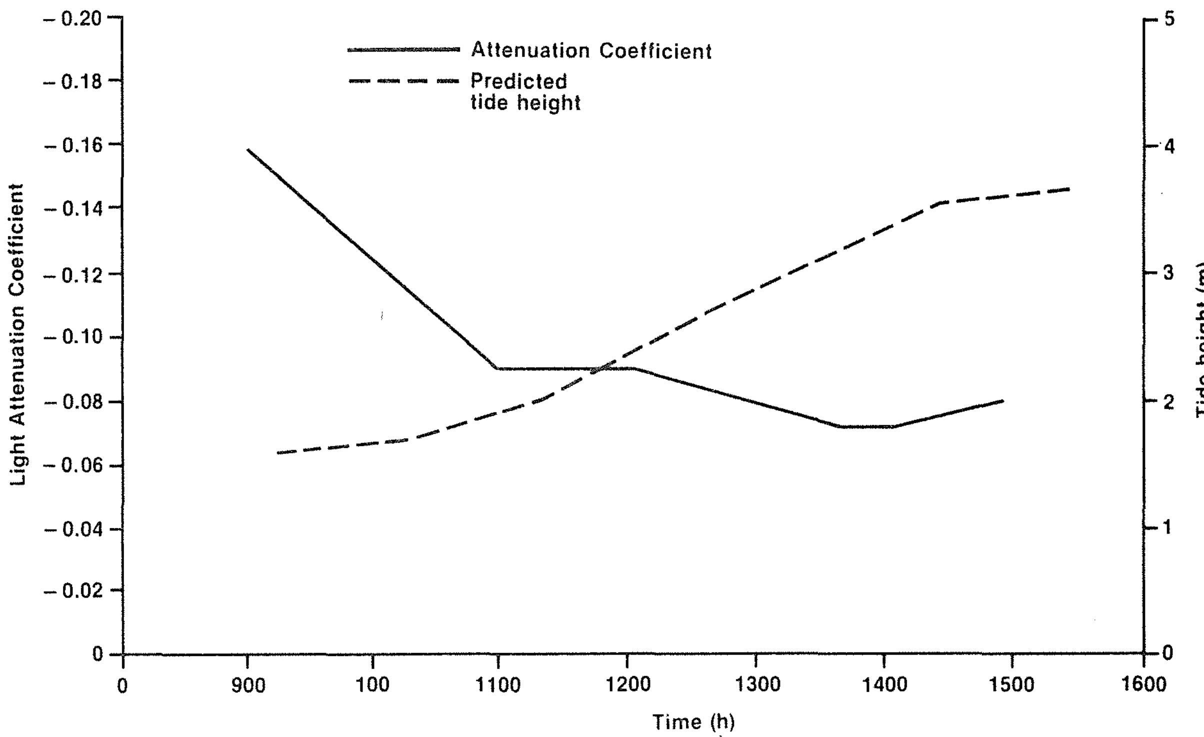

Figure 4.5 Change in light attenuation at Nelson Rocks over a six hour period, 28 June, 1982.

4.4 DISCUSSION

The replicate analyses of suspended load and organic content of water samples taken at Nelson Rocks gave standard deviations of about 15%, and indicate that single spot samples should give reasonable estimates of the actual values at the time of sampling. This conclusion is supported by the similar values of the two samples collected simultaneously at different depths at Nelson Rocks.

However, the disparity between the results from the two sampling series, in March and December 1983, questions the validity of using light attenuation solely as an indication of the mass of suspended material. Duckrow and Everhart (1971) have shown that although turbidity is linearly related to the concentration of a particular suspended solid, the same concentration of different materials can result in different turbidity values.

The substrates of Mermaid Sound display a gradient of increasing colour and silica content and decreasing grain size from the inner continental shelf to the mainland (Chapters 1 and 5). If a proportion of the material in suspension has been resuspended locally, then that material should display a spatial variation similar to that of the sediments. Differences in colour cause different degrees of light absorption, and a linear decrease in grain size diameter results in a linear increase in surface area to mass ratio. Small grain size material will, therefore, both absorb and scatter more light than the same mass of the same material of larger grain size.

This suggests that the composition of material sampled during March 1983 was more consistent than that sampled in December 1983. The differences between the two sampling periods were variation in sampling location, the occurrence of blooms of the blue-green alga, *Trichodesmium*, in the December period, and the time of the year. Although the blooms were easily seen, the analyses for chlorophyll a and phaeophytin did not indicate high phytoplankton content. The strength of the correlation found between light attenuation coefficients and suspended load over the March sampling indicates, however, that the two parameters sampled were linearly related over the area sampled at that time. This is supported by the light attenuation coefficient of 0.064 for waters free of suspended matter, interpolated from the regression equation, which is similar to 0.052 established by Jerlov (1977).

The spatial trends indicate that the waters of the northern reaches of the Sound have oceanic characteristics while the southern end has turbid condition more typical of coastal waters.

The increase in turbidity over the summer may be explained in terms of the environmental factors which change with the seasons. These are wind conditions and water temperature. The summer wind conditions are characterised by south-west to north-west winds, while the winter winds are essentially from the east and south-east (Chapter 2). The summer breezes therefore have greater fetch and, as such, could resuspend more material, especially in the shallow areas adjacent to the mainland (Chapter 5). Water temperature could also affect the vertical attenuation of light indirectly, by influencing biological production rates. *Trichodesmium* blooms and increased biological fouling rates are associated with increasing temperatures. The varying water temperature also caused changes in water structure which, when combined with the dominant wind conditions, generated density currents along the length of the Sound (Chapter 3).

The summer pattern of inshore water flowing over the more oceanic water offshore, may carry turbid water far enough away from the Sound to cause the increased light attenuation recorded at the outer site in March. Density currents may contribute to the clearer conditions occurring in winter. The influx of more oceanic water over the departing inshore water would result in decreased light attenuation.

High light attenuation occurred near the southern opening of Flying Foam Passage throughout the study, and over a large area from near Withnell Bay in December 1982. Current speeds in Flying Foam Passage can exceed 2 ms^{-1}. A turbid stream emanating from the southern opening can affect the tidal regime of Mermaid Sound to a distance of 5 km (Chapter 3). This turbid stream could therefore have caused the observed increase in turbidity near the southern opening of Flying Foam Passage. The other isolated area of increased turbidity was obvious only in the December profiles. Dredging of the island berth turning basin was in progress in December 1982, and the area of increased turbidity appeared to be a result of that dredging. Those latter measurements gave the highest values of light attenuation taken in Mermaid Sound, and indicate both the area of influence and degree of increased turbidity resulting from dredging.

The light profiles, taken at Nelson Rocks over 6 h indicated the effect of tidal excursion upon local water conditions. The decrease in light attenuation as the tide moved from low towards high, indicated the influx of oceanic water. This trend is expected to reverse as the tide falls and water from within the Archipelago moves over the area. These data emphasise the need to consider and select the tidal conditions appropriate to the problems being studied.

4.5 CONCLUSIONS

Light measurements alone should not be used as an indication of the mass of suspended material. Turbidity of the waters of Mermaid Sound increased with proximity to the shore ie from north to south. Turbidity was greater in summer than in winter in the Sound. Increases in turbidity occurred over the southern half of the Sound as a result of dredging.

5. VARIATION OF SUSPENDED LOAD IN MERMAID SOUND BASED ON SEDIMENT TRAP DATA

5.1 INTRODUCTION

Suspended load is an environmental parameter which can influence the structure of marine communities by placing constraints on some organisms (Bakus, 1969); corals are known to have developed different tolerances (Bak & Elgershuizen, 1976). Suspended load is readily influenced by anthropogenic activities such as dredging operations, effluent discharge and perturbations to natural runoff such as damming of rivers or deforestation of catchment areas.

Water sampling and filtration techniques are methods that have been widely used to estimate suspended load (Gellenne, 1973; Bohlen et al, 1979; Bothner et al, 1981; Smith, 1982). These techniques, however, provide instantaneous estimates and are suitable only for comparison with other measurements taken on similar time scales (eg light attenuation coefficients). They are not suitable, even over short-time scales, for the estimation of suspended loads in areas with markedly variable suspended loads. The Pilbara region of Western Australia is characterised by large tidal excursion (about 2-10m range) and the presence of water bodies with markedly variable suspended loads.

Another common method of estimating flux of suspended material involves sediment traps. Initial sediment trapping studies were done by Heim in 1900, and, to 1980, over 125 reports of sediment trap findings had been documented (Blomquist & Hakanson, 1981). These studies have described deployment of traps under a range of conditions; in calm lakes to energetic estuaries, and in nearshore coastal locations to offshore deep oceans. Shape of sediment collectors has ranged from cylinders and funnels to wide-mouthed jars, bottles and basins. In addition, a range of baffles and collars have been incorporated into designs.

Sediment trap design has never been standardised, and, until the work of Gardner in 1977, no comprehensive attempts had been made to evaluate collection efficiency. Gardner's work and subsequent studies (Hargrave & Burns, 1979; Gardner 1980a, b; Blomquist & Hakanson, 1981) have demonstrated the necessity of a sediment trap which forms a turbulence-free boundary layer, below which collected material cannot be resuspended. In addition, sediment traps must collect material at rates relative to their aperture, so that the rates can be related to surface area. Most studies have concluded that simple open-topped cylinders are the most useful sediment collectors. In addition, the height to width ratio (aspect ratio) was found to be the most important single factor affecting efficiency. In flume experiments with maximum current speeds of 0.095 ms^{-1}, Gardner (1980a) found that aspect ratios of 2 - 3 were most suitable. Various field experiments, (Hoskin, et al, 1978; Gardner, 1980b; Hargrave & Burns, 1979), however, have found that aspect ratios >5 are necessary for valid estimates of downward flux of particulate material. Blomquist and Hakanson (1981) suggested that differences in optimum aspect ratio reported by researchers may be a consequence of local hydrodynamic conditions.

For this study, a suitable sediment trap aspect ratio was evaluated in field trials in Mermaid Sound. On that basis, sediment traps were then designed for the suspended sediment monitoring programme. Results are discussed with reference to vertical, temporal and between-site variation. The relationships between wind and wave energy, and suspended load in different areas of Mermaid Sound, are also discussed.

5.2 MATERIALS AND METHODS

5.2.1 Field evaluation of appropriate sediment trap aspect ratio

The sediment trap assembly used for this evaluation consisted of five identical arrays suspended on a taut-wire mooring.

The arrays were spaced at 2 m depth intervals, between 0.5 and 8.5 m above the sea-floor. Each array consisted of three identical arms upon which four sediment traps were attached. Traps consisted of open-topped PVC cylinders (internal diameter 50 mm), with aspect ratios of 2, 4, 6 and 10. These traps were positioned on the arms such that no trap was within 3 diameters (150 mm) of another, thus eliminating effects from the sphere of turbulent influence caused by each sediment trap (Gardner, 1980a, b).

The assembly was moored near the West 5 channel marker (Site 11, Fig. 5.1) on 12 September 1981 and recovered after 9 days. Sediment traps were then sealed and road freighted to Perth for analyses.

Seven of these 60 samples were discarded owing to damage during transport or problems during analyses. The analytical problem resulted from an attempt to recover material from sediment traps using the filtration technique of Brewer et al (1976). Sample mass proved too great for that technique, and a decanting method (See 5.2.3) was used subsequently.

5.2.2 Design of monitoring programme

Sediment trap assemblies consisted of a four-armed array mounted on taut-wire mooring (Fig. 5.2). Each arm was fitted with two stainless steel clips by which two sediment collectors were attached. These collectors were simple PVC cylinders (300 mm long and 50 mm wide) which were sealed at the bottom and open at the top.

Sediment traps were deployed at 13 sites in Mermaid Sound between November 1981 and August 1983. Ten of these sites were maintained for monitoring purposes; however, Site 3 was abandoned after June 1982 (Fig. 5.1). Sites ranged in depth from 1.5 m (below mean low water) at Site 13, to 20 m (below MLW) at Site 7. Arrays were deployed 0.5 m above the sea-floor at all sites and at 6.0 m above the sea-floor where depth

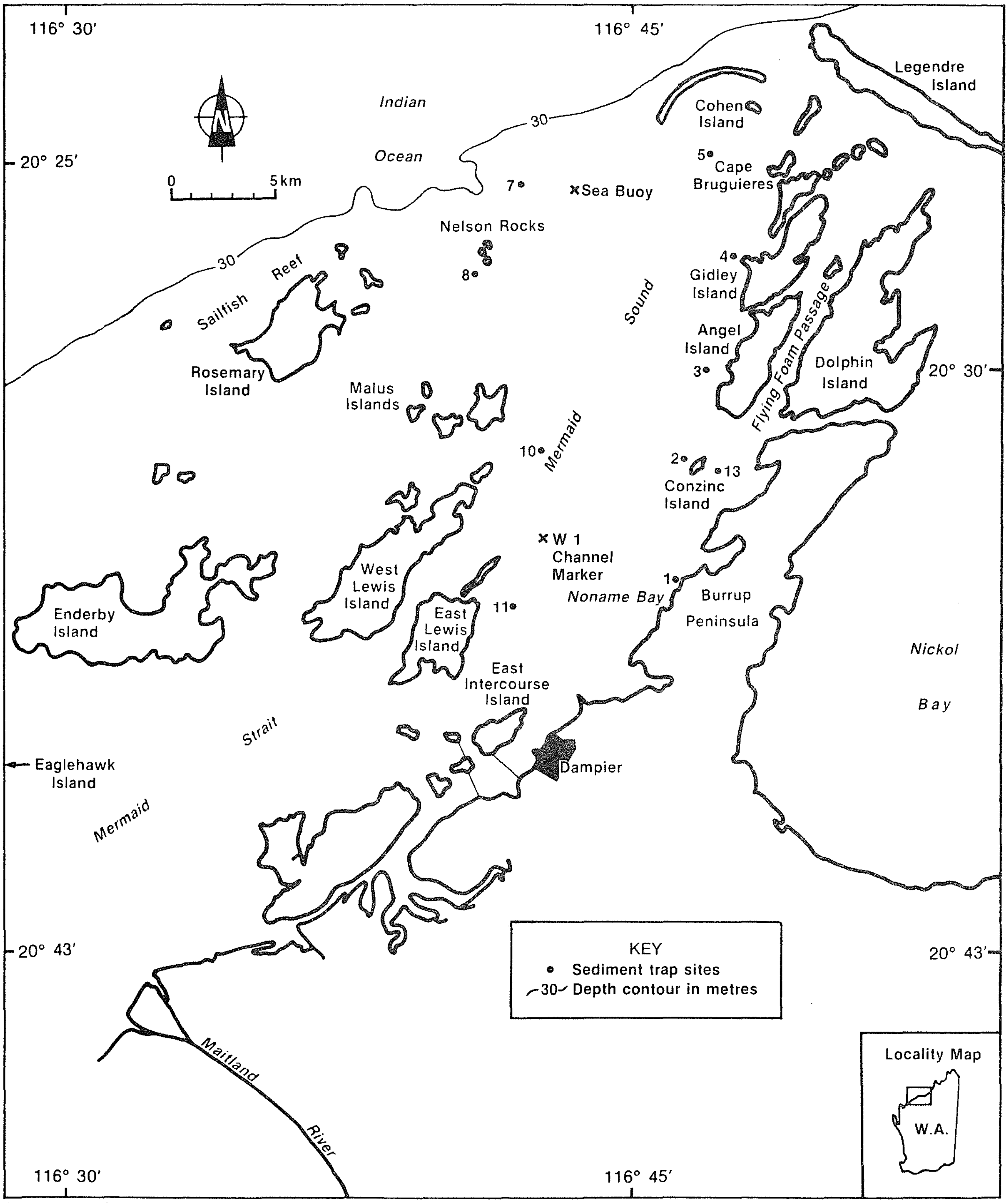

Figure 5.1 Sediment trap sites in Mermaid Sound.

permitted (Sites 3, 5, 7, 10 and 11). The collection periods were usually about 8 days, although some were deployed for 30-40 days.

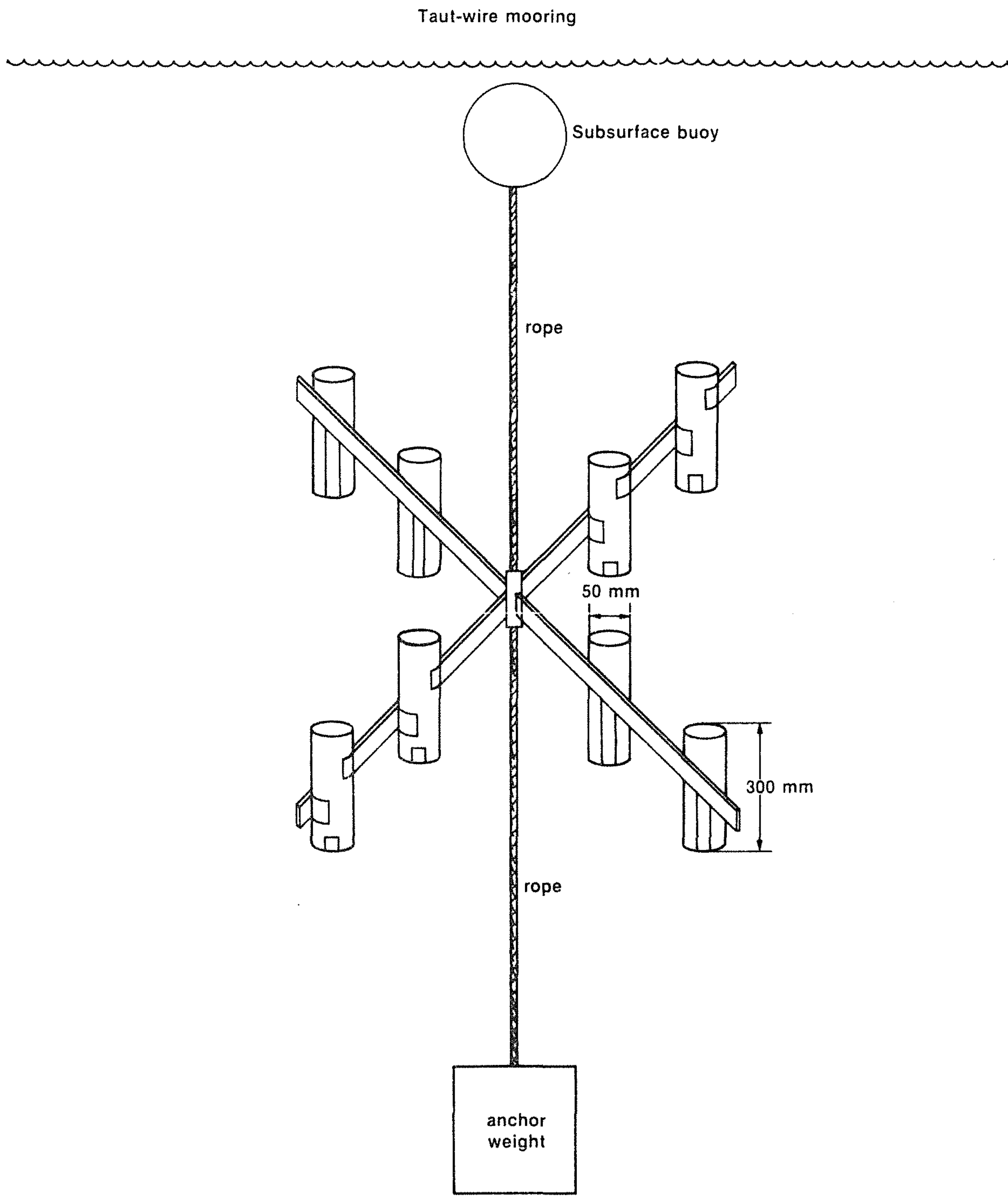

Figure 5.2 Sediment trap assembly.

Sediment traps were deployed and retrieved by SCUBA divers, who fitted the collection cylinders and cleaned the arrays of fouling organisms. To avoid contamination or sample loss, the cylinders were sealed with plastic caps underwater, prior to removal from the array.

5.2.3 Sample analysis

Sediment traps were allowed to settle for a minimum of 3 h after return to the Dampier laboratory. Excess water was then decanted and the residue washed with freshwater into 500 ml settling cylinders. After another settling period of > 3 h, excess water was decanted, and the samples washed with tap water into 140 ml vials. This was made up to volume with water and formaldehyde such that the final solution approximated a 6% formaldehyde-water mixture. These preserved samples were then road freighted to Perth and stored for a few weeks prior to analysis.

To determine total dry weight, the samples were decanted and washed with deionized water into pre-weighed porcelain crucibles. These were placed in a drying oven at $120^{0}C$ for 18 h, and weighed to 0.001 g (Sartorius; model 1265 MP). Organic and calcium carbonate contents were determined by loss on ignition after 90 min at $600^{0}C$ and $1000^{0}C$ respectively in a muffle furnace. To prevent condensation, crucibles were cooled in a desiccator prior to weighing. Results are expressed as the weight in grams of suspended solids trapped per square metre, per day ($g\ m^{-2}\ d^{-1}$).

5.2.4 Surface sediments: sampling and analysis

SCUBA divers collected core samples of the surface 50 mm of sediment at all study sites where deposits were available. These were frozen and air freighted to the Botany Department, University of Western Australia. Samples were analysed for organic, calcium carbonate and refractory contents using the loss on ignition technique. Replicate samples were sent to the

Geology Department for grain size determination. Granulometric analysis, using the method of Folk (1968), was undertaken using a CSIRO-Warman cyclocyser. The results are presented as percentage of total dry weight.

5.3 MONITORING SITES

The nine monitoring sites used within Mermaid Sound varied in depth, energy regime and bottom type as follows:

Site 1 - Adjacent to the rocky shoal immediately west of Noname Bay (Noname Rocks; Fig. 5.1). A sandy sea-floor sloped gently from the emergent granophyre rocks to about 6 m. The sediment trap was located on the slope in 2.0 m depth (below MLW). Sediments of the slope were composed of grains in a bimodal distribution, with dominant modes of 0.5 - 0.25 mm, and in the clay-particle size range (Table 5.1). Corals occupied the shallow areas surrounding the emergent rocks, and sparse sea grasses *(Halophylla sp.)* occurred on the soft sediments of the slope.

Table 5.1 Grain size analysis of core samples from the surface 50 mm at the sediment trap sites. Cores collected 1982, analysed 1983.

Site	%			Sand fractions (% of total)						Silt fractions (% of total)				
	Sand	Silt	Clay	7-2 mm	2-1 mm	1-0.5 mm	0.5-0.25 mm	0.25-0.125 mm	0.125-0.0625 mm	38 µm	28 µm	20 µm	14 µm	10 µm
1	66.0	11.8	22.2	1.6	2.8	8.2	23.5	20.2	9.6	2.9	2.9	2.4	2.3	1.3
2	99.5	0.5	-	6.2	11.0	30.0	37.6	12.7	1.3	-	-	-	-	-
3	96.4	3.6	-	0.9	0.5	1.0	6.8	60.3	26.4	2.0	1.6	-	-	-
4	00	-	-	0.2	0.6	1.6	46.6	50.8	0.1	-	-	-	-	-
5	98.4	1.6	-	-	0.3	1.9	12.9	58.3	24.6	-	-	-	-	-
7				Limestone Pavement										
8				Coral Reef and Rubble										
10	69.5	16.8	13.7	1.7	1.6	3.2	6.8	25.8	30.4	4.4	4.3	3.8	2.8	1.5
11	21.0	29.4	49.6	-	0.4	0.7	2.3	4.4	12.9	6.1	7.4	7.2	5.5	3.2
13	99.8	0.2	-	7.2	11.7	32.0	36.4	11.1	0.8	-	-	-	-	-

Site 2 - Adjacent to the north-west shore of Conzinc Island (Fig. 5.1), in 2.5 m depth. Corals were abundant on a limestone pavement where sediments were coral rubble and coarse sand. Granulometric analysis of these sands revealed a leptokurtic distribution with a dominant modal range of 0.5 - 0.25 mm (Table 5.1).

Site 3 - Located near the south-west corner of Angel Island (Fig. 5.1) in 8 m depth. The sea-floor consisted of even sands devoid of benthos. Ripples, resulting from high energy events, were occasionally observed. This site was abandoned after June 1982.

Site 4 - Located near Gidley Island (Fig. 5.1) in 4 m depth. A limestone crest sloped away from the island, to a deeply rippled sand flat in 6 m of water.

Granulometric analysis of the sands showed a leptokurtic distribution of grains with a dominant modal range of 0.25 - 0.125 mm (Table 5.1). The sand flat was devoid of benthos, while small macroalgae populated the limestone crest. This was a high energy area, with waves breaking on the crest during periods of high swell activity or strong westerly winds.

Site 5 - Approximately 4.5 km west of Cape Brugiures (Fig. 5.1) in 11.5 m depth. The sea-floor was composed of even, sandy deposits, devoid of rocky projections or macrobiota. Sand ripples, indicating occasional high wave energy, were observed while a patchy algal turf was observed at times of low turbidity and energy. Granulometric analysis of the sediments indicated a leptokurtic distribution of grain size, with a dominant modal range of 0.25 - 0.125 mm (Table 5.1).

Site 7 - Adjacent to the outermost channel marker (Sea Buoy, Fig. 5.1) on the outer edge of the Sound, and the deepest area sampled (20 m depth). The sediment trap was positioned on a continuous limestone pavement, which provided a sea-floor for a benthic community dominated by filter-feeding organisms. Sediments were limited to some superficial accumulations of coarse shelly sand, with some fine material trapped within the biota.

Site 8 - On the coral reef on the eastern side of Nelson Rocks (Fig. 5.1) in 4.2 m depth. This site was within 400 m of the 20 m depth contour and was, therefore, susceptible to high energy conditions. Those areas of the reef not occupied by corals were covered with coral rubble of unknown depth.

Site 10 - Adjacent to West 1 channel marker (Fig 5.1) in 16 m depth. The sea-floor was composed of muddy sands devoid of macroalgae or rocky projections. Granulometric analysis of sediments showed a positively skewed distribution with a dominant modal range of a 0.125 - 0.0625 mm. (Table 5.1).

Site 11 - Near the West 5 channel marker (Fig. 5.1) in 11 m depth. The brown muddy sediments were devoid of benthos or rocky projections, and had a negatively skewed distribution. Dominant modal grain size was in the clay size range (Table 5.1). This was the only site where calcium carbonate did not dominate the composition of the sediments (Table 5.2). Both organic and refractory materials were more abundant here than at any other site (Table 5.2).

Table 5.2 Muffle oven analysis of core samples from the surface 50 mm at the sediment trap sites.

Site	Organic %	$CaCO_3$ %	Refractory %
1	3.2	92.3	3.9
2	7.2	85.7	7.1
3	8.6	81.0	10.4
4	4.3	91.0	4.7
5	5.9	86.7	7.4
7		Limestone Pavement	
8		Coral Reef and Rubble	
10	7.1	74.4	18.5
11	14.8	28.0	57.2
13	6.1	87.3	6.6

Site 13 - Situated on the opposite side of Conzinc Island to Site 2 (Fig. 5.1), in 2 m depth over a uniformly flat, sandy area supporting a dense coral community. Granulometric analysis of the sediments showed a leptokurtic distribution of sand-size grains with a dominant modal range of 0.5 - 0.25 mm (Table 5.1).

5.4 RESULTS

5.4.1 Field evaluation of appropriate sediment trap aspect ratio

Figure 5.3 shows a number of trends with regard to collection rates and aspect ratios: The collection rates of sediment traps of aspect ratio 2, were generally lower than those with higher ratios at the same height above the sea-floor.

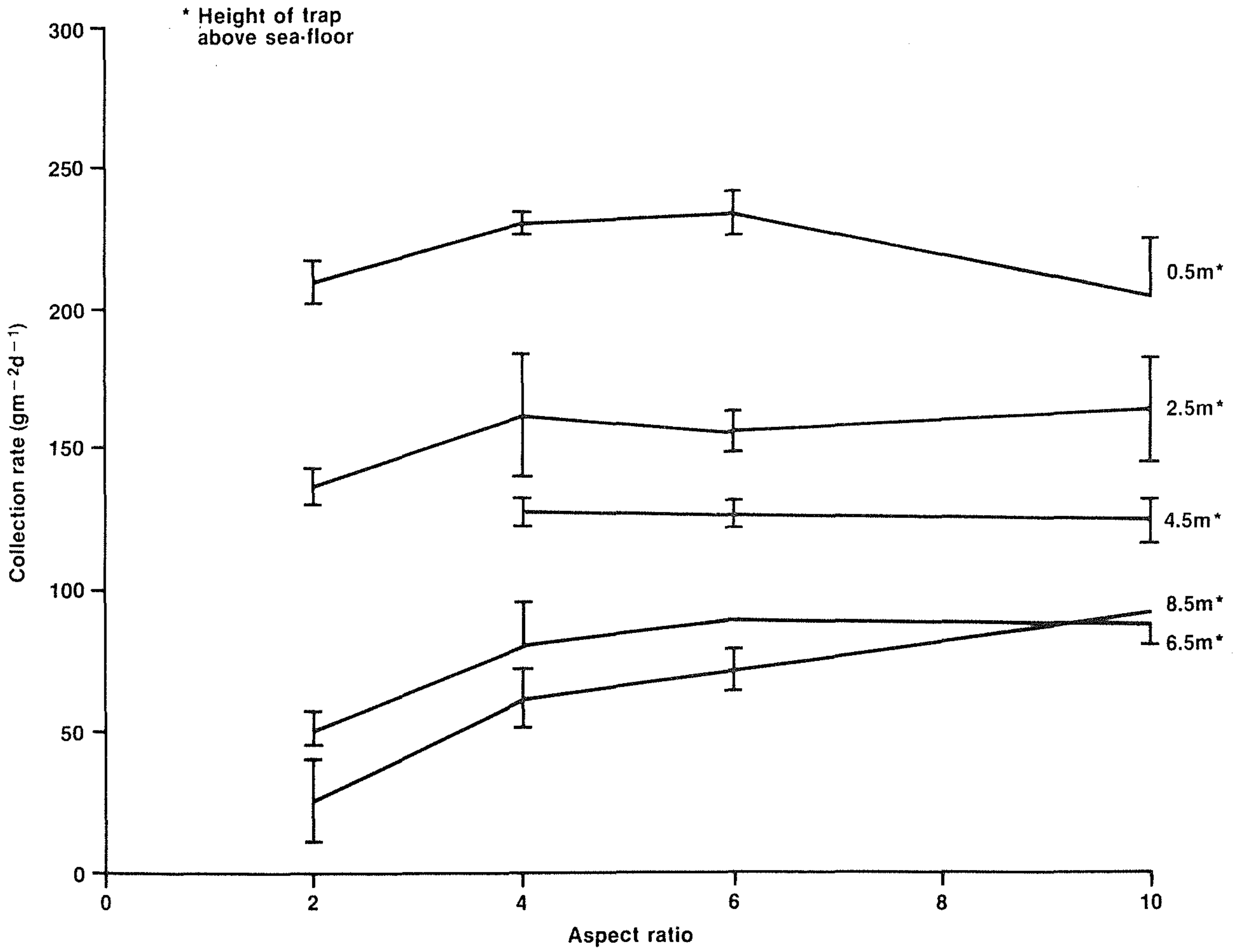

Figure 5.3 The collection rates of sediment traps with different aspect ratios at heights ranging from 0.5 m to 8.5 m above the sea-floor at Site 11.

The collection rates of sediment traps of aspect ratio 4, were lower than those of ratio 6 and 10 at heights of 6.5 m and 8.5 m above the sea-floor.

The traps with aspect ratio 10 had the largest variation between replicates in collection rates and yielded an unexpectedly low mean value at the 0.5 m elevation.

The traps which produced the consistently lowest variation between replicates, for total solids and proportion of organic content, were of aspect ratio 6. Thus, the most appropriate sediment trap chosen for the present study was one with an aspect ratio of 6.

Figure 5.4 shows there were no significant differences between mean proportions of organic material collected in sediment traps of different aspect ratio.

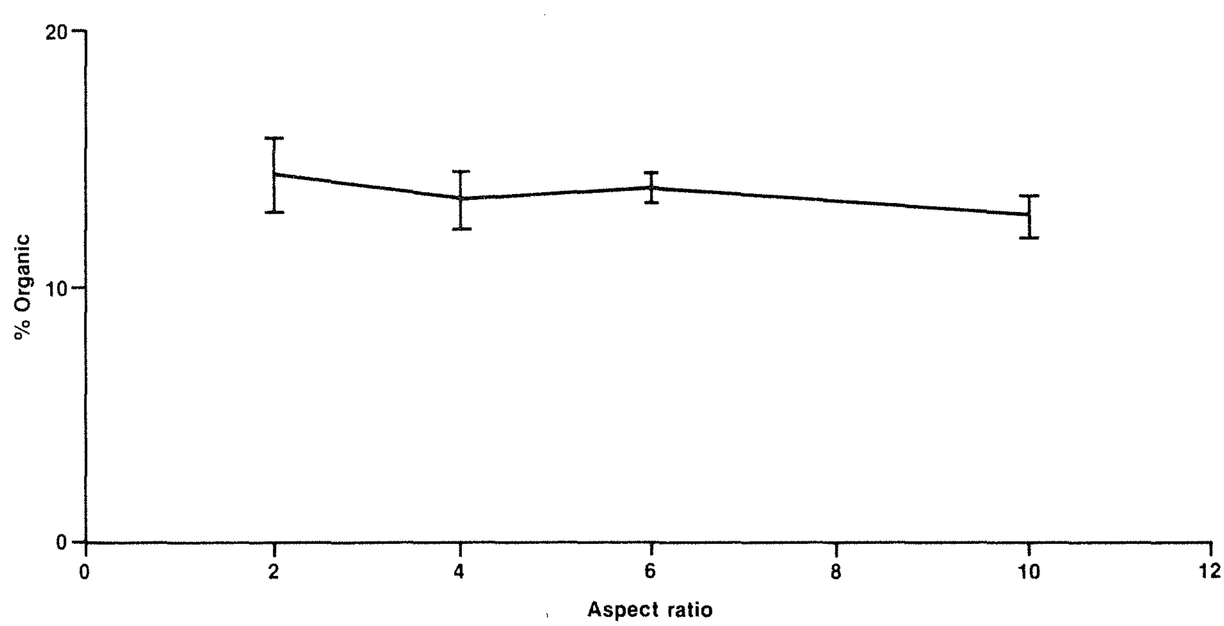

Figure 5.4 Percentage of a mean weight of organic material in sediment traps of different aspect ratios at Site 11.

5.4.2 Variation of suspended load with height above sea-floor

From the aspect ratio study, the accumulation rate of suspended solids was indirectly proportional to the height of the sediment trap above the sea-floor ($r_3 = -0.9662$, $p<0.01$, for sediment traps of aspect ratio 6).

Analyses of material collected in sediment traps is tabulated in Appendix 1. Data from sites where paired traps were deployed are presented in Appendix Tables 3a & b, 5a & b, 8a & b, and 9a & b. For ease of presentation, data used as examples are taken from Tables 6 and 8 (Sites 7 and 10, Fig. 5.1).

Where pairs of traps were deployed, a number of trends were observed: at all sites the total suspended load (Appendix 1; Fig 5.5), and the loads of organic (Fig. 5.6), calcium carbonate (Fig 5.7) and refractory (Fig. 5.8) materials were consistently greater in the sediment traps at 0.5 m than those 6 m above the sea-floor. The percentage of calcium carbonate in the suspended load also followed this trend (Appendix 1).

This was not so with mean organic percentage of the suspended load (Fig. 5.9), where higher values occurred in the 6 m sediment traps at all sites.

The percentage of suspended refractory material showed no consistent differences between sediment traps moored 0.5 and 6 m above the sea-floor.

5.4.3 Temporal variation in suspended load

The monitoring programme allowed assessment of variation in suspended load from deployment to deployment, and from season to season. As there are two dominant weather patterns in the Pilbara region (Chapter 2), seasonal variations will be discussed in terms of the 'summer' and the 'winter' periods.

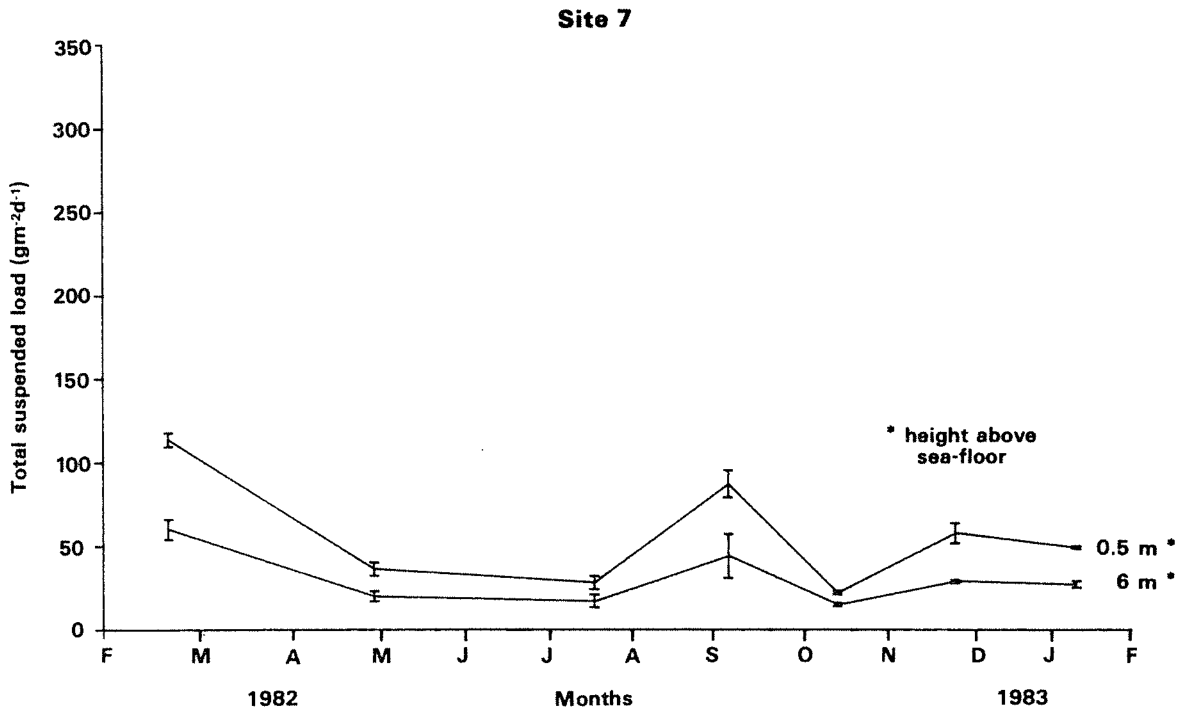

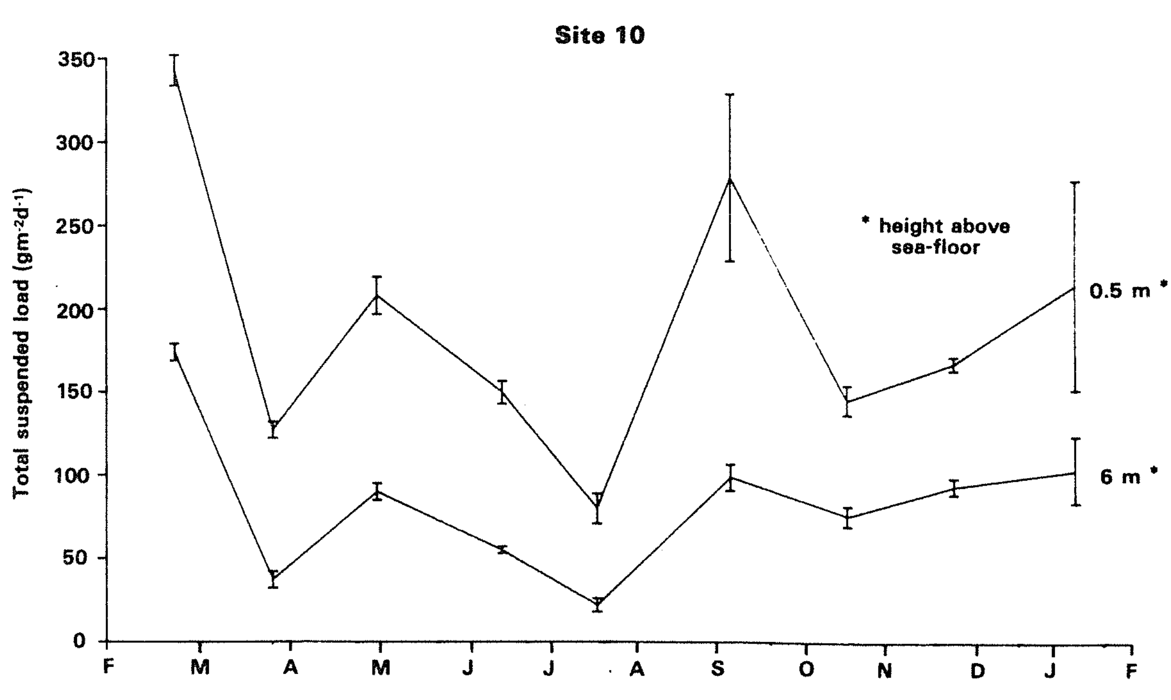

Figure 5.5 Total suspended load collected in sediment traps 0.5 m and 6 m above the sea-floor in Sites 7 and 10.

Site 7

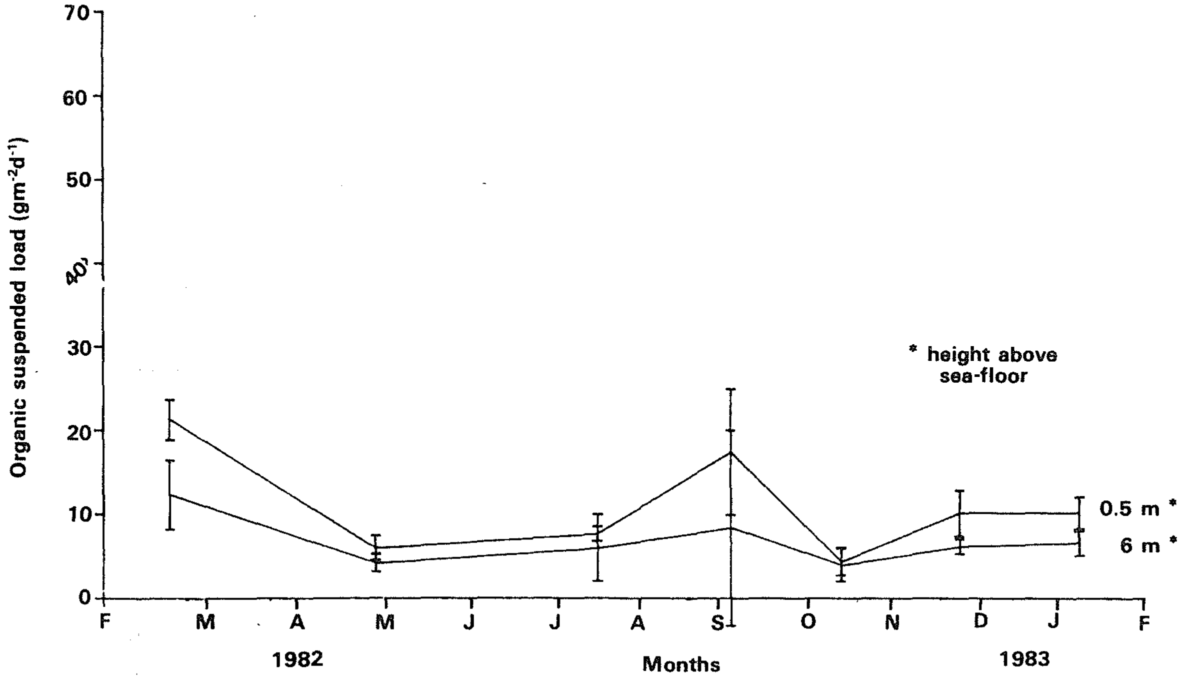

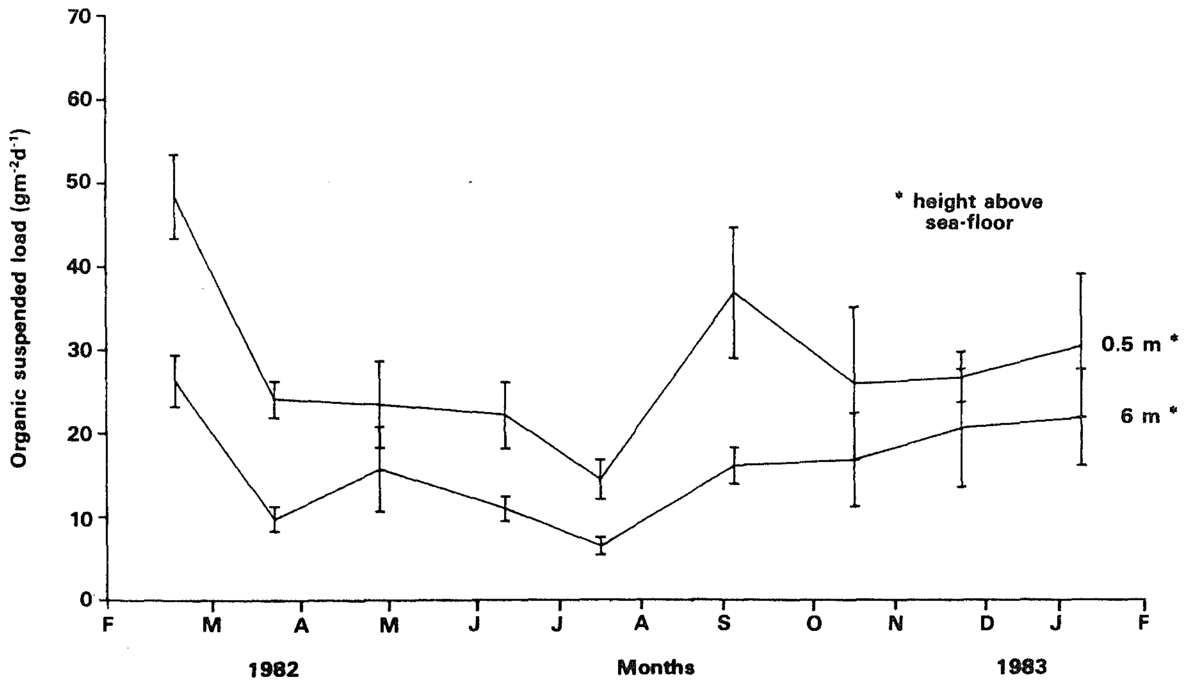

Figure 5.6 Organic suspended load collected in sediment traps 0.5 m and 6 m above the sea-floor at Sites 7 and 10.

Site 7

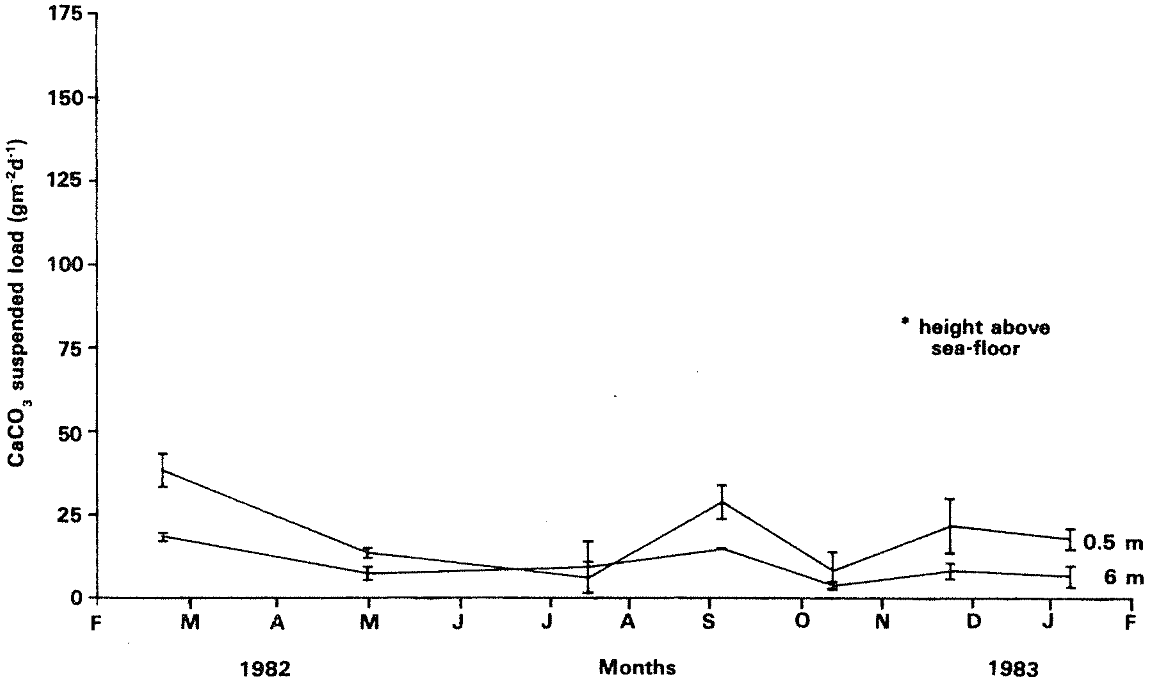

Site 10

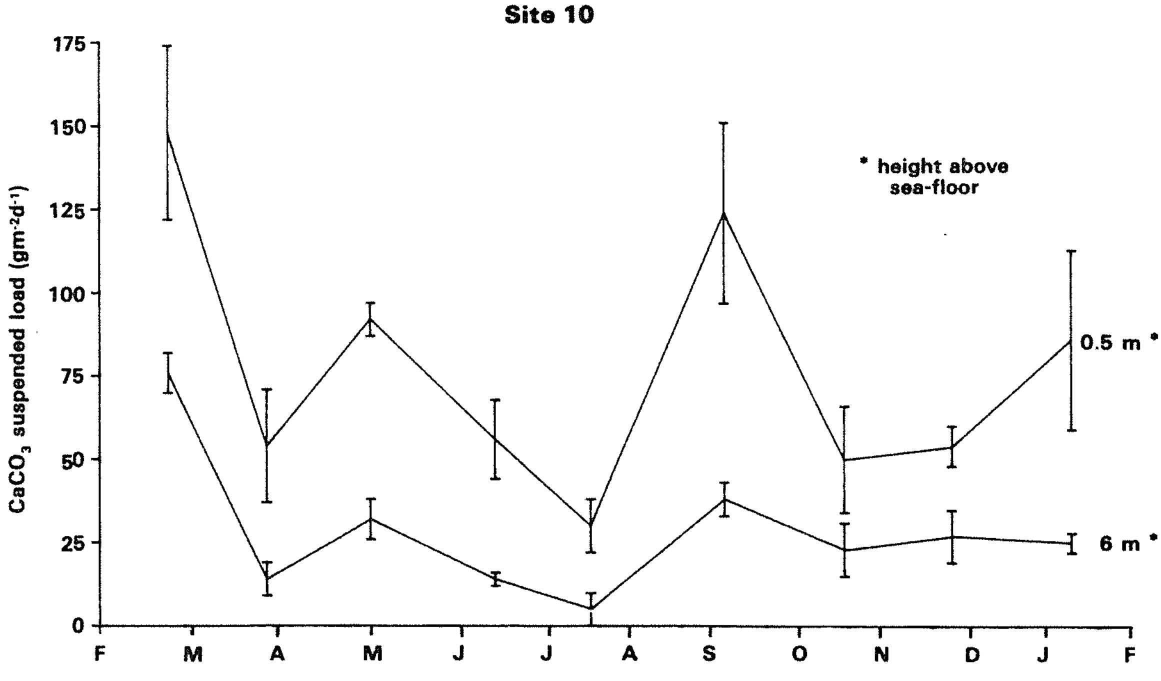

Figure 5.7 Calcium carbonate suspended loads collected in sediment traps 0.5 m and 6 m above the sea-floor at Sites 7 and 10.

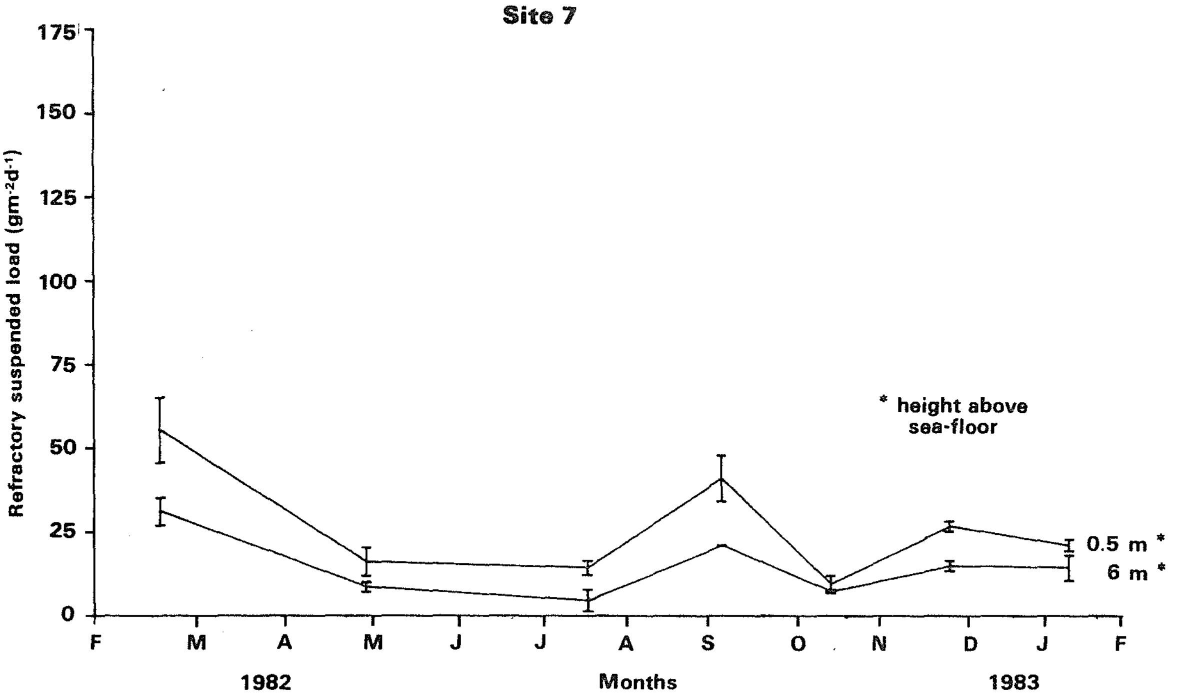

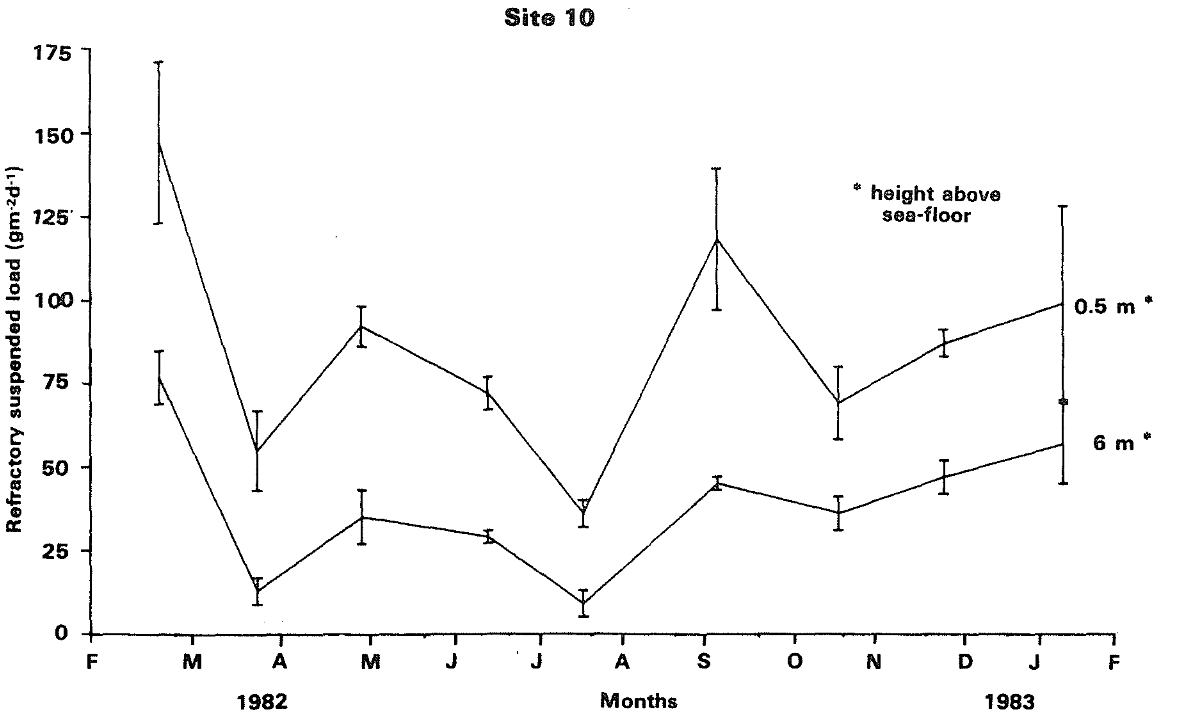

Figure 5.8 Suspended refractory loads collected in sediment traps 0.5 m and 6 m above the sea-floor at Sites 7 and 10.

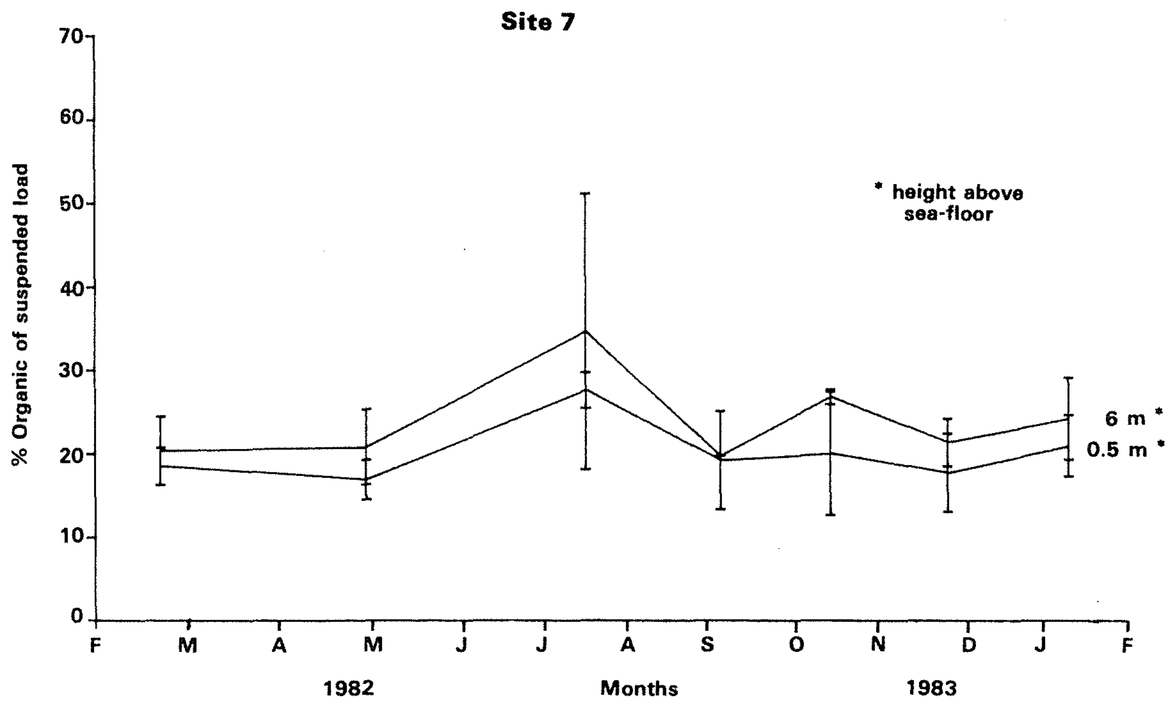

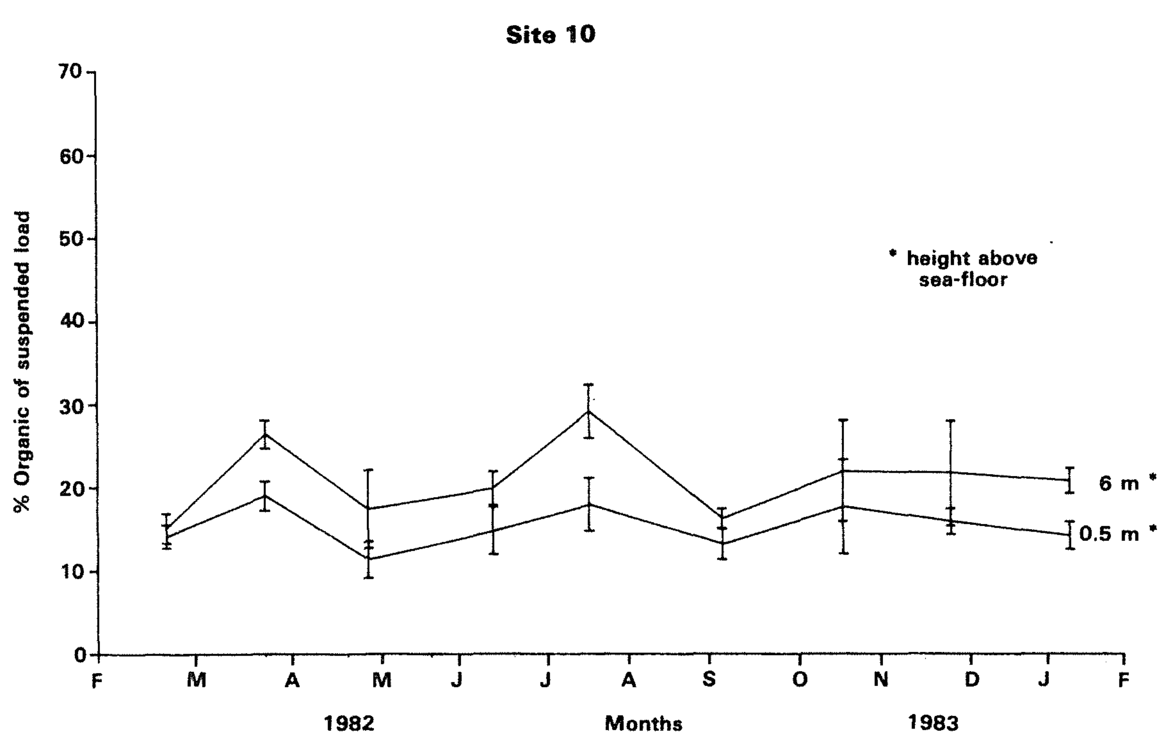

Figure 5.9 Percentage of mean weight of organic material in suspended loads collected in sediment traps 0.5 m and 6 m above the sea-floor at Sites 7 and 10.

Variations in suspended load from one deployment to another were evident at all of the study sites; however, only at Sites 1, 8 and 13 were sufficient data collected for statistical analysis.

At Site 1, the suspended loads were significantly correlated with both mean wind speed and the index for mean specific wave energy under normal conditions ie unaffected by cyclones (r_{11} = 0.793, $p < 0.002$ and r_9 = 0.809, $p < 0.005$ respectively; Figs 5.10 & 5.11).

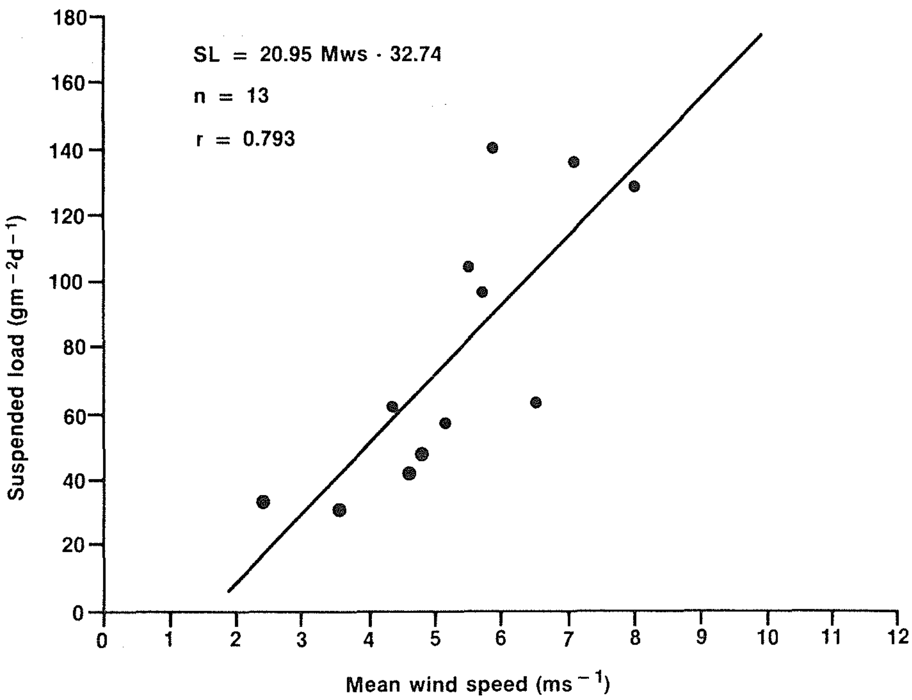

Figure 5.10 The relationship between suspended load and mean wind speed at Site 1.

At Site 8, the suspended loads were not significantly correlate with mean wind speed, but were positively correlated with the index for mean specific wave energy (r_{10} = 0.711, $p < 0.01$; Figs. 5.12 and 5.13).

The suspended load was also correlated to the peak specific wave energy of each sample period (r_{10} = 0.7475, $p < 0.01$ excluding the period incorporating cyclone 'Lena', and r_{11} = 0.9256, $p < 0.001$, including that period).

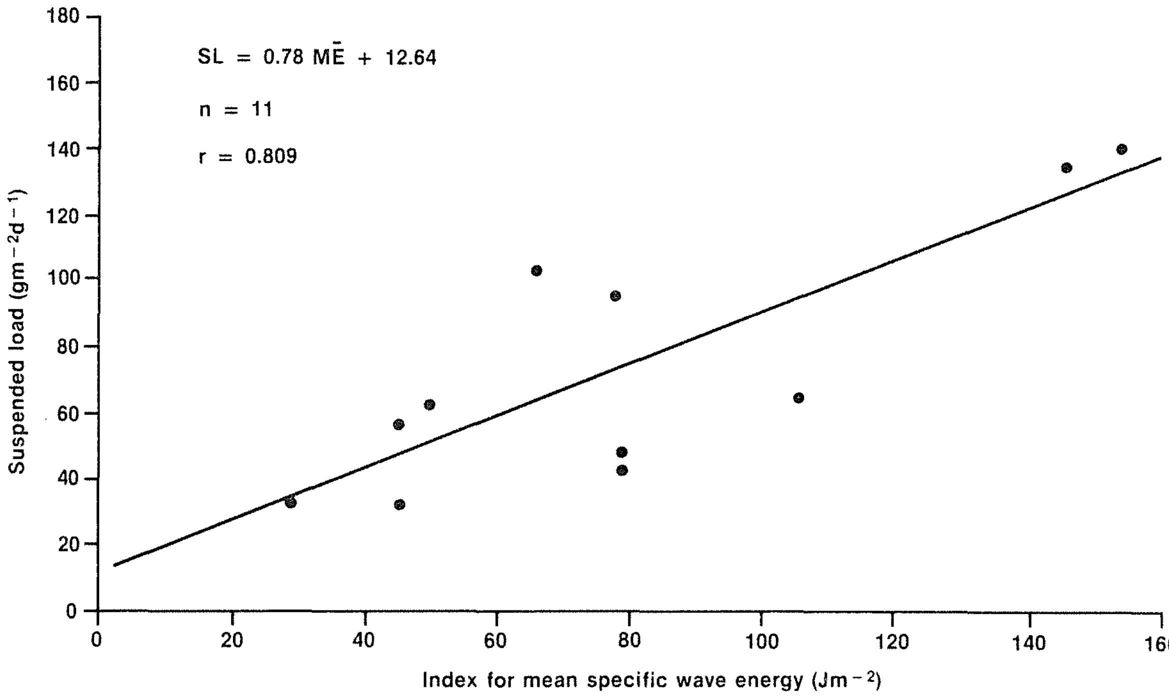

Figure 5.11 The relationship between suspended load and the index for mean specific wave energy at Site 1.

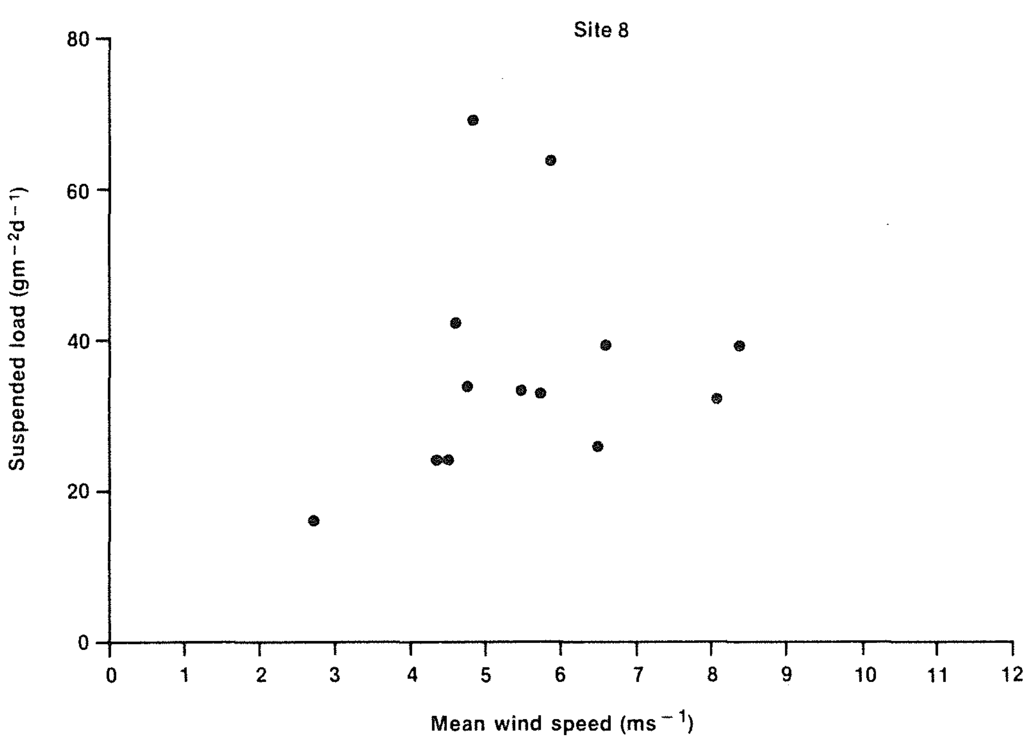

Figure 5.12 The relationship between suspended load and mean wind speed at Site 8.

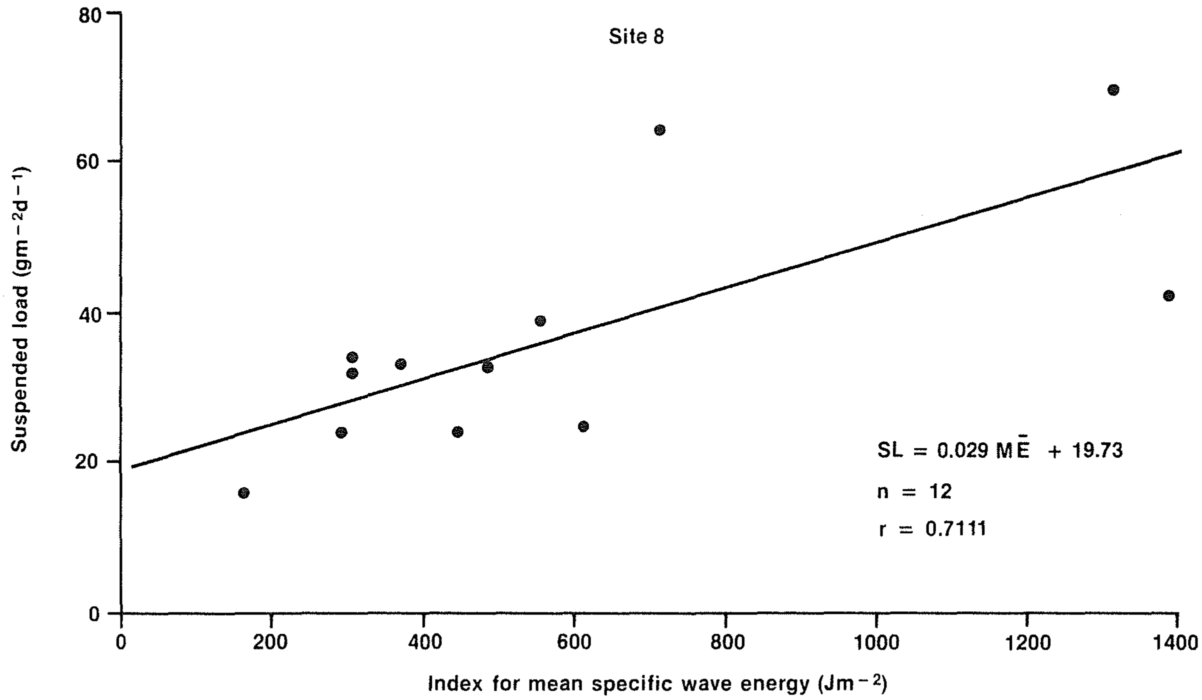

Figure 5.13 The relationship between suspended load and the index for mean specific wave energy at Site 8.

The suspended loads at Site 13 were significantly correlated with both mean wind speed and the index for mean specific wave energy (r_8 = 0.820, $p < 0.005$ and r_8 = 0.930, $p < 0.001$ respectively; Figs. 5.14 and 5.15).

The compositional fractions at each site displayed similar correlations with both mean wind speed and the index for mean specific wave energy, as did the total suspended loads. The one exception was at Site 8, where refractory load was not significantly correlated with the index for mean wave energy (Table 5.3).

Sufficient data for assessment of seasonal variation were collected at Sites 1, 8 and 13.

At Sites 1 and 13, the suspended load was significantly greater in summer than in winter (t_{13} = 5.83, $p < 0.0005$, and t_9 = 4.7, $p < 0.001$, respectively; Figs. 5.16 and 5.17).

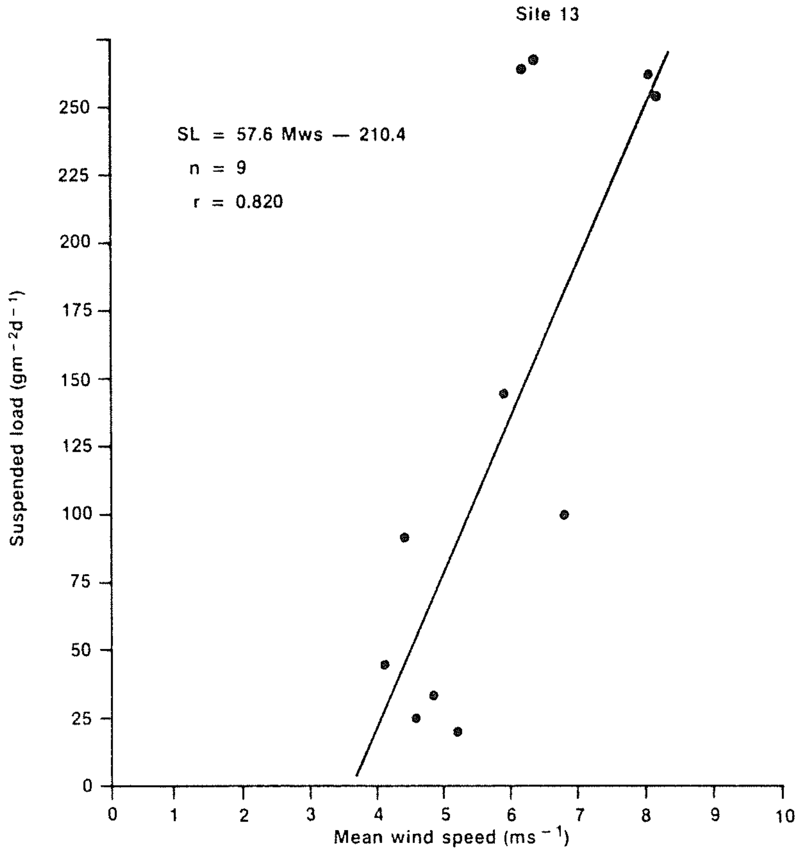

Figure 5.14 The relationship between suspended load and mean wind speed at Site 13.

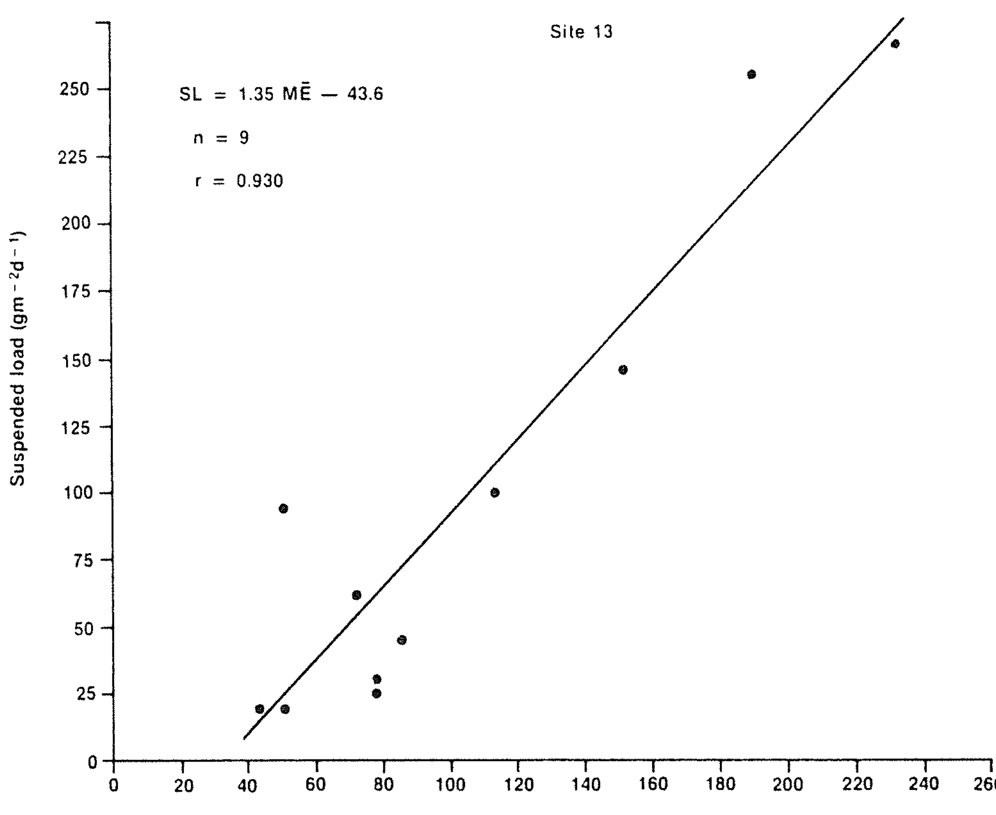

Figure 5.15 The relationship between suspended load and the index for mean specific wave energy at Site 13.

There was no significant difference in suspended load between the summer and winter periods at Site 8 (Fig. 5.18).

There were no observed seasonal variations in the composition of trapped material at any of the three study sites.

5.4.4 Spatial variation in suspended load

The sites monitored for suspended load were separated into two categories according to depth. The shallow sites (1,2,4,8,13) with single arrays ranged in depth from 1.5 m to 4 m (below MLW), while the deeper sites with paired arrays (5,7,10,11) ranged in depth from 11.5 m to 20 m (below MLW). Suspended loads at different sites were compared only within these two categories and not between them.

Single array sites:

Statistical analysis of seasonal trends in suspended loads for Sites 2 and 4 was not possible because of low sample numbers. The mean suspended load at shallow offshore Site 8 was significantly lower than at the shallow inshore Site 1 (t_{20} = 3.420 $p < 0.0025$; Fig. 5.16 and Fig. 5.18). When the data are separated into periods of 'summer' and 'winter', loads were

Table 5.3 Significant relationships of suspended load (total and component proportions) with mean wind speed (MWS) and the index for mean specific wave energy (ME) at three shallow sites.

Site	Environmental factors	Relationship	Significance
1	Suspended load and MWS	r_{11} = 0.793, Y= 20.95x - 32.74	P<0.001
	Suspended load and $M\bar{E}$	r_{12} = 0.809, Y= 0.781x + 12.64	P<0.0005
	Organic suspended load and MWS	r_{11} = 0.752, Y= 2.32 x + 0.34	P<0.0025
	Organic suspended load and $M\bar{E}$	r_{12} = 0.750, Y= 0.086x = 5.43	P<0.001
	$CaCO_3$ suspended load and MWS	r_{11} = 0.692, Y= 8.61 x - 17.73	P<0.005
	$CaCO_3$ suspended load and $M\bar{E}$	r_{12} = 0.793, Y= 0.33 x - 1.26	P<0.0005
	Refractory suspended load and MWS	r_{11} = 0.826, Y= 10.67x - 17.39	P<0.0005
	Refractory suspended load and $M\bar{E}$	r_{12} = 0.795, Y= 0.365x + 8.05	P<0.0005
	MWS and $M\bar{E}$	r_{10} = 0.798, Y= 0.026x + 3.02	P<0.001
8	Suspended load and $M\bar{E}$	r_{11} = 0.711, Y= 0.029x + 19.73	P<0.005
	Organic load and $M\bar{E}$	r_{11} = 0.664, Y= 0.006x + 3.99	P<0.01
	$CaCO_3$ load and $M\bar{E}$	r_{11} = 0.572, Y= 0.012x + 11.32	P<0.05
13	Suspended load and MWS	r_9 = 0.820, Y= 57.6 x -210.4	P<0.001
	Suspended load and $M\bar{E}$	r_9 = 0.930, Y= 1.35x - 43.6	P<0.0005
	Organic suspended load and MWS	r_9 = 0.823, Y= 6.55x - 20.3	P<0.001
	Organic suspended load and $M\bar{E}$	r_9 = 0.915, Y= 1.56x - 1.52	P<0.0005
	$CaCO_3$ suspended load and MWS	r_9 = 0.790, Y= 24.91x - 94.83	P<0.0025
	$CaCO_3$ suspended load and $M\bar{E}$	r_9 = 0.940, Y= 0.60x - 25.37	P<0.0005
	Refractory suspended load and MWS	r_9 = 0.836, Y= 26.1 x - 95.24	P<0.001
	Refractory suspended load and $M\bar{E}$	r_9 = 0.907, Y= 0.59x - 16.79	P<0.0005
	MWS and $M\bar{E}$	r_8 = 0.728, Y= 36.40x - 88.89	P<0.01

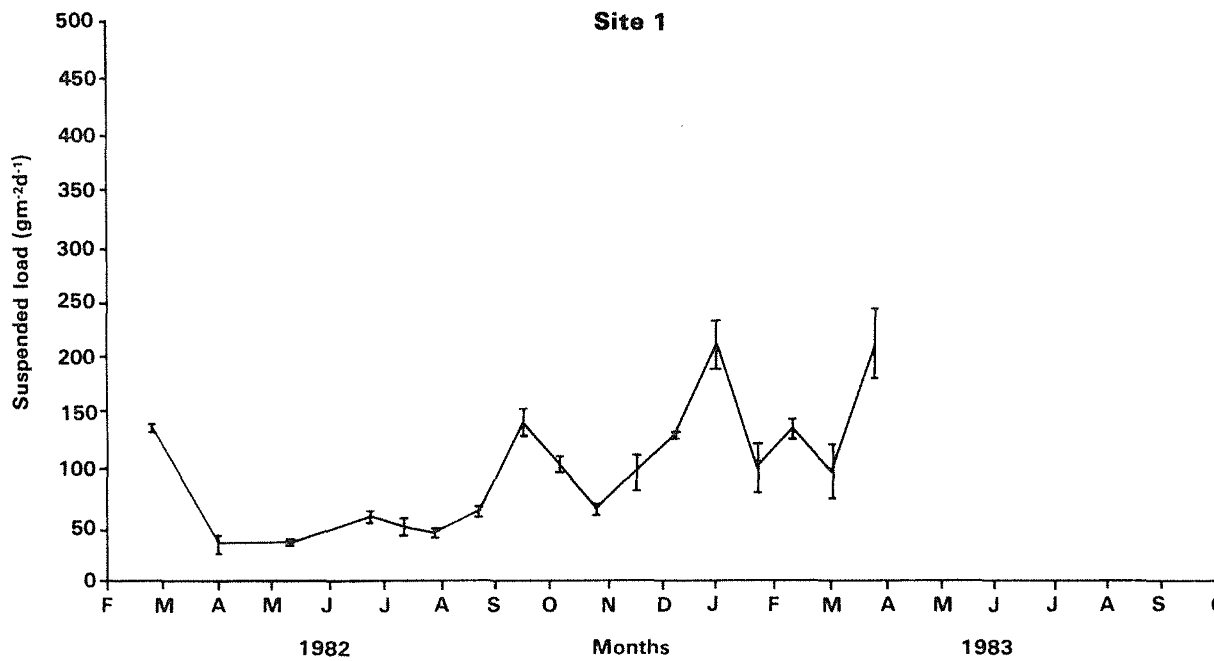

Figure 5.16 Suspended loads between February 1982 and March 1983 at Site 1. Peaks in January and March-April 1983 coincide with the timing of cyclones 'Jane' and 'Lena'.

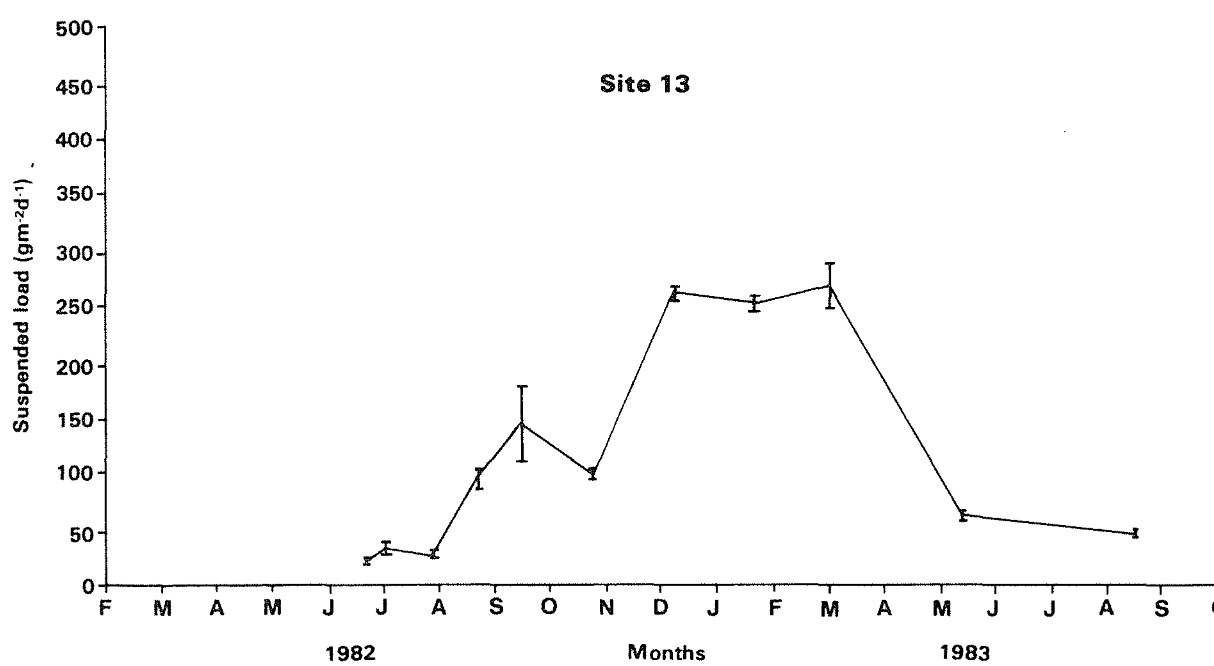

Figure 5.17 Suspended loads between June 1982 and August 1983 at Site 13.

significantly lower at Site 8 than at Site 1 in summer (t_{10} = 4.450, $p < 0.002$) but not significantly different in winter. The only period during summer when the suspended load at Site 8 exceeded that at Site 1 was in March-April 1983, when cyclone 'Lena' affected the area (Fig. 5.18).

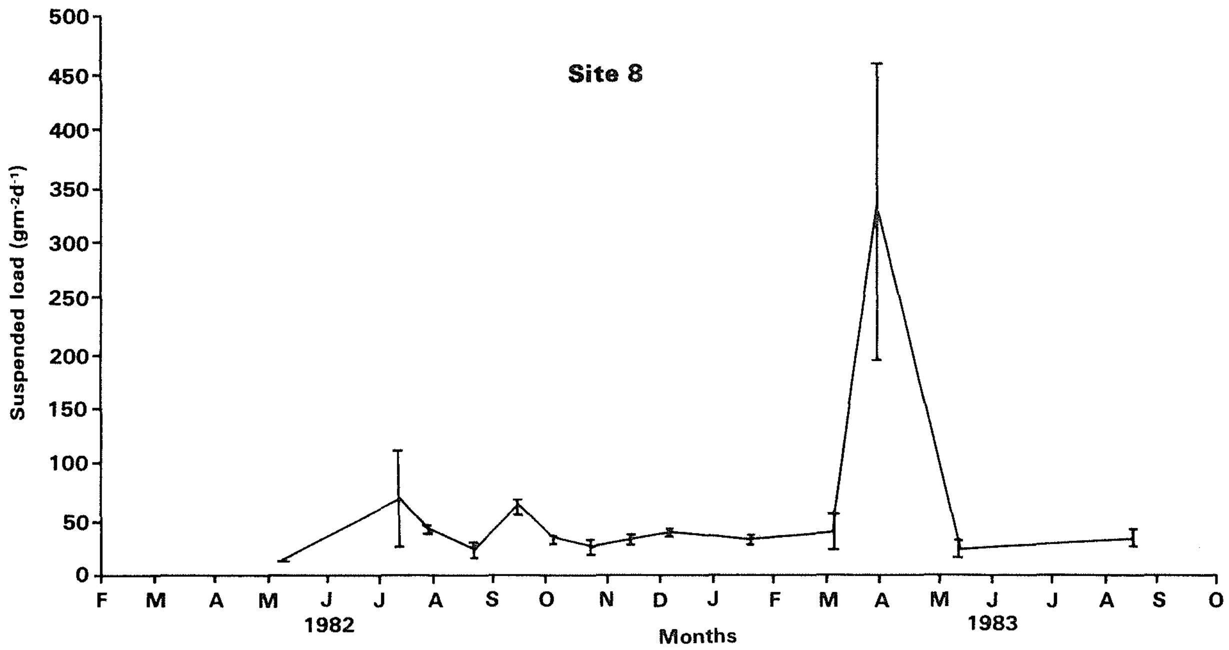

Figure 5.18 Suspended load between May 1982 and August 1983 at Site 8. The peak in March-April 1983 coincides with the timing of cyclone 'Lena'.

The mean suspended loads over the entire monitoring period at the two inshore Sites, 1 and 13, were not significantly different (Fig. 5.16 and Fig. 5.17). The loads over the summer period, however, were significantly higher at Site 13 (t_8 = 2.687, $p < 0.0276$). There were no significant differences over the winter period.

On the other hand, the mean suspended load at inshore Site 13 was significantly higher than offshore Site 8 (t_8 = 2.91, $p < 0.01$ Fig. 5.17 and Fig. 5.18). This difference arose from the higher values over the summer period (t_8 = 4.7645, $p < 0.0015$), as the winter loads were not significantly different.

Thus suspended load was greater inshore than offshore. It was also greater in summer than in winter at inshore sites. No such seasonal difference was recorded at the shallow offshore site.

The composition of suspended matter at the three inshore shallow sites, 1, 2 and 13, was not significantly different. (Table 5.4a, b).

The percentage of organic material in the suspended load was significantly higher at offshore Site 8 than at any other site (Table 5.4a, b).

Table 5.4a Significant differences between shallow sites in content of suspended load.

Fraction	Site	t value	Significance
Mean proportion (%) of organic content	8 > 1	2.74	$p < 0.01$
	8 > 2	3.02	$p < 0.005$
	8 > 13	2.70	$p < 0.01$
	8 > 4	4.03	$p < 0.001$
Mean proportion (%) of Ca CO_3 content	8 > 1	2.76	$p < 0.01$
	4 > 1	5.48	$p < 0.0005$
	4 > 2	4.37	$p < 0.001$
	4 > 13	3.97	$p < 0.0025$
	4 > 8	2.80	$p < 0.01$
Mean proportion (%) of refractory content	1 > 8	5.03	$p < 0.0005$
	2 > 8	3.72	$p < 0.0025$
	13 > 8	2.95	$p < 0.01$
	1 > 4	6.79	$p < 0.0005$
	2 > 4	5.57	$p < 0.0005$
	13 > 4	4.24	$p < 0.001$

Table 5.4b Proportions (%) of the organic, calcium carbonate and refractory material in the mean suspended load at each shallow site.

Fraction	Site 1	Site 2	Site 4	Site 8	Site 13
Organic %	17.8	17.4	13.8	23.3	17.8
$CaCO_3$ %	32.8	37.5	62.6	43.8	37.4
Refractory %	49.0	45.0	24.6	32.7	46.0

The percentage of calcium carbonate in the suspended load was significantly higher at Site 4 than at any other site (Table 5.4a, b) and was significantly higher at Site 8 than at Site 1 (Table 5.5a, b).

The three inshore Sites, 1, 2 and 13, all had a significantly higher proportion of refractory material than Sites 4 and 8 (Table 5, 4a, b).

Paired array sites

The mean suspended loads at deep Sites 10 and 11 were not significantly different in either the 0.5 m or 6 m arrays. The variations in loads at each site were positively correlated ($r_5 = 0.966$, $p < 0.001$ and $r_5 = 0.962$, $p < 0.001$ for arrays 0.5 m and 6 m above the sea-floor respectively) and were similar over time (Fig. 5.19 for 0.5 m depth).

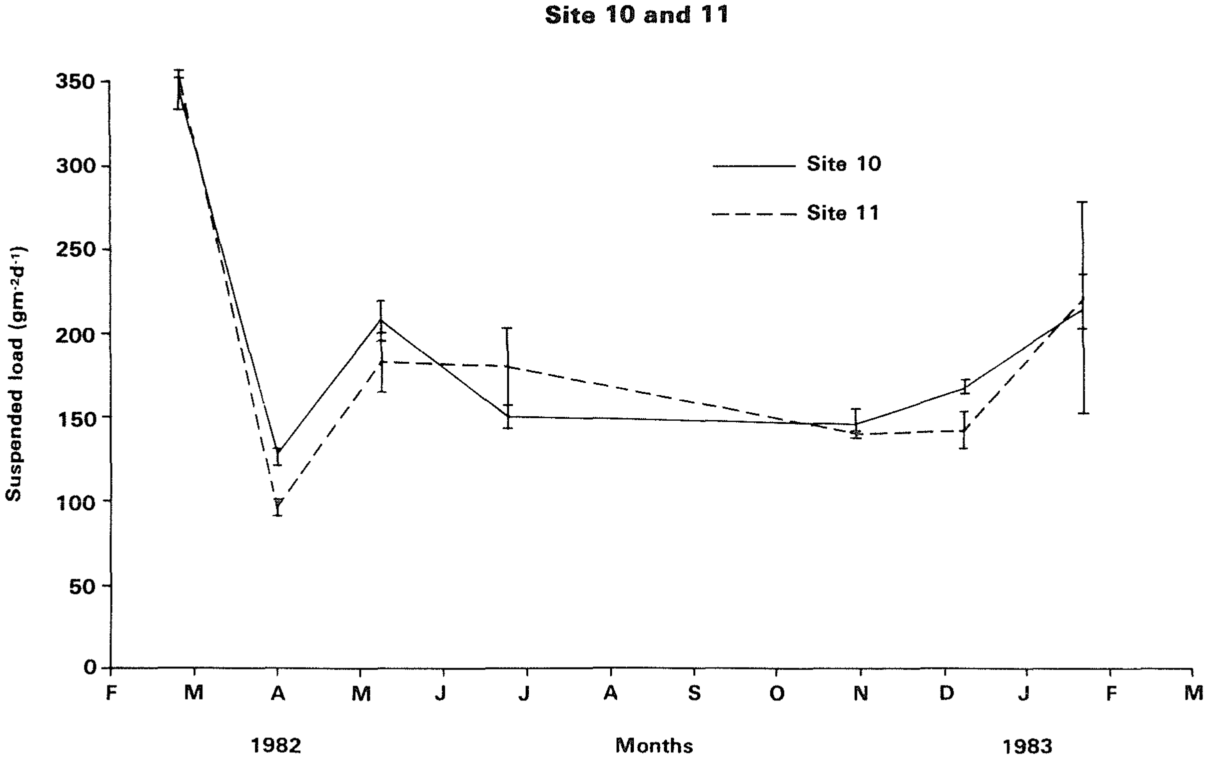

Figure 5.19 Comparison of total suspended load in traps, at 0.5 m deployed concurrently at Sites 10 and 11.

The mean suspended loads for both the 0.5 m and 6 m elevations were significantly lower at Site 7 than Site 10 ($t_{12} = 4.2483$, $p < 0.001$ and $t_{12} = 3.3246$, $p < 0.005$ respectively). The mean suspended load at Site 10, over the same collection periods, was about 4 times greater at the 0.5 m array and 3 times greater at the 6 m array than at Site 7, which is farther offshore ($\bar{x} = 205.5$ g $m^{-2}d^{-1}$ and $\bar{x} = 56.3$ g $m^{-2}d^{-1}$ at the 0.5 m array, Sites 10 and 7 respectively; $\bar{x} = 94.1$ g $m^{-2}d^{-1}$ and 30.4 gm $^{-1}d^{-1}$ at the 6 m arrays, Sites 10 and 7 respectively). Variations with time in sediment loads at Site 7 and 10 were, however, positively correlated (r_5 = 0.896 $p < 0.01$ and r_5 = 0.8411, $p < 0.02$).

The suspended load at Site 5 was significantly greater than at Site 7 (t_8 = 2.702, $p < 0.025$) but was not significantly different from that at Site 10. Variations in sediment loads at Site 5 were, however, significantly correlated with those at Sites 7 and 10 (r_3 = 0.981, $p < 0.005$ and r_3 = 0.889, $p < 0.005$ respectively).

The mean proportion (%) of organic material in the suspended load was significantly higher at Site 7 than at Sites 5, 10 and 11 (Table 5.5a, b).

Table 5.5a Significant differences of suspended loads between deep sites with paired arrays.

Fraction	Sites	t value	Significance
Mean proportion (%) of organic content	7 > 5	2.893	$p < 0.01$
	7 > 10	3.170	$p < 0.005$
	7 > 11	2.050	$p < 0.05$
Mean proportion (%) of $CaCO_3$ content	5 > 11	4.593	$p < 0.0005$
	7 > 11	2.730	$p < 0.01$
	10 > 11	6.814	$p < 0.0005$
	10 > 7	2.240	$p < 0.025$
Mean proportion (%) refractory content	11 > 5	5.357	$p < 0.0005$
	11 > 7	7.044	$p < 0.0005$
	11 > 10	7.485	$p < 0.0005$

Table 5.5b* Proportions (%) of the organic, calcium carbonate and refractory material in the mean suspended load at each of the sites with paired arrays.

Fraction	Site 5	Site 7	Site 10	Site 11
Organic %	15.3	20.1	15.3	16.5
$CaCO_3$ %	37.5	33.6	39.4	27.1
Refractory %	47.1	46.3	45.6	55.8

* Data presented here are only from sediment traps at 0.5 m above sea-floor.

The mean proportion (%) of calcium carbonate in the suspended load was significantly lower at Site 11 than at Sites 5, 7 and 10. The mean proportion (%) of refractory matter at Site 11, however, was significantly greater than at Sites 5, 7 and 10 (Table 5.5a, b).

5.5 DISCUSSION

The results of the aspect ratio experiment conducted in Mermaid Sound are consistent with the findings of earlier workers (Hoskin et al, 1978; Gardner, 1980b; Hargrave & Burns, 1979). The sediment traps of aspect ratio 2 lack an effective turbulent-free boundary zone, resulting in resuspension and loss of trapped material from the sediment traps, and consistently collected less material than the other traps. The low collection rates of sediment traps with aspect ratio 4, when suspended at 6.5 m or 8.5 m above the sea-floor, are attributed to a similar phenomenon: when close to the surface, they are subject to more energetic conditions than traps in deeper water. Gardner (1980a) found sediment traps with aspect ratios between 2 and 3 to be suitable in low energy conditions (<0.095 ms^{-1} current speed). The inefficiency, in more energetic conditions, of the sediment traps with an aspect ratio of ≤4 make their use inappropriate in such high energy areas as Site 8.

The inconsistency between replicates and the low collection rate obtained from traps of aspect ratio 10, 0.5 m above the sea-floor, may have been caused by analytical technique. The length of these traps (500 mm) reduced the efficiency of the decanting procedure and more water was required to remove the sample. This increased the opportunity for error and may have caused the low value obtained from the traps at 0.5 m. In response to the findings of this study, sediment traps of aspect ratio 6 were used in the monitoring programme.

Suspended load decreased proportionately with height above the sea-floor. This is consistent with the findings of Tsunogai et al (1980) in Funka Bay, Japan, who concluded that higher loads measured near the sea-floor were caused by resuspension of fine material from bottom sediments. The height above the sea-floor, to which material will be resuspended, is dependent upon the energy available and the cohesion and fall velocity of the sediments. The suspended load will, therefore, be greatest near the sea-floor and decrease with height above it.

Another factor contributing to higher loads near the sea-floor may be the resuspension of material in distant locations and subsequent transport by currents into the study area. This material may be derived from dredging activities, resuspension in more energetic areas, or from fluviatile inputs. In non-turbulent water, however, it will migrate downwards at fall velocity, irrespective of origin thus being progressively depleted from the surface water with time.

The pattern of the organic, calcium carbonate and refractory fractions, which all demonstrate decreasing load with height above the sea-floor, suggests that all fractions are influenced by the same processes. The consistently differing composition of suspended material with height, however, indicates varying responses to those processes. The greater proportion of organic material, compared with other fractions in the suspended load at 6 m, suggests a higher fall velocity for the non-organic material; that is, the organic fractions remain suspended longer than the non-organic fractions.

Another factor which can contribute to greater proportions of organic matter near the water surface is the production of organic matter on, or near, the surface. This material (e.g. faecal pellets or dead plankton) should maintain a constant concentration throughout the water column, (Hoskin et al, 1978). If the flux density of resuspended material decreases with height however, the relative percentage of the non-organic fraction within the total suspended load will decrease with height, thus increasing the organic proportion, as was found in Mermaid Sound.

Some organic material in suspension will possess fall velocities identical to the inorganic material, as all marine surface sediments have a covering of organic material (Hargrave & Phillips, 1977; Jumors et al,1980). Micro-organisms such as diatoms, blue-green algae and bacteria account for most of this material. These organisms possess slime sheaths by which they attach to sediments (Risk & Yeo, 1980, Parmenter et al, 1983).

The trend of a decreasing proportion of calcium carbonate in the suspended load, with height above the sea-floor, was not as consistent as the opposite trend, observed for organic content. This inconsistency may result partly from variation within the analytical technique (the replicates for calcium carbonate determination being more variable than for organic analysis), or partly from inputs of biogenic calcium carbonate originating in the water column (e.g. Foraminifera). This trend, however, suggests that some fraction of the suspended calcium carbonate material had a higher fall velocity than the organic or refractory matter. According to Stokes Law, grain size and specific gravity (of both the particles and the medium) determine particle fall velocity. The specific gravity of calcium carbonate and refractory material (mainly terrigenous silicates: Talbot and Creagh, 1985) were similar, with ranges of 2.71-2.91 and 2.6-2.75 respectively. This implies that a larger grain size was responsible for the lower rates of resuspension of the calcium carbonate material than those of the refractory material. A comparison of the composition of the surface sediments and material collected in sediment traps supports this view. The sediments were largely composed of calcium carbonate materials at all sites except Site 11 (Table 5.2), and carbonate always formed a higher percentage in the sediments than in trapped material (Appendix 1).

In addition to this vertical variation, seasonal variation was evident. The suspended load, which was significantly higher in summer than in winter at Sites 1 and 13, was consistent with the seasonal change in light attenuation found over the same period (Chapter 4). This variation in suspended load was related to the wind and wave conditions. The correlation of suspended load with wind speed and the index for wave energy at inshore sites implies that direct resuspension of sediments, through locally-induced waves, was the major mechanism determining variations in suspended load.

Mechanisms responsible for changes in suspended sediment loads at Site 8 appeared to differ from those operating at sites farther inshore. At Site 8, suspended load was not related to wind speed nor was it seasonal. The suspended load was, however, correlated to the index for wave energy. The low correlation between wind speed and wave energy indicated that another factor was contributing to wave conditions and resuspension of material. Observations of long period waves, breaking on the outer escarpment (Lawson & Treloar, 1983), indicated that swell energy was that factor. The correlation between swell energy and suspended load indicated that resuspension of local sediments was the major cause of variation in suspended load at Site 8. This was further supported by the correlation between mean suspended load and peak wave energy over the period sampled. The r^2 value for the correlation between the index for mean specific wave energy and suspended load, of approximately 0.5, indicates, however, that other factors could influence variations in suspended load. The influx of water, e.g. tidal movement with varying suspended loads, from other areas could account for some of this (Chapter 4).

The sediment distribution in the Sound (Lawson & Treloar, 1983) is partly a consequence of energy characteristics (Chapter 2). Fine material is proportionately less in the outer areas (Lawson & Treloar, 1983) where the sea-floor is typically limestone pavements and rubbles (Semeniuk et al, 1982). Sediment deposits become progressively finer farther into the Sound, ranging from sands to muds with clay-sized particles as the energy regime decreases (Lawson & Treloar, 1983).

Offshore sediments are predominantly calcareous, being mainly modern skeletal remains of molluscs, bryozoa, calcareous algae, foraminifera and hermatypic corals. These corals are prevalent in areas along the outer escarpment, and are damaged by wave action associated with storm events. The sediment generated by these events is removed by currents and deposited in less energetic areas: for instance, the deposits of modern debris south of Courtenay Shoal and north of Nelson Rocks. Both of these sediment deposits are thought to have originated from coral reefs at Nelson Rocks (Lawson & Treloar, 1983).

The sediments in the southern sector of the Sound are composed predominantly of terrigenous silicates. The source of this fine material is fluviatile runoff and shoreline erosion: hence it is a consequence of rain and wave energy (Lawson and Treloar, 1983). Tropical cyclones, therefore, are important contributing factors to these sediment deposits.

Cyclones may have peak gusts of 63.9 ms^{-1} (230 km h^{-1}) (Chapter 2), and may result in storm beach deposits to elevations of 8.5 m above mean sea level near Dampier (Lawson & Treloar, 1983). Cyclones generate both swell and high energy local waves; hence they accelerate the erosional and depositional processes operating in both the outer and inner areas. Cyclones may also cause abnormal currents, with extended periods of unidirectional flow and increased current speed (Chapter 3). These conditions, combined with the observed large scale resuspension of sediments under cyclonic conditions, provide a mechanism for marked redistribution of marine sediments.

An indication of the degree of such local resuspension can be gained from the sediment traps deployed at Dampier when cyclonic effects were evident. Lengthy deployments, at Sites 1 and 8, started in December 1982 and March 1983 and so covered the period when cyclones 'Jane' and 'Lena' occurred. Deployment periods at Site 1 were for 34 and 40 days respectively. On both occasions mean suspended loads were about 210 gm^{-2} d^{-1}. These loads were the highest measured at Site 1, and were 64-118% greater than loads measured immediately before or after the cyclone periods.

It is believed that Site 8 was not affected by dredging; however, the sediment trap was partially damaged, presumably by cyclone-generated waves during the January period. One arm was snapped from the array and all the collection cylinders were detached from the remaining arms. Some of the traps were also lost during cyclone 'Lena' in April; however, sufficient data were recovered to indicate the suspended load. That load, averaged over a 40 day period, was 348 gm^{-2} d^{-1}: an order of magnitude greater than loads measured immediately before. Most of this material was coarse and calcium carbonate made up 75% of its content. The high fall velocity of such material indicates that it was the product of local short-term resuspension, probably over the five days when direct cyclone effects were evident. The material of smaller grain size would, however, be resuspended for longer periods and, therefore, be available for transport by currents prevailing during that period.

Sediment trap data were scarce also from Cohen Island, Gidley Island and Angel Island chain (Sites 4 and 5); areas exposed to heavy weather. No data were collected when sea conditions were unsuitable for diver access to the traps, and when traps were damaged or lost. The largest loads measured during the monitoring programme were from this area, at Site 4, near Gidley Island. The high calcium carbonate content (Appendix 1) combined with the sandy nature of the material collected in those sediment traps, indicated short-term resuspension as responsible for much of that suspended load. These sands were white indicating that they were of recent origin (Chapter 1) and may have been derived from the extensive coral reefs of Hammersley Shoal and the more patchy reefs of the island chain.

Although the deeper sites varied in location, depth, type of seabed and energy regime, the pattern of variation in suspended loads at each site was similar. This indicates that common processes may cause the variations in suspended load at all sites. These could be direct resuspension mechanisms, such as wave action, or some indirect process involving transport of suspended material. This similarity in trends of suspended load was particularly evident at Sites 10 and 11. Although these sites were 7 km apart, and varied in depth and surface sediment composition, the loads (as well as the pattern of variation) were similar over the monitoring period. However, the trapped sediments at Site 10 were of larger grain size and had a greater calcium carbonate content than those of Site 11.

The higher fall velocity of the sediments and the increased water depth at Site 10 was apparently negated by the more energetic conditions there, than at Site 11, resulting in similar suspended loads. Vertical light attenuation values from the two sites (Chapter 4), and observations by divers replacing and cleaning the traps, suggested that the water was more turbid at Site 11 than 10. This indicated that the material in suspension at Site 11 was, like the bottom sediments, finer than that at Site 10; a decrease in grain size results in an increase in surface area for equivalent mass, thus increasing light attenuation for similar suspended loads.

The dredging operations in progress over the 1982-83 summer period might have biased the monitoring programme's data. Operations which could have affected the inshore areas include the dredging of the island berth turning basin and the submarine trunkline backfill (Chapter 1). Although the dredging of the turning basin resulted in obvious widespread increase in light attenuation in adjacent waters (Chapter 4) there is evidence to suggest that the effects upon Site 1 were minimal. Observations made while visiting the sediment traps indicated that the area was locally sheltered, with less turbid water than that surrounding it. This conclusion was supported by aerial reconnaissance and photography in December 1983.

These dredging operations, however, could have had more effect on the suspended loads at Site 13. Widespread turbid water was observed around the dredge sites and sediment trap Site 13. Suspended loads at Site 13 were uniformly higher, between December 1982 and March 1983, by 260% and 425% respectively, than the loads immediately before or after (Appendix 1). Suspended loads at Sites 1 and 13 before December were similar, but varied widely during the dredge period (Fig. 5.16 and 5.17), possibly indicating the effect of resuspended spoil at Site 13. Further circumstantial evidence of atypical conditions at Site 13 over the summer period was the uniform suspended load recorded despite varying wind speed. Suspended loads inshore were found to correlate with wind speed, but, in March, when the maximum load was recorded at that site, mean wind speed was more than 20% lower than on the previous sampling occasions. Without summer data recorded prior to dredging operations for this site, no conclusions can be made as to the extent of trapped sediment contributed by dredging.

Thus, effects of dredging, although widespread, mainly influenced one sampling site, Site 13, where unusually high sediment loads were recorded. Effects at Site 1 were minimal despite its proximity to the operations.

SUMMARY

WIND ENERGY

- Local wind conditions in the Dampier Archipelago were monitored between September 1981 and July 1983 using a Woeffle anemometer. Woodside Offshore Petroleum Pty Ltd supplied measurements of wave conditions from within and beyond the Archipelago, over the period May 1980 to December 1982.

- Winds had a seasonal pattern, with the summer winds occurring predominantly from the west, while the winter winds were mainly from the south and east.

- Locally generated wind waves and oceanic swell waves were more energetic at the offshore measuring sites than at the site within Mermaid Sound. An index of wave energy was between six and 64 times greater offshore than inshore over the monitoring period.

- Tropical cyclones are the most intensely energetic natural events occurring in the area. They destroy calcareous structures, such as corals, and severely disturb the benthos. This damage is evident in subsequent years.

- The effects of a cyclone on the Archipelago depend on its severity, origin and trajectory. Cyclones passing through or just seaward of the Archipelago are the most disruptive.

WATER MOVEMENT

- Water movement was monitored between 1981 and 1984 in and around the Dampier Archipelago using untethered trivane drogues and moored acoustic current meters. Physical structure was recorded using a temperature-salinity bridge.

. Instantaneous water movements are caused mainly by the semi-diurnal tides, but, because they reciprocate they contribute little to longer term circulation. This is affected mainly by seasonal variations in wind condition and to a lesser extent by density structure.

. The summer winds drive water in an easterly direction past the islands to the west of Burrup Peninsula and northwards through Mermaid Sound, while the winter winds generate a reverse flow. The most extreme wind-generated currents occur during the passage of cyclones.

. Variations in density structure result in a subsurface exodus of dense inshore water from the Sound during the winter period, and a northerly movement of less dense surface waters from the Sound over the summer period.

LIGHT ATTENUATION

. Six series of light profiles were recorded from throughout Mermaid Sound between April 1982 and March 1983. In addition, in March and December 1983 water samples from the Dampier Archipelago were collected concurrently with the measurement of light attenuation profiles. The samples were assessed for suspended matter content.

. March 1983 data showed a linear relationship between light attenuation and dry weight of suspended matter. December 1983 data showed no such relationship possibly because of variations in composition of suspended matter and sporadic blooms of the blue-green alga, *Trichodesmium* .

. The light attenuation properties of water in Mermaid Sound varied; the offshore areas were always less turbid than those inshore, while the entire area was more turbid in summer than in winter.

- The seasonal variations in wind condition, water temperature and water structure were thought to be responsible for the temporal variation in light attenuation.

- The effects of dredging were observed in December 1982. They caused increased turbidity over areas at least 10 km from the site of operation.

VARIATION IN SUSPENDED LOAD

- An initial experiment was undertaken in September 1981 to find a sediment trap design suitable for use in the Dampier Archipelago. The chosen design was an open topped cylindrical trap of aspect ratio 6 and internal diameter 50 mm. Traps of this design were deployed at 10 sites in Mermaid Sound between November 1981 and August 1983.

- There was an inverse correlation between suspended load and height above the sea-floor indicating that sediment was being resuspended.

- The composition of suspended material varied with height. The organic fraction was greatest near the water surface and the calcium carbonate fraction greatest near the sea-floor.

- Suspended load was consistently higher at a shallow inshore site, than at a comparable site on the outer escarpment.

- The suspended loads at two shallow inshore sites were greater in summer than in winter.

- The highest collection rates occurred near Gidley Island; apparently the product of short-term resuspension of sediment by wave action.

- Mean wind speed, the index for mean specific wave energy and suspended load were all significantly correlated at a shallow inshore site, indicating that local wind conditions regulated wave energy which in turn affected suspended load by resuspending bottom sediments.

. At a shallow offshore site suspended load was correlated with the index for mean specific wave energy, but not with mean wind speed. A combination of wind induced waves and swell energy was likely to have caused resuspension, and hence variations in suspended load, at that site.

. Very high suspended loads, obtained from both an inshore and offshore site after the passing of a cyclone, were evidence that tropical cyclones can cause large scale, short-term resuspension. Cyclones also generate abnormal currents which flow in one direction for extended periods and thus are responsible for the relocation of massive quantities of sediment suspended in the water column.

Considerable damage to benthic communities and accumulations of calcareous rubble and sands were features observed in Mermaid Sound after cyclones. Rainfall, causing erosion of the hinterland associated with these events, is responsible for some terrigenous sediment input to the Sound.

. Further monitoring for background levels of suspended sediment should include a full summer period during which no dredging activities occur in the area of study.

REFERENCES

Aller, R.C. & Dodge, R.E. (1974). Animal sediment relations in a tropical lagoon Discovery Bay, Jamaica. *Journal of Marine Research* **32**, 209-32.

Bak, R.P.M & Elgershuizen, J.H.B.W (1976). Patterns of oil-sediment rejection in corals. *Marine Biology* **37**, 105-13.

Bakus, G.J. (1969). Some effects of sedimentation on benthic invertebrates of atoll lagoons, Lagunas costeras, in Simposio-Mem. Simp. Intern. Lagunas costeras UNAM-UNESCO Nov 28-30, MEXICO: 503-4.

Biggs, E.R. & Denman, P.D. (1981). Dampier Archipelago limestones and limesands, Geological Survey of Western Australia, Record 1978/6.

Blomquist, S. & Hakanson, L. (1981). A review on sediment traps in aquatic environments. *Archives of Hydrobiology* **91**, 101-32.

Bohlen, W.F., Lundy, D.F., & Tramontano, J.M. (1979). Suspended material distributions in the wake of estuarine channel dredging operations. *Estuarine and Coastal Marine Science* 9, 699-711.

Bothner, M.H., Parmenter, C.M. & William, J.D. (1981). Temporal and spatial variations in suspended matter in continental shelf and slope waters of north-eastern United States. *Estuarine, Coastal and Shelf Science* **13**, 213-234.

Brewer, P.G., Spenser, D.W., Biscay, P.E., Harley, A., Sachs, D.L., Smith, C.C., Kadar, S. & Fredericks, J. (1976). The distribution of particulate matter in the Atlantic Ocean. *Earth and Planetary Science Letters* **32**, 393-402.

Chalker, B.E., Dunlap, W.C. & Oliver, J.K. (1983). Bathymetric adaptations of reef-building corals at Davis Reef, Great Barrier Reef, Australia. 11, Light saturation curves for photosynthesis and respiration. *Journal of Experimental Marine Biology and Ecology* **73**, 37-56.

Chapman, V.J., & Chapman, D.J. (1973). 'The Algae', 2nd edition, (Macmillan: London).

Chittleborough, R.G. (1983). The Dampier Archipelago Marine Study: A progress report. Bulletin No. 141, (Western Australian Department of Conservation and Environment, Perth 12pp.

Department of the Interior, Bureau of Meteorology, (1972). Climate survey, north west, Region 6 - Western Australia, (Australian Government Publishing Service, Canberra.)

Duckrow, R.M. & Everhart, W.H. (1971). Turbidity measurement. *American Fisheries Society Transactions* **100**, 682-90.

Duinker, J.C. (1980). Suspended matter in estuaries: Absorption and desorption processes, pp 121-51, *in* E. Olausson & I. Cats (Eds), 'Chemistry and Biogeochemistry of Estuaries', (Wiley: Chichester, New York, Brisbane, Toronto).

Endean, R. (1976). Destruction and recovery of coral reef communities, *in* 'Biology and Geology of Coral Reefs, III' (Academic Press: New York, San Francisco, London).

Folk, R.L. (1968). "Petrology of Sedimentary Rocks". (Hemphill's: Austin).

Gallenne, B. (1974). Study of the fine material in suspension in the estuary of the Loire and its dynamic grading. *Estuarine and Coastal Marine Science* **2**,261-72.

Gardner, W.D. (1980a). Sediment trap dynamics and calibration: a laboratory evaluation. *Journal of Marine Research* **38**, 17-39.

Gardner, W.D. (1980b). Field assessment of sediment traps. *Journal of Marine Research* **38**, 41-51.

Godfrey, J.S. & Ridgeway, K.R. (1985). The large-scale environment of the poleward-flowing Leeuwin current, Western Australia: Longshore steric height gradients, wind stresses and geostrophic flow. *Journal of Physical Oceanography* (in press).

Gordon, D.M. (1983). A preliminary study of the mangroves of the Dampier Archipelago, Western Australia, Environmental Note No. 141 (Western Australian Department of Conservation and Environment Perth), 34pp.

Hargrave, B.T. & Phillip, G.A. (1977). Oxygen uptake of microbial communities on solid surfaces. Pp 545-87, *in* J. Courris (Ed), 'Aquatic Microbial Communities', (Garland: New York).

Hargrave, B.T. & Burns, N.A. (1979). Assessment of sediment trap collection efficiency. *Limnology and Oceanography* **24** (6), 1124-36.

Holloway, P.E. & Nye, H.C. (1985). The Leeuwin current and wind distributions on the southern part of the Australian North West Shelf between January 1982 and July 1983. *Australian Journal of Marine and Freshwater Research* **36**, 123-37.

Hoskin, C.M., Burrell, D.C. & Freitag, G.R. (1978). Suspended Sediment dynamics in Blue Fjord, Western Prince William Sound, Alaska. *Estuarine and Coastal Marine Science* **7** 1-16.

Jerlov, N.G. (1977). Classification of sea water in terms of quanta irradiance. *Journal du Conseil Conseil International pour L'Exploration de la Mer* **37**, 281-87.

Jumano, P.A., Nowell, A.R.M. & Self, R.F.L. (1981). A simple model of flow-sediment organism interactions. *Marine Geology* **42**, 155-72.

Jumors, P.A., Nowell, A.R.M. & Self, R.F.I. (1981). Simple model of flow-sediment-organism interaction. *Marine Geology* **42**, 155-75.

Kirk, J.T.O. (1977). Use of quanta meter to measure attenuation and underwater reflectance of photosynthetically active radiation in some inland and coastal south-eastern Australian waters. *Australian Journal of Marine and Freshwater Research* **28** (1), 9-21.

Kirk, J.T.O. (1981). Monte Carlo study of the nature of the underwater light field in, and the relationships between optical properties of, turbid yellow waters. *Australian Journal of Marine and Freshwater Research* **32**, 517-32.

Kriewaldt, M.J.B. (1964). Dampier and Barrow Island, Western Australia. Western Australian Geological Survey, 1:250,000 Geological Series, Explanatory Notes, 24pp.

Larkum, A.W.D. (1983). The primary productivity of plant communities on coral reefs. Pp 221-30 *in* D.J. Barnes (Ed), 'Perspectives on coral reefs' (Clouston: Manuka).

Lasker, H.R. (1980). Sediment rejection by reef corals: the roles of behaviour and morphology in *Monastrea cavernosa* (Linneaus). *Journal of Experimental Marine Biology and Ecology* **47**, 77-87.

Lawson, & Treloar Pty Ltd. (1981). Coastal Engineering Study - Port of Dampier, Vol III: Current predictions. (Prepared for Hamersley Iron Pty Ltd, Perth).

Lawson & Treloar Pty Ltd. (1983). Coastal Engineering Study - Port of Dampier - Stage 2. Vol IV: Sediment Transport Study. (Prepared for Hamersley Iron Pty Ltd, Perth).

Lourensz, R.A. (1981). Tropical cyclones in the Australian region July 1909 to June 1980. (Australian Government Printing Service, Canberra).

Marsh, L.M. (1978). Report on the corals and some associated invertebrates of the Dampier Archipelago, *In* 'Report on the marine fauna and flora of the Dampier Archipelago,' (Unpublished report, W.A. Museum, Perth).

Mills, D.A. (1985). The development of a numerical hydrodynamic model and its application to the tidal dynamics of the Dampier Archipelago. Bulletin No. 190 (Western Australian Department of Conservation and Environment, Perth). 30pp.

Parmenter, C.M., Bothner, M.H. & Butman, B. (1983). Characteristics of resuspended sediment from Georges Bank collected with a sediment trap. *Estuarine, Coastal and Shelf Science* **17**, 521-533.

Raven, J.A. & Glidewell, F.A. (1975). Photosynthesis, respiration and growth in the shade algae *Hydrodictyon africanum*. *Photosynthetica* **9**, 361-377.

Risk, M.J. & Yeo, R.K. (1980). Animal - Sediment relations in the Minas Basin, Bay of Fundy. Pp 189-194. *In* S.B. McCann (Ed), 'The Coastline of Canada', (Geological Survey of Canada).

Semeniuk, V., Chalmer, P.N. & Le Provost, I. (1982). The marine environments of the Dampier Archipelago, *Journal of* *the Royal Society of Western Australia* **65**, 97-144.

Smith, W.O. (1982). The relative importance of chlorophyll, dissolved and particulate material, and seawater to the vertical extinction of light. *Estuarine, Coastal and Shelf Science* **15**, 459-65.

Soutar, A., Kling, S.A., Crill, P.A., Duffrin, E & Bruland, K.W. (1977). Monitoring the marine environment through sedimentation. *Nature* **266**, 136-39.

Simpson, C.J. (1985). Environmental factors affecting coral growth in the Dampier Archipelago, Western Australia. (Western Australian Department of Conservation and Environment, Perth). Environmental Note No 168. 24pp.

Steedman R.K. & Associates (1982). Prediction of oil spill trajectories for the proposed South Pepper No. 1 exploration well, WA 149P-South of Barrow Island. (Prepared for Mesa Australia Ltd., Perth).

Steedman R.K. & Associates (1983). Wave measurements - Mermaid Sound adjacent to Legendre Island and Withnell Bay, May 1980 to December 1982. (Prepared for Woodside Offshore Petroleum Pty. Ltd., Perth). Document No. A 9620RC045.

Strickland, J.D.H. & Parsons, T.R. (1972). 'A Practical Handbook of Seawater Analysis' (2nd edition). Bulletin No. 167. (Fisheries Research Board of Canada, Ottawa).

Talbot, V. (1985). Heavy metal concentrations in the oysters *Saccostrea cuccullata* and *Saccostrea* sp. from the Dampier Archipelago, Western Australia. *Australian Journal of Marine and Freshwater Research* **36**, 169-75.

Talbot, V. & Creagh, S. (1985a). The derivation of threshold mean concentrations of copper and zinc in seawater, to protect the edible tropical rock oyster, *Saccostrea* *cucullata* from exceeding the health (food) standards. Bulletin 212 (Western Australian Department of Conservation and Environment, Perth). 25pp.

Talbot, V. & Creagh, S. (1985b). Mineralogical variation within the marine sediments of the Dampier region: a dynamic approach, in preparation, (Western Australian Department of Conservation and Environment, Perth). 29pp.

Tsunogai, S., Uematsu, M., Tanaka, N. & Harada, K. (1980). A sediment trap experiment in Funka Bay, Japan: "upward flux" of particulate matter in seawater. *Marine Chemistry* 9, 321-334.

U S Army Coastal Engineering Research Centre (1975). Shore Protection Manual 1, 2nd edn, 2-27.

Woodside Petroleum Development Pty Ltd. (1979). North West Shelf Development Project, Draft Environmental Impact Statement and Environmental Review and Management Programme, B.1-B.24.

Woodside Petroleum Development Pty Ltd. (1980). Environmental conditions in and around Mermaid Sound. Document number A9640RG015.

APPENDIX 1

APPENDIX 1

SEDIMENT TRAP DATA

Sediment traps were deployed in Mermaid Sound from November 1981 to August 1983 inclusive. The mean rate of collection in these sediment traps is expressed as weight per square metre per day ($gm^{-2}d^{-1}$).

The statistic E refers to the one tailed 97.5% confidence interval of the population mean (u), such that

$$E = t_{0.025} \frac{S}{\sqrt{n}}$$

Where S is the standard deviation and n is the sample number. The 95% confidence interval of the population mean is, therefore

$$\bar{x} - E < u < x + E$$

Reference

Lapin, L. (1978). Statistics for modern business decisions, 2nd edition. (Harcourt Brace Jovanovich: New York).

Table 1 Suspended load and composition, 0.5 m above the sea-floor at Site 1.

Date deployed	Total no. days deployed		Total dry weight $gm^{-2}d^{-1}$	ORGANIC Dry weight $gm^{-2}d^{-1}$	ORGANIC %	$CaCO_3$ Dry weight $gm^{-2}d^{-1}$	$CaCO_3$ %	REFRACTORIES Dry weight $gm^{-2}d^{-1}$	REFRACTORIES %
		$\bar{x}$	136.7	16.7	12.2	57.2	41.9	62.8	45.9
21.02.82	9.9	E	3.6	3.6	3.1	6.7	5.0	4.2	2.5
		n	5	5	5	5	5	5	5
		$\bar{x}$	33.0	8.4	25.4	11.0	33.3	13.6	41.1
31.03.82	5.1	E	7.6	1.7	5.0	8.9	21.1	4.6	18.3
		n	7	7	7	4	4	4	4
		$\bar{x}$	34.4	8.3	23.6	9.2	26.5	16.9	49.2
08.04.82	7.0	E	2.0	1.1	3.2	2.7	6.6	1.6	6.1
		n	5	5	5	5	5	5	5
		$\bar{x}$	56.8	10.6	18.7	14.7	25.8	31.5	55.5
22.06.82	8.0	E	4.7	1.7	3.1	3.7	5.6	2.7	2.9
		n	5	5	5	6	5	5	5
		$\bar{x}$	48.1	7.1	14.6	15.0	31.6	25.7	53.4
30.06.82	27.9	E	8.4	0.6	2.4	1.6	5.8	3.7	7.7
		n	5	5	5	5	5	5	5
		$\bar{x}$	42.7	7.7	17.6	14.2	32.7	21.2	49.3
27.07.82	8.0	E	4.2	0.6	1.4	4.6	7.0	1.0	5
		n	5	5	5	4	4	4	4
		$\bar{x}$	62.1	9.2	14.9	20.9	33.5	32.0	51.6
04.08.82	41.0	E	3.5	0.4	1.2	3.0	3.1	10.8	1.9
		n	5	5	5	5	5	5	5
		$\bar{x}$	140.6	20.8	14.8	51.2	36.2	68.6	48.9
14.09.82	8.0	E	12.3	2.0	1.4	11.0	5.0	3.8	4.0
		n	5	5	5	5	5	5	5
		$\bar{x}$	104.3	17.2	16.5	33.8	32.5	53.2	51.0
22.09.82	31.1	E	7.2	3.2	2.2	3.7	5.1	6.4	2.9
		n	4	4	4	4	4	4	4
		$\bar{x}$	64.4	15.2	23.4	12.8	20.1	36.5	56.5
23.10.82	8.9	E	5.2	2.9	4.3	5.0	9.1	6.4	6.2
		n	5	5	5	5	5	5	5

Table 1 (continued)

		$\bar{x}$	96.2	14.2	14.9	33.8	35.0	48.2	50.1
01.11.82	35.2	E	16.1	2.2	2.2	8.0	3.5	8.1	1.9
		n	4	4	4	4	4	4	4
		$\bar{x}$	128.8	17.7	13.6	42.3	32.8	66.8	51.9
06.12.82	7.8	E	3.1	1.5	1.6	5.0	3.0	0.6	1.6
		n	5	5	5	5	5	5	5
		$\bar{x}$	210.4	32.6	15.5	75.0	35.9	102.7	48.7
15.12.82	34.0	E	22.4	6.1	2.1	5.5	4.7	18.7	4.5
		n	5	5	5	5	5	5	5
		$\bar{x}$	100.4	13.7	13.8	43.2	42.3	43.5	43.9
19.01.83	7.0	E	21.6	3.0	3.0	17.1	9.3	6.3	6.6
		n	5	5	5	5	5	5	5
		$\bar{x}$	135.1	19.4	13.3	53.1	39.4	62.6	46.3
25.01.83	36.0	E	9.5	7.3	5.2	14.6	11.4	11.4	7.0
		n	4	4	4	4	4	4	4
		$\bar{x}$	96.7	14.5	15.3	35.31	36.2	46.9	48.5
02.03.83	7.0	E	24.3	3.7	2.6	9.4	3.6	14.6	1.6
		n	5	5	5	5	5	5	5
		$\bar{x}$	211.2	28.0	13.3	89.5	42.0	94.0	44.7
10.03.83	40.0	E	30.7	6.4	3.8	29.9	8.4	9.4	4.6
		n	4	4	4	4	4	4	4

Table 2 Suspended load and composition, 0.5 m above the sea-floor at Site 2.

Date deployed	Total no. days deployed		Total dry weight $gm^{-2}d^{-1}$	ORGANIC Dry weight $gm^{-2}d^{-1}$	ORGANIC %	$CaCO_3$ Dry weight $gm^{-2}d^{-1}$	$CaCO_3$ %	REFRACTORIES Dry weight $gm^{-2}d^{-1}$	REFRACTORIES %
		$\bar{x}$	152.0	28.0	18.3	-	-	-	-
17.11.81	8.0	E	6.7	4.1	2.5	-	-	-	-
		n	8	8	8	-	-	-	-
		$\bar{x}$	19.6	4.8	24.7	10.1	52.0	4.2	21.7
31.03.82	5.1	E	2.9	1.1	5.7	-	-	-	-
		n	4	4	4	1	1	1	1
		$\bar{x}$	38.4	9.0	23.4	13.4	35.6	16.1	44.4
08.05.82	7.0	E	3.2	2.7	6.3	5.7	15.1	4.2	10.4
		n	5	5	5	3	3	3	3
		$\bar{x}$	225.6	31.7	14.1	101.9	45.0	92.0	40.9
22.06.82	7.9	E	45.1	6.1	0.9	23.4	2.4	16.7	1.5
		n	5	5	5	5	5	5	5
		$\bar{x}$	52.2	10.3	19.7	17.1	32.3	25.5	48.2
04.08.82	8.0	E	4.1	1.7	3.2	5.2	8.1	1.9	4.9
		n	5	5	5	5	5	5	5
		$\bar{x}$	376.3	55.3	14.7	161.0	42.9	159.9	42.4
14.09.82	8.0	E	59.8	11.9	0.2	18.0	2.4	30.7	1.6
		n	4	4	4	4	4	4	4
		$\bar{x}$	176.1	26.1	14.9	65.1	36.7	84.9	48.4
06.12.82	7.8	E	51.6	2.0	3.2	32.7	7.4	62.0	15.3
		n	3	3	3	3	3	2	2
		$\bar{x}$	120.9	19.9	16.5	41.0	33.8	60.1	49.8
19.01.83	7.0	E	6.1	3.0	2.6	8.7	6.3	3.5	3.7
		n	5	5	5	5	5	5	5
		$\bar{x}$	212.3	29.1	13.7	81.9	35.6	101.2	47.7
02.03.83	8.0	E	6.3	1.9	0.7	4.7	2.0	4.1	1.2

Table 3a Suspended load and composition, 6 m above the sea-floor at Site 3.

Date deployed	Total no. days deployed		Total dry weight $gm^{-2}d^{-1}$	ORGANIC Dry weight $gm^{-2}d^{-1}$	ORGANIC %	$CaCO_3$ Dry weight $gm^{-2}d^{-1}$	$CaCO_3$ %	REFRACTORIES Dry weight $gm^{-2}d^{-1}$	REFRACTORIES %
		$\bar{x}$	22.5	5.7	25.1	-	-	-	-
17.11.81	8.0	E	0.7	0.8	3.2	-	-	-	-
		n	8	8	8	-	-	-	-
		$\bar{x}$	97.2	11.6	11.9	51.5	51.7	36.1	36.4
22.02.82	7.9	E	4.2	1.4	1.4	72.7	33.2	8.1	19.8
		n	7	7	7	2	2	2	2
		$\bar{x}$	14.5	4.5	33.3	8.4	47.3	2.2	1
31.03.82	5.1	E	3.0	1.1	8.0	6.2	45.6	4.5	31.0
		n	7	7	7	3	3	3	3
		$\bar{x}$	13.7	4.7	34.7	6.1	44.0	2.8	21.3
08.05.82	4.9	E	1.7	0.3	4.8	4.1	23.5	2.4	19.1
		n	4	4	4	4	4	4	4
		$\bar{x}$	13.6	4.2	30.3	1.9	13.2	7.6	56.0
22.06.82	8.0	E	2.7	0.6	5.3	2.0	11.5	0.7	7.3
		n		5	5	5	5	5	5

Table 3b Suspended load and composition, 0.5 m above the sea-floor at Site 3.

Date deployed	Total no days deployed		Total dry weight $gm^{-2}d^{-1}$	ORGANIC Dry weight $gm^{-2}d^{-1}$	ORGANIC %	$CaCO_3$ Dry weight $gm^{-2}d^{-1}$	$CaCO_3$ %	REFRACTORIES Dry weight $gm^{-2}d^{-1}$	REFRACTORIES %
		$\bar{x}$	38.0	8.3	21.8	-	-	-	-
17.11.81	8	E	1.5	1.1	2.6	-	-	-	-
		n	8	8	8	-	-	-	-
		$\bar{x}$	287.6	30.5	10.6	166.6	59.0	87.8	31.1
22.02.82	7.9	E	6.4	3.7	1.2	2.2	5.0	12.6	2.2
		n	9	9	9	3	3	3	3
		$\bar{x}$	25.4	7.2	29.5	9.8	40.5	5.6	26.2
31.03.82	5.1	E	6.3	1.0	5.8	16.4	55.3	8.7	46.6
		n	7	6	6	3	3	3	3
		$\bar{x}$	46.3	11.2	24.5	21.9	48.3	17.0	33.3
08.05.82	4.9	E	5.2	6.1	12.4	25.8	53.1	5.1	32.5
		n	5	5	5	3	3	3	3
		$\bar{x}$	27.0	6.1	22.8	7.1	26.0	13.8	51.2
22.06.82	8.0	E	2.1	1.0	4.3	3.2	11.0	1.7	6.9
		n	5	5	5	5	5	5	5

Table 4 Suspended load and composition, 0.5 m above the sea-floor at Site 4.

Date deployed	Total no. days deployed		Total dry weight $gm^{-2}d^{-1}$	ORGANIC Dry weight $gm^{-2}d^{-1}$	ORGANIC %	$CaCO_3$ Dry weight $gm^{-2}d^{-1}$	$CaCO_3$ %	REFRACTORIES Dry weight $gm^{-2}d^{-1}$	REFRACTORIES %
		$\bar{x}$	64.7	12.1	18.8	-	-	-	-
17.11.81	8.0	E	5.7	1.5	2.5	-	-	-	-
		n	9	9	9	-	-	-	-
		$\bar{x}$	159.3	34.1	21.5	69.2	43.4	5.6	35.2
08.05.82	6.0	E	9.5	4.3	2.5	9.8	5.5	5.3	3.0
		n	5	5	5	5	5	5	5
		$\bar{x}$	338.3	35.5	9.2	291.5	75.0	61.3	15.8
22.06.82	8.0	E	33.4	5.5	1.4	33.5	4.0	10.0	2.6
		n	5	5	5	5	5	5	5
		$\bar{x}$	408.5	34.5	8.4	315.3	77.3	61.1	14.3
04.08.82	8.0	E	51.8	5.3	0.7	40.4	1.7	2.6	1.1
		n	5	5	5	5	5	5	5
		$\bar{x}$	803.3	81.7	10.2	521.9	64.8	199.7	25.0
14.09.82	8.0	E	106.5	6.2	1.0	94.5	3.1	12.9	2.1
		n	5	5	5	5	5	5	5
		$\bar{x}$	128.3	18.8	14.7	67.6	52.7	41.8	32.6
23.10.82	8.0	E	6.7	1.0	1.0	7.6	4.0	3.0	2.9
		n	4	4	4	4	4	4	4

Table 5a Suspended load and composition, 0.5 m above the sea-floor at Site 5.

Date deployed	Total no. days deployed		Total dry weight $gm^{-2}d^{-1}$	ORGANIC Dry weight $gm^{-2}d^{-1}$	ORGANIC %	$CaCO_3$ Dry weight $gm^{-2}d^{-1}$	$CaCO_3$ %	REFRACTORIES Dry weight $gm^{-2}d^{-1}$	REFRACTORIES %
		$\bar{x}$	73.4	12.7	19.6	-	-	-	-
17.11.81	8.0	E	4.2	2.7	2.9	-	-	-	-
		n	6	6	6	-	-	-	-
		$\bar{x}$	181.1	27.0	14.9	65.1	36.0	89.0	49.1
23.02.82	8.0	E	4.2	2.1	1.0	3.4	2.1	3.8	1.2
		n	7	7	7	7	7	7	7
		$\bar{x}$	22.9	4.4	18.3	10.8	40.3	10.0	35.1
08.05.82	5.9	E	5.2	1.1	4.1	4.1	10.7	3.0	19.0
		n	5	5	5	5	5	5	5
		$\bar{x}$	21.9	6.0	26.5	11.2	50.6	6.9	30.8
04.08.82	8.0	E	5.8	1.6	1.9	5.3	15.3	2.2	9.7
		n	5	5	5	5	5	5	5
		$\bar{x}$	33.1	6.3	19.0	10.4	31.5	16.4	49.4
23.10.82	8.9	E	2.1	2.7	7.9	6.1	18.2	3.7	10.3
		n	5	5	5	5	5	5	5

Table 5b Suspended load and composition, 0.5 m above the sea-floor at Site 5.

Date deployed	Total no. days deployed		Total dry weight $gm^{-2}d^{-1}$	ORGANIC Dry weight $gm^{-2}d^{-1}$	ORGANIC %	$CaCO_3$ Dry weight $gm^{-2}d^{-1}$	$CaCO_3$ %	REFRACTORIES Dry weight $gm^{-2}d^{-1}$	REFRACTORIES %
		$\bar{x}$	216.6	30.8	14.2	-	-	-	-
17.11.81	8.0	E	4.9	3.1	1.4	-	-	-	-
		n	8	8	8	-	-	-	-
		$\bar{x}$	315.6	52.8	15.1	123.8	35.1	177.0	49.8
23.02.82	8.0	E	11.0	8.1	2.6	23.2	6.1	9.8	3.5
		n	8	8	8	8	8	8	8
		$\bar{x}$	151.4	21.0	13.9	62.0	41.0	68.4	45.1
08.05.82	5.9	E	21.9	2.1	1.0	9.2	2.1	11.9	2.7
		n	5	5	5	5	5	5	5
		$\bar{x}$	133.1	19.4	14.6	50.3	38.0	63.4	47.4
04.08.82	8.0	E	12.2	2.1	1.9	25.4	19.6	30.2	19.9
		n	4	4	4	4	4	4	4
		$\bar{x}$	255.2	36.7	14.4	112.9	44.0	106.5	41.7
14.09.82	8.0	E	8.8	1.4	0.7	7.7	1.7	2.2	1.0
		n	5	5	5	5	5	5	5
		$\bar{x}$	72.9	14.1	19.4	21.4	29.3	37.3	51.3
23.10.82	8.0	E	4.3	2.1	2.9	5.8	7.1	3.1	4.3
		n	5	5	5	5	5	5	5

Table 6a Suspended load and composition, 6 m above the sea-floor at Site 7.

Date deployed	Total no. days deployed		Total dry weight $gm^{-2}d^{-1}$	ORGANIC Dry weight $gm^{-2}d^{-1}$	ORGANIC %	$CaCO_3$ Dry weight $gm^{-2}d^{-1}$	$CaCO_3$ %	REFRACTORIES Dry weight $gm^{-2}d^{-1}$	REFRACTORIES %
		$\bar{x}$	60.4	12.3	20.4	18.4	29.6	31.2	50.1
21.02.82	8.0	E	5.6	4.1	4.1	1.2	6.4	4.1	2.2
		n	5	5	5	3	3	3	3
		$\bar{x}$	19.9	4.2	20.8	7.2	36.0	8.6	43.2
08.05.82	5.9	E	3.1	1.1	4.5	2.0	5.7	1.5	7.3
		n		5	5	5	5	5	5
		$\bar{x}$	16.9	6.0	34.6	9.3	42.3	4.5	25.6
04.08.82	7.9	E	3.5	4.0	16.5	7.8	49.0	3.2	6.2
		n	5	5	5	4	4	4	4
		$\bar{x}$	44.3	8.4	19.7	14.8	33.2	21.0	47.5
14.09.82	8.0	E	12.6	11.7	29.6	46.7	52.1	21.6	62.9
		n	2	2	2	2	2	2	2
		$\bar{x}$	14.9	4.0	26.8	3.7	24.4	7.2	48.8
23.10.82	9.0	E	0.6	2.0	0.9	1.0	6.1	0.6	6.0
		n	5	5	5	5	5	5	5
		$\bar{x}$	29.2	6.2	21.3	8.1	27.6	14.9	51.1
06.12.82	7.1	E	0.6	0.9	2.9	2.4	7.9	1.5	5.5
		n	5	5	5	5	5	5	5
		$\bar{x}$	27.4	6.6	24.2	6.5	24.0	14.3	51.8
19.01.83	7.0	E	2.4	1.5	4.9	3.2	21.2	3.8	8.9
		n	4	4	4	4	4	4	4

Table 6b Suspended load and composition, 0.5 m above the sea-floor at Site 7.

				ORGANIC		$CaCO_3$		REFRACTORIES	
Date deployed	Total no. days deployed		Total dry weight $gm^{-2}d^{-1}$	Dry weight $gm^{-2}d^{-1}$	%	Dry weight $gm^{-2}d^{-1}$	%	Dry weight $gm^{-2}d^{-1}$	%
		$\bar{x}$	114.3	21.3	18.5	38.3	33.2	55.4	48.3
21.02.82	0.8	E	3.5	2.4	2.2	5.0	20.1	9.7	8.9
		n	8	8	8	3	3	3	3
		$\bar{x}$	35.5	6.0	16.9	13.4	38.3	16.0	44.9
08.05.82	5.9	E	4.2	1.5	2.4	1.6	7.8	4.3	6.7
		n	5	5	5	5	5	5	5
		$\bar{x}$	28.0	7.7	27.6	6.0	20.7	14.3	51.7
04.08.82	7.9	E	3.5	0.9	2.1	4.8	14.1	2.1	13.0
		n	5	5	5	5	5	5	5
		$\bar{x}$	87.0	17.5	19.2	28.7	33.2	41.0	47.1
14.09.82	8.0	E	7.8	7.5	5.9	5.0	16.9	6.8	4.1
		n	4	4	4	4	4	4	4
		$\bar{x}$	21.9	4.4	20.0	8.1	36.9	9.4	43.1
23.10.82	9.0	E	0.6	1.7	7.4	5.7	20.1	2.6	12.2
		n	5	5	5	5	5	5	5
		$\bar{x}$	58.3	10.2	17.7	21.6	36.5	26.6	45.8
06.12.82	7.7	E	5.8	2.7	4.7	8.3	14.0	1.5	5.8
		n	5	5	5	5	5	5	5
		$\bar{x}$	48.8	10.2	20.9	17.7	36.2	20.9	42.9
19.01.83	7.0	E	1.4	1.9	3.7	3.2	6.6	1.7	3.5
		n	5	5	5	5	5	5	5

Table 7 Suspended load and composition, 0.5 m above the sea-floor at Site 8.

				ORGANIC		$CaCO_3$		REFRACTORIES	
Date deployed	Total no. days deployed		Total dry weight $gm^{-2}d^{-1}$	Dry weight $gm^{-2}d^{-1}$	%	Dry weight $gm^{-2}d^{-1}$	%	Dry weight $gm^{-2}d^{-1}$	%
		$\bar{x}$	15.9	4.2	26.5	5.8	36.4	5.9	37.1
08.05.82	8.9	E	0.0	0.9	8.4	0.9	11.0	0.0	2.7
		n	2	2	2	2	2	2	2
		$\bar{x}$	69.5	8.9	12.9	38.2	55.1	22.2	31.9
30.06.82	28.0	E	43.1	8.9	20.7	4.5	56.2	43.1	61.1
		n	2	2	2	2	2	2	2
		$\bar{x}$	42.3	12.2	28.6	18.7	44.3	11.5	28.0
27.07.82	8.0	E	4.2	4.0	9.2	2.4	16.4	3.7	8.1
		n	5	5	5	4	4	4	4
		$\bar{x}$	24.4	3.7	15.1	12.0	49.6	8.7	35.3
04.08.82	41.0	E	7.2	1.3	1.9	4.8	15.1	4.6	16.4
		n	4	4	4	4	4	4	4
		$\bar{x}$	64.1	13.9	21.7	24.5	38.0	25.7	40.3
14.09.82	8.0	E	5.1	3.6		10.3	14.8	5.1	8.8
		n	5	5	5	5	5	5	5
		$\bar{x}$	33.0	5.4	17.3	16.7	50.3	10.7	32.4
22.09.82	31.1	E	4.2	1.1	3.5	4.0	8.1	1.6	4.7
		n	5	5	5	5	5	5	5
		$\bar{x}$	25.8	6.4	24.4	10.4	38.9	8.9	34.7
23.10.82	9.0	E	7.3	3.2	7.4	4.3	17.1	3.2	8.8
		n	5	5	5	5	5	5	5
		$\bar{x}$	32.7	6.2	19.0	14.9	45.6	11.6	35.4
01.11.82	35.2	E	4.1	1.1	2.5	1.2	2.7	2.1	2.1
		n	5	5	5	5	5	5	5
		$\bar{x}$	39.3	9.4	24.0	13.1	33.4	16.7	42.6
08.12.82	5.9	E	3.4	2.0	4.7	3.8	8.7	1.7	3.8
		n	5	5	5	5	5	5	5
		$\bar{x}$	32.2	7.5	23.7	16.4	50.8	8.3	25.5
19.01.83	7.0	E	4.3	2.5	7.1	3.3	4.8	2.0	2.9
		n	5	5	5	5	5	5	5
		$\bar{x}$	39.1	7.0	18.1	17.3	44.5	14.6	37.3
05.03.83	7.0	E	16.3	2.9	1.1	7.0	1.6	9.8	1.4
		n	4	4	4	4	4	4	4

Table 7 (continued)

09.03.83	48.0	x̄	326.5	27.6	8.4	242.8	74.3	56.3	17.3
		E	132.9	0.9	3.6	16.6	6.3	12.6	3.6
		n	2	2	2	2	2	2	2
26.04.83	39.0	x̄	23.6	2.4	10.2	17.4	73.9	3.8	15.9
		E	7.2	0.6	0.3	5.2	1.7	1.3	1.7
		n	4	4	4	4	4	4	4
13.08.83	14.0	x̄	34.1	7.4	21.4	20.4	59.9	6.4	18.8
		E	8.0	3.2	5.4	4.3	8.1	2.4	5.7
		n	4	4	4	4	4	4	4

Table 8a Suspended load and composition, 6 m above the sea-floor at Site 10.

				ORGANIC		$CaCO_3$		REFRACTORIES	
Date deployed	Total no. days deployed		Total dry weight $gm^{-2}d^{-1}$	Dry weight $gm^{-2}d^{-1}$	%	Dry weight $gm^{-2}d^{-1}$	%	Dry weight $gm^{-2}d^{-1}$	%
21.02.82	9.0	x̄	174.3	26.3	15.1	75.6	43.3	76.8	44.0
		E	5.2	3.1	1.8	5.7	3.0	8.2	1.5
		n	9	9	9	3	3	3	3
31.03.82	6.1	x̄	36.6	9.7	26.4	13.8	37.7	13.4	35.8
		E	5.2	1.5	1.7	5.2	13.1	4.2	13.4
		n	7	7	7	3	3	3	3
08.05.82	5.8	x̄	90.0	15.7	17.4	31.6	35.2	34.6	47.4
		E	5.1	5.1	4.7	5.6	5.7	7.6	4.3
		n	5	5	5	5	5	5	5
22.06.82	7.0	x̄	54.6	10.9	19.9	14.4	26.4	29.3	53.7
		E	2.0	1.5	2.1	2.2	4.6	2.2	2.5
		n	5	5	5	5	5	5	5
04.08.82	8.0	x̄	22.2	6.4	29.1	4.9	21.3	9.3	49.5
		E	4.0	1.0	3.2	4.8	18.3	3.8	13.0
		n	4	4	4	4	4	4	4
14.09.82	8.0	x̄	98.6	16.1	16.3	37.7	38.1	44.9	45.6
		E	8.2	2.2	1.2	5.1	14.8	2.5	2.4
		n	5	5	5	5	5	5	5
28.10.82	5.3	x̄	75.6	16.8	22.0	23.2	30.7	35.7	47.3
		E	6.4	5.6	6.1	8.1	10.7	4.7	6.9
		n	5	5	5	5	5	5	5
06.12.82	7.8	x̄	94.0	20.6	21.7	26.6	28.5	46.8	49.8
		E	5.2	7.1	6.3	8.3	9.3	5.0	4.0
		n	5	5	5	5	5	5	5
19.01.83	7.1	x̄	104.0	21.8	20.8	25.3	24.6	56.8	54.5
		E	20.5	5.8	1.5	2.9	2.9	12.4	1.6
		n	5	5	5	5	5	5	5

Table 8b Suspended load and composition, 0.5 m above the sea-floor at Site 10.

Date deployed	Total no. days deployed		Total dry weight $gm^{-2}d^{-1}$	ORGANIC Dry weight $gm^{-2}d^{-1}$	ORGANIC %	$CaCO_3$ Dry weight $gm^{-2}d^{-1}$	$CaCO_3$ %	REFRACTORIES Dry weight $gm^{-2}d^{-1}$	REFRACTORIES %
		$\bar{x}$	343.3	48.4	14.1	147.6	43.9	147.2	43.8
21.02.82	9.0	E	9.2	5.0	1.4	26.3	6.9	24.1	3.7
		n	9	9	9	3	3	3	3
		$\bar{x}$	126.7	24.0	19.0	53.9	40.8	55.0	41.6
31.03.82	6.1	E	5.1	2.2	1.8	17.4	12.9	12.4	10.2
		n	8	8	8	3	3	3	3
		$\bar{x}$	207.6	23.4	11.3	92.0	44.3	91.9	44.4
08.05.82	5.8	E	10.8	5.2	2.2	5.2	2.7	6.2	1.2
		n	5	5	5	5	5	5	5
		$\bar{x}$	149.8	22.1	14.8	55.9	37.3	71.8	48.0
22.06.82	7.0	E	6.6	4.0	2.9	11.8	6.9	5.2	4.0
		n	5	5	5	5	5	5	5
		$\bar{x}$	80.8	14.4	17.9	30.1	37.0	36.5	45.1
04.08.82	8.0	E	9.3	2.4	3.2	7.7	5.8	4.1	4.8
		n	5	5	5	5	5	5	5
		$\bar{x}$	278.9	36.8	13.2	124.4	44.6	117.6	42.2
14.09.82	8.0	E	49.6	7.8	1.9	26.7	4.5	21.0	2.7
		n	4	4	4	4	4	4	4
		$\bar{x}$	145.5	25.9	17.7	50.2	34.6	69.4	47.7
28.10.82	5.3	E	9.1	9.2	5.7	16.1	11.7	10.8	6.3
		n	5	5	5	5	5	5	5
		$\bar{x}$	167.9	26.7	15.9	54.0	32.2	87.1	51.9
06.12.82	7.8	E	3.6	3.0	1.6	6.1	3.6	4.1	2.1
		n	5	5	5	5	5	5	5
		$\bar{x}$	214.6	30.4	14.2	85.6	39.9	98.6	45.9
19.01.82	7.1	E	62.5	8.6	1.7	26.5	3.5	29.0	1.9
		n	5	5	5	5	5	5	5

Table 9a Suspended load and composition, 6 m above the sea-floor at Site 11.

Date deployed	Total no. days deployed		Total dry weight $gm^{-2}d^{-1}$	ORGANIC Dry weight $gm^{-2}d^{-1}$	ORGANIC %	$CaCO_3$ Dry weight $gm^{-2}d^{-1}$	$CaCO_3$ %	REFRACTORIES Dry weight $gm^{-2}d^{-1}$	REFRACTORIES %
		$\bar{x}$	159.6	26.9	15.4	43.6	28.8	90.9	56.0
21.02.82	9.0	E	5.4	5.2	1.2	29.8	5.7	25.5	8.9
		n	8	8	8	3	3	3	3
		$\bar{x}$	21.7	5.7	26.6	9.3	22.5	24.8	59.7
31.03.82	6.0	E	4.5	0.9	3.0	1.9	4.5	2.9	3.8
		n	8	8	8	3	3	3	3
		$\bar{x}$	41.6	7.5	17.9	9.3	22.5	24.8	59.7
08.05.82	5.8	E	3.3	1.0	2.0	1.9	4.5	2.9	3.8
		n	5	5	5	5	5	5	5
		$\bar{x}$	36.0	8.7	24.2	3.9	11.0	22.8	65.0
22.06.82	7.0	E	3.7	1.7	4.5	3.2	8.4	3.0	4.3
		n	5	5	5	5	5	5	5
		$\bar{x}$	59.9	14.1	23.6	12.8	21.2	33.0	55.2
28.10.82	5.3	E	3.1	0.6	1.5	5.8	8.4	2.9	7.1
		n	5	5	5	5	5	5	5
		$\bar{x}$	76.4	13.9	18.2	15.8	20.6	46.8	61.2
06.12.82	7.8	E	1.9	1.3	1.9	1.9	4.0	1.6	2.1
		n	4	4	4	4	4	4	4
		$\bar{x}$	93.1	18.3	19.7	18.5	19.8	56.3	60.5
19.01.83	7.1	E	12.6	6.9	8.4	18.1	19.0	12.1	10.9
		n	3	3	3	3	3	3	3

Table 9b Suspended load and composition, 0.5 m above the sea-floor at Site 11.

Date deployed	Total no. days deployed		Total dry weight $gm^{-2}d^{-1}$	ORGANIC Dry weight $gm^{-2}d^{-1}$	ORGANIC %	$CaCO_3$ Dry weight $gm^{-2}d^{-1}$	$CaCO_3$ %	REFRACTORIES Dry weight $gm^{-2}d^{-1}$	REFRACTORIES %
		x̄	354.3	53.1	15.4	100.2	28.9	196.6	56.6
21.02.82	9.0	E	3.0	4.2	1.2	18.1	5.7	11.2	2.2
		n	8	8	8	3	3	3	3
		x̄	96.4	18.7	19.4	24.9	25.0	54.0	54.4
31.03.82	6.0	E	5.1	3.1	2.4	8.9	7.8	5.9	9.9
		n	7	7	7	4	4	4	4
		x̄	183.1	23.2	12.7	54.1	29.5	105.8	57.8
08.05.82	5.8	E	18.5	2.1	0.7	8.2	2.4	10.0	1.6
		n	5	5	5	5	5	5	5
		x̄	180.00	27.3	15.2	48.1	27.3	103.6	57.6
22.06.82	7.0	E	23.2	6.7	2.2	9.2	3.8	12.2	2.5
		n	5	5	5	5	5	5	5
		x̄	139.7	30.0	21.5	35.4	25.3	74.3	53.2
28.10.82	5.3	E	2.4	3.0	2.1	8.3	5.7	5.0	4.0
		n	5	5	5	5	5	5	5
		x̄	141.9	23.0	16.2	16.2	25.4	82.9	54.4
06.12.82	7.8	E	11.4	3.3	1.6	4.2	4.2	7.1	11.9
		n	5	5	5	5	5	5	5
		x̄	218.9	35.5	15.4	62.5	28.3	122.9	56.4
19.01.83	7.1	E	16.5	2.4	1.5	20.7	7.0	4.4	5.4
		n	5	5	5	5	5	5	5

Table 10 Suspended load and composition, 0.5 m above the sea-floor at Site 13.

Date deployed	Total no. days deployed		Total dry weight $gm^{-2}d^{-1}$	ORGANIC Dry weight $gm^{-2}d^{-1}$	ORGANIC %	$CaCO_3$ Dry weight $gm^{-2}d^{-1}$	$CaCO_3$ %	REFRACTORIES Dry weight $gm^{-2}d^{-1}$	REFRACTORIES %
		x̄	21.5	4.9	22.5	4.5	18.5	12.8	59.0
22.06.82	8.0	E	0.5	0.6	3.1	1.7	9.8	1.4	6.8
		n	5	5	5	5	5	5	5
		x̄	32.3	5.3	16.2	10.7	33.9	16.1	49.9
30.06.82	27.9	E	5.3	1.4	3.6	1.6	9.5	3.0	9.4
		n	5	5	5	5	5	5	5
		x̄	25.5	6.1	23.8	11.0	42.8	8.3	33.0
27.07.82	8.0	E	2.2	0.9	2.5	5.7	18.3	3.3	16.4
		n	5	5	5	5	5	5	5
		x̄	95.3	15.1	15.8	33.0	35.0	47.0	49.0
04.08.82	41.0	E	8.9	5.7	6.0	18.6	21.1	16.4	14.9
		n	3	3	3	3	3	3	3
		x̄	146.5	21.1	14.6	51.4	35.4	74.0	49.9
14.09.82	8.0	E	34.0	2.1	3.5	4.1	4.8	30.0	8.1
		n	4	4	4	4	4	4	4
		x̄	100.0	17.1	17.1	36.0	36.0	46.7	46.9
26.10.82	6.0	E	3.5	4.8	4.7	10.3	10.4	6.2	5.7
		n	5	5	5	5	5	5	5
		x̄	263.0	32.0	12.2	115.6	43.9	115.4	43.9
06.12.82	7.8	E	6.4	3.0	1.24	11.5	3.6	5.1	2.4
		n	5	5	5	5	5	5	5
		x̄	253.1	33.7	13.3	100.2	39.6	119.1	47.1
19.01.83	7.0	E	7.2	2.4	5.6	5.6	2.0	5.1	1.1
		n	5	5	5	5	5	5	5
		x̄	268.7	32.6	11.9	123.1	45.9	113.5	42.2
02.03.83	7.0	E	20.0	4.8	1.3	6.8	2.5	10.7	1.3
		n	5	5	5	5	5	5	5
		x̄	63.1	9.5	15.0	23.2	36.6	30.6	48.4
19.04.83	55.0	E	4.1	0.6	0.7	3.5	4.0	2.2	3.3
		n	5	5	5	5	5	5	5
		x̄	46.0	10.8	23.7	17.7	38.1	17.5	3.83
18.08.83	9.3	E	3.2	1.1	3.8	7.1	13.0	3.3	9.5
		n	5	5	5	5	5	5	5